



## A Theory of the Connectivity Dimensionality Field in Edge-Vertex Graphs and Discrete-Continuous Dual Spaces

THOMAS A. MANZ

email:tom@space-mixing-theory.com

Please see [www.space-mixing-theory.com/authors.htm](http://www.space-mixing-theory.com/authors.htm) for current address.

Published on the web December 11, 2008.

### ABSTRACT

*Over the years, a number of measures have been defined for the purpose of determining the number of independent dimensions contained in a space. The most common dimensionality measures are the topological dimensionality and various kinds of fractal dimensionalities. While each of these dimensionality measures is useful in its own right, none of them accurately quantifies the effective number of independent directions passing through locations contained in a local region of a space. This article introduces a new dimensionality measure, called the connectivity dimensionality field, which is the true measure for the effective number of independent directions passing through locations in a space. In contrast to the fractal dimensionality, the connectivity dimensionality field is a topological property because its value at each material location is invariant to deformations of the space preserving connectivity.*

*The connectivity dimensionality field is a fundamental concept that applies to many different kinds of discrete spaces, continuous spaces, and discrete-continuous dual spaces. A discrete space is a space in which positions cannot be varied differentially, and a continuous space is a space in which positions can be varied differentially. A discrete-continuous dual space has complementary discrete and continuous representations, and a process called discrete-continuous dual matching relates the discrete and continuous representations to each other. This article formally defines two basic types of discrete-continuous duality: (a) asymptotic and (b) strict. A rigorous method is provided for computing the connectivity dimensionality field in edge-vertex graphs, continuous spaces, and discrete-continuous dual spaces. Many examples are given to illustrate the key concepts.*

*Single points, unbranched lines, and periodic lattices are examples of discrete-continuous dual spaces in which the connectivity dimensionality field is a constant nonnegative integer. In other types of discrete-continuous dual spaces, the connectivity dimensionality field contains inherent uncertainty. For the first time, a comprehensive theory is derived that predicts the inherent uncertainty associated with the connectivity dimensionality field in discrete-continuous dual spaces. The study of discrete-continuous dual spaces with variable connectivity dimensionality fields transcends variable-based mathematics.*

**Keywords:** connectivity dimensionality field, discrete-continuous duality, strictly and asymptotically discrete-continuous dual spaces, graph theory, edge-vertex graphs, large-world networks, lattices, fractals, topological dimensionality, fractal dimensionality, mathematical dimensionality, quartropy, hyperability, hypercalculus, compact cross-section, discrete-continuous dual matching, hyperbubbles, compact or hidden dimensions, complementarity, transcending variable-based mathematics

**LIST OF CONTENTS**

1.	INTRODUCTION.....	4
1.1	Statement of the Problem .....	4
1.2	The Mathematical Dimensionality, Quartropy, and Hyperability of a Variable-Based System of Mathematics .....	5
1.3	The Topological Dimensionality .....	6
	Figure 1: A cover of the von Koch fractal .....	7
	Figure 2: The topological dimensionality of every edge-vertex graph is one.....	8
	Figure 3: The topological dimensionality of a solid rectangle is two .....	8
	Figure 4: The union of two topological spaces with different topological dimensionalities .....	8
1.4	The Manifold Covering Dimensionality.....	9
1.5	The Euclidean Covering Dimensionality (n-Embeddable).....	10
1.6	Fractal Dimensionalities .....	11
1.6.1	General Definition.....	11
1.6.2	Fractal Coastlines .....	11
	Figure 5: Procedure for constructing the von Koch fractal .....	12
1.6.3	The Box-Counting Dimensionality .....	13
	Figure 6: The fractal pattern of ferns .....	14
	Figure 7: Computing the fractal dimensionality of the von Koch fractal .....	15
	Figure 8: Computing the fractal dimensionality of the Sierpiński gasket.....	16
1.6.4	The Hausdorff Dimensionality.....	16
1.6.5	Multiple Fractals and Nonfractals in the Same Space.....	17
1.7	The Need for a New Type of Dimensionality Measure.....	17
2.	THE CONNECTIVITY DIMENSIONALITY FIELD DEFINED.....	18
2.1	Hyperspheres .....	18
2.2	General Method for Computing the Connectivity Dimensionality .....	19
2.3	The Connectivity Dimensionality Field is Nonnegative and Real-valued .....	22
2.4	The Connectivity Distance, Connectivity Radius, and Count Function .....	23
	Figure 9: Vertex-labeled graph used to illustrate the connectivity distance function .....	24
	Table 1: Correspondence between generic and edge-vertex graph functions.....	26
2.5	Efficient Computational Algorithms .....	26
	Table 2: A table representation of the edge-vertex graph shown in Figure 9 .....	27
3.	DISCRETE-CONTINUOUS DUALITY .....	28
3.1	Overview .....	28
3.2	Strictly Discrete-Continuous Dual Space Defined .....	30
3.3	Examples of Strictly Discrete-Continuous Dual Spaces .....	31
	Figure 10: The human circulatory system is an example of a strictly discrete-continuous dual network .....	32
3.4	Asymptotically Discrete-Continuous Dual Space Defined .....	33
3.5	Example of an Asymptotically Discrete-Continuous Dual Space .....	34
	Figure 11: A system of roads is an example of an asymptotically discrete-continuous dual network .....	35
3.6	Method for Determining Whether an Edge-Vertex Graph is Discrete-Continuous Dual.....	35
	Figure 12: Examples of (a.) unconnected and (b.) connected graphs .....	37
	Figure 13: A graph that is not discrete-continuous dual because it is small-world.....	37
	Figure 14: Example of a worm-hole edge.....	38
	Figure 15: Example of an asymptotically discrete-continuous dual graph .....	38
	Figure 16: Example of a strictly discrete-continuous dual graph.....	39
3.7	Tree-like Networks .....	39
	Figure 17: A tree-like graph in which the branches are not gradual or smooth .....	40
	Figure 18: A tree-like graph in which the branches are gradual and smooth.....	40

4.	COMPUTING THE CONNECTIVITY DIMENSIONALITY IN DISCRETE-CONTINUOUS DUAL SPACES.....	41
4.1	Minimum Connectivity Radius for Computing the Connectivity Dimensionality.....	41
4.2	Estimating the Average Connectivity Dimensionality of a Local Region.....	43
	Table 3: The minimum connectivity radius for evaluating the connectivity dimensionality.....	44
4.3	When and Why the Connectivity Dimensionality Contains Inherent Uncertainty.....	45
	Figure 19: A lattice companion graph superimposed on the lattice it represents.....	46
4.4	How Uncertainty in Average Connectivity Dimensionality Depends on Connectivity Radius.....	48
	Figure 20: A plot of the function $K[z]$ .....	52
	Figure 21: A plot of the function $K[z]/\sqrt{z}$ .....	54
4.5	Hypergradients in the Connectivity Dimensionality.....	55
	Figure 22: Space containing a connectivity dimensionality hypergradient.....	56
	Table 4: Local average connectivity dimensionalities for the labeled vertices.....	56
4.6	How to Compute the Connectivity Dimensionality Field of Edge-Vertex Graphs.....	57
4.7	Example: The Sierpiński Gasket.....	58
	Figure 23: The Sierpiński Gasket.....	59
	Figure 24: A plot of count function versus connectivity radius for the Sierpiński gasket.....	60
	Figure 25: Plot to determine the local connectivity dimensionality in the Sierpiński gasket.....	61
	Table 5: Data for computing the local connectivity dimensionality in the Sierpiński gasket.....	62
	Figure 26: The upper uncertainty in the average connectivity dimensionality.....	63
	Figure 27: A plot of count function versus connectivity radius for a corner vertex in the Sierpiński gasket.....	65
	Figure 28: Plot to determine the connectivity dimensionality of a corner vertex in the Sierpiński gasket.....	66
4.8	Isolated Point and Straight Line.....	67
4.9	Tilings and Lattices.....	67
4.9.1	Types of Lattices.....	67
	Figure 29: Examples of Penrose tilings.....	68
	Figure 30: Examples of regular lattices.....	69
	Figure 31: Section of an untiled lattice.....	69
4.9.2	Removing the Connectivity Dimensionality Error for Periodic Lattices.....	69
	Table 6: Count function for a Penrose tile compared to a 2-dimensional periodic lattice.....	71
4.10	Tree-like Networks.....	71
	Figure 32: Noncrosslinked infinite tree.....	71
	Figure 33: A partially crosslinked tree.....	73
5.	DISCRETE-CONTINUOUS DUAL MATCHING.....	73
5.1	The Need for a New Field of Mathematics Studying Discrete-Continuous Dual Spaces.....	73
5.2	What is Discrete-Continuous Dual Matching?.....	75
	Figure 34: Connectivity versus hypercoordinate radius.....	76
5.3	An Example Space with a Fractional Connectivity Dimensionality Field.....	78
	Table 7: Count function for the graph of Figure 9.....	78
	Figure 35: Plot used to determine the connectivity dimensionality of vertex P in Figure 9.....	79
5.4	Other Hypercoordinate Bases and Vertexal Density Variations.....	79
5.5	Compact and Hidden Dimensions.....	80
	Figure 36: Space containing a compact dimension.....	81
	Table 8: Count function for the indicated vertex in Figure 36.....	81
	Figure 37: Plot of the count function for a space containing a compact dimension.....	82
5.6	Hyperbubbles and Porous Spaces.....	84
	Figure 38: Hyperbubbles and porous spaces.....	85
6.	CONCLUSIONS.....	86
7.	GLOSSARY.....	87
	REFERENCES.....	90

## 1. INTRODUCTION

### 1.1 Statement of the Problem

There are different types of dimensions and associated dimensionalities described in the literature. Some of these assign a scalar value to the space as a whole. Others assign a scalar value that depends upon location within the space; these are called dimensionality fields.

**Definition 1: Dimensionalities** are quantitative measures of the number of dimensions in a space.

**Definition 2: A dimensionality field** assigns a dimensionality to each position within a space.

This Introduction section discusses several basic kinds of dimensionality measures and then explains why a new dimensionality measure is needed to quantify the effective number of independent directions passing through points in edge-vertex graphs and discrete-continuous dual spaces. The most common method for computing the number of independent dimensions in a space is to simply count the number of independent continuous coordinates needed to locate a position within that space; however, this method only works when the number of independent dimensions is a constant nonnegative integer. A variety of methods for computing or measuring fractal dimensionalities of a space have also been developed, but connectivity dimensionality is a different concept than fractal dimensionality. In particular, fractal dimensionality depends upon both a space's connectivity and degree of crumpledness whereas the connectivity dimensionality field depends upon the space's connectivity but not its degree of crumpledness. Fractal dimensionality has been the subject of many scholarly articles, but the connectivity dimensionality field is new. A generally applicable method for computing or measuring the connectivity dimensionality field needs to be developed from first principles.

The main purposes of this article are to (i) describe how to properly measure the connectivity dimensionality field in edge-vertex graphs and discrete-continuous dual spaces, (ii) formalize the mathematical description of discrete-continuous dual spaces, and (iii) derive basic mathematical properties of the connectivity dimensionality field in discrete-continuous dual spaces. Two basic types of discrete-continuous dual spaces are formally defined: (a) strictly discrete-continuous dual spaces and (b) asymptotically discrete-continuous dual spaces.

Strictly discrete-continuous dual spaces have been previously studied, but they are more commonly referred to in the literature by other terms like lattices or grids. On April 24, 2008, each of the phrases "discrete-continuous dual space" and "discrete-continuous dual network" returned no matches on Google's Scholar and worldwide web searches, but each of the terms "lattice" and "grid" returned millions of matches on these same two search engines. The integers form a widely studied discrete space whose interpolated continuous space is the widely studied set of real numbers; therefore,  $\{\mathbb{Z}, \mathbb{R}\}$  is a strictly discrete-continuous dual space where  $\mathbb{Z}$  is the set of integers and  $\mathbb{R}$  is the set of real numbers. Similarly,  $\{\mathbb{Z}^N, \mathbb{R}^N\}$  is a strictly discrete-continuous dual space where  $\mathbb{Z}^N$  is the set of integer N-tuples and  $\mathbb{R}^N$  is the set of real N-tuples. These examples of discrete-continuous dual spaces have a constant connectivity dimensionality field N.

In the literature, the concept of edge-vertex graphs dual to continuous spaces is usually restricted to continuous spaces of nonnegative integer dimensionality. To the best of my knowledge, the concept of a discrete-continuous dual space embedding a variable connectivity dimensionality field is not discussed in the prior literature. The concept of spaces with a variable fractal dimensionality exists in the prior literature, but this is a different concept than a discrete-continuous dual space embedding a variable connectivity dimensionality field. As discussed later in this article, discrete-continuous dual spaces embedding a variable connectivity dimensionality field transcend variable-based mathematics. A new subject area of mathematics called hypercalculus is introduced to describe their properties.

## 1.2 The Mathematical Dimensionality, Quartropy, and Hyperability of a Variable-Based System of Mathematics

A mathematical system describes a particular solution or a family of possible solutions. Each particular solution of a mathematical system is called a self-consistent solution. For example, when a dice is rolled, an integer from 1 to 6 is selected. The set of integers 1 through 6 is the family of possible solutions for this system. The system selects exactly one of these possible solutions, and the selection of one particular solution means the alternative possible solutions are not selected.

In a variable-based mathematical system, there are three different types of degrees of freedom:

**Definition 3:** A measure of one type of degrees of freedom, we shall call the **mathematical dimensionality** of the mathematical system  $\mathbb{S}$ , refers to the number of continuous independent variables that must be specified to locate a particular point within a single self-consistent solution of the mathematical system  $\mathbb{S}$ .

**Definition 4:** A measure of another type of degrees of freedom, we shall call the **hyperability** of the mathematical system  $\mathbb{S}$ , is the number of continuous boundary conditions and continuous parameters that must be specified to give a particular self-consistent solution of the mathematical system  $\mathbb{S}$ .

**Definition 5:** A measure of a third type of degrees of freedom, we shall call the **quartropy** of the mathematical system  $\mathbb{S}$ , refers to the base 2 logarithm of the number of discrete possibilities in the family of possible solutions out of which one particular must be chosen in order to specify a self-consistent solution. (The quartropy is the number of distinguishable quarter flips that produces a discrete probability space of the same size.)

For example, consider the straight line  $y = mx + b$ . This system has one continuous independent variable ( $x$ ), one dependent variable ( $y$ ), and two continuous parameters ( $m$  and  $b$ ). Two continuous parameters ( $m$  and  $b$ ) must be specified to give a particular line, thus the hyperability of this system is 2. Because the system has one independent variable, its mathematical dimensionality is one. The quartropy of this system is zero since it doesn't involve any discrete variables.

Now consider the hyperbola

$$\frac{x^2}{a^2} - \frac{y^2}{b^2} = 1. \quad (1)$$

Two continuous parameters ( $a$  and  $b$ ) must be specified to give a particular hyperbola, so the hyperability of this system is 2. There are two continuous variables ( $x$  and  $y$ ). One of these two variables is independent while the other is dependent, so the mathematical dimensionality of this system is 1. Finally, the hyperbola consists of two discrete branches (a left branch and a right branch), so the quartropy of the system is  $\log_2 [2] = 1$ .

Next, consider the game of Yatzee<sup>®</sup> which is based on the roll of 5 indistinguishable dice, each of which selects an integer from 1 to 6. Because the dice are indistinguishable, for each roll of the five dice there are 117 different possible outcomes and the quartropy is  $\log_2 [117]$ . Since no continuous variables are present in this system, both the mathematical dimensionality and the hyperability are zero.

Next, consider the eigenvalue problem  $\nabla^2 f[x, y, z] = -\lambda^2 f[x, y, z]$ . The mathematical dimensionality is three since a particular self-consistent solution  $f[x, y, z]$  has three independent continuous coordinates:  $x$ ,  $y$ , and  $z$ . In order to specify a particular self-consistent solution, we must specify a value for the parameter  $\lambda$  plus two boundary conditions each for the variables  $x$ ,  $y$ , and  $z$  since

<sup>®</sup> Registered trademark of Milton Bradley.

the differential equation is second order with respect to derivatives of each of these variables. If and only if (iff.) these six boundary conditions plus the parameter  $\lambda$  can be varied continuously to give self-consistent solutions then the hyperability of the system is seven and the quartropy is zero.

Finally, consider the system of equations

$$\begin{cases} x + y = 2\sqrt{12.5} \\ x^2 + y^2 + z^2 = 25 \end{cases} \quad (2)$$

that describes the intersection of a particular plane and sphere. Because there are three variables and two equations, one might expect there to be one independent variable in this system; however, this is not the case. The intersection of this plane with the sphere occurs through the single point  $(x, y, z) = (\sqrt{12.5}, \sqrt{12.5}, 0)$ ; therefore, there are no independent variables in this system and the mathematical dimensionality of system (2) is zero. This example shows that the number of independent variables cannot be obtained merely by subtracting the total number of equations from the total number of variables. On the other hand, the mathematical dimensionality of the system

$$\begin{cases} x + y = 5 \\ x^2 + y^2 + z^2 = 25 \end{cases} \quad (3)$$

is one since the intersection of this plane and sphere is a circle. For systems (2) and (3), both the hyperability and quartropy are zero.

Because the system  $x^2 + 2x + 1 = 0$  has a single solution  $x = -1$ , its quartropy is zero, its hyperability is zero, and its mathematical dimensionality is zero. Because the system  $x^2 + 2x - 3 = 0$  has two self-consistent solutions ( $x = 1$  or  $-3$ ), its quartropy is 1, its hyperability is zero, and its mathematical dimensionality is zero. The sphere  $x^2 + y^2 + z^2 = R^2$  has a hyperability of 1 (since the radius  $R$  must be specified to give a particular sphere), a mathematical dimensionality of 2, and a quartropy of zero.

We now focus more specifically on the mathematical dimensionality. Since the mathematical dimensionality of a linear path is one, the mathematical dimensionality of a space in the vicinity of location  $\odot$  is the number of linearly independent directions passing through location  $\odot$ . Notice the key phrase ‘in the vicinity of.’ Dimensionality is not the property of a single location, but rather the property of a group of adjacent locations in space. For simplicity of speech, we may often say the ‘dimensionality of the location  $\odot$ ’ or the ‘dimensionality at the location  $\odot$ ’, but one must keep in mind that dimensionality is not an internal property of the location  $\odot$ . Rather, dimensionality is an expression of how the location  $\odot$  is connected to adjacent locations in space. That is, dimensionality is a property of a neighborhood of locations.

### 1.3 The Topological Dimensionality

The term ‘dimension’ is often used in the place of dimensionality; consequently, topological dimensionality and fractal dimensionality are often called ‘topological dimension’ and ‘fractal dimension’, respectively. However, using the term ‘dimension’ to mean dimensionality can lead to confusion. Consider the statement: “~~A 3-dimensional Euclidean space has a topological dimension equal to three~~”. Taken literally, this statement does not tell us how many topological dimensions a 3-dimensional Euclidean space has; it merely states that a 3-dimensional Euclidean space has at least one topological dimension and that this particular topological dimension happens to equal a numeric constant, namely the number three. The statement does not rule out the possibility that a 3-dimensional Euclidean space has at least two topological dimensions, one equal to the number three and another equal to the number five. However, a dimension cannot equal a numeric constant because a numeric constant (e.g. the number three) is zero-dimensional. On the other hand, a variable can represent a dimension. For example, we can represent locations in a 3-dimensional Euclidean space by means of the variables  $(x, y, z)$ , so it is meaningful to speak of the  $x$ -dimension, the  $y$ -dimension, and the  $z$ -dimension. To avoid confusion, the term ‘dimension’ should not be used to mean ‘the number of dimensions’. The crossed out statement



should be revised to “A 3-dimensional Euclidean space has three topological dimensions” or “A 3-dimensional Euclidean space has a topological dimensionality equal to three”.

The number of topological dimensions (the topological or Lebesgue covering dimensionality)  $\mathbb{T}$  of a topological space is always a nonnegative integer. To determine the number of topological dimensions of a space, one first constructs a collection of open subsets whose union covers the entire space. Next, we find a set of even smaller open subsets which covers the entire space, and this cover is said to be a refinement of the first cover. Figure 1 shows a cover of the von Koch fractal. A space is said to have  $m$  topological dimensions if constructing refined covers requires at least one point in the space to be at most a subset of  $m+1$  open subsets in the refined cover.<sup>1</sup> In Figure 1, we can see that the cover can be constructed so that a point in the von Koch fractal belongs to at most two of the open subsets forming the cover; hence, the von Koch fractal has one topological dimension.

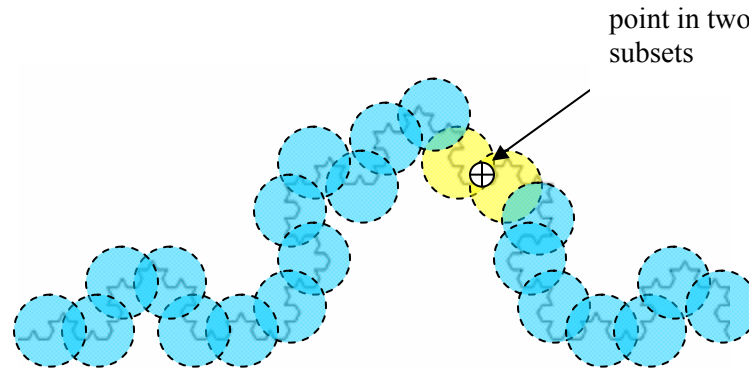


**Figure 1: A cover of the von Koch fractal**

*Notice that the solid circles entirely cover the fractal. An individual point of the fractal is at most a subset of two solid circles, and this means the topological dimensionality of the fractal is one.*

As commonly known, every edge-vertex graph has exactly one topological dimension. As we make the open sets of the cover smaller and smaller, they eventually become smaller than the size of an edge joining two vertices in the graph. For this very refined cover, some of the open sets enclose a vertex while others enclose a subsegment of an edge. See Figure 2. The open sets of the cover overlap at points along the edge that belong to two open sets of the cover; hence, the edge-vertex graph has exactly one topological dimension. Because the topological dimensionality of every edge-vertex graph is one, the topological dimensionality does not tell us anything at all about how one edge-vertex graph differs from another. Consequently, the topological dimensionality is not very useful for describing edge-vertex graphs or networks.

The topological dimensionality of the set of  $m$ -tuples of real numbers,  $\mathbb{R}^m$ , is  $m$ . Also, the topological dimensionality of a  $m$ -dimensional Euclidean space is  $m$ . Figure 3 shows that the topological dimensionality of a solid rectangle is two because constructing the refined cover requires points to belong to at most three open subsets of the cover.

One of the fundamental limitations of the topological dimensionality is that it describes only the overall properties of a topological space. Imagine the union of a 1-dimensional topological space with a 2-dimensional topological space. (For example, by gluing a line segment to the edge of a rectangle to form a sign-like structure, Figure 4.) The topological dimensionality of this combined space is 2. Because the topological dimensionality refers to the space as a whole and is not a field, it does not tell us that the space locally looks 1-dimensional in some parts and 2-dimensional in other parts.

<sup>1</sup> Weisstein, Eric W. "Lebesgue Covering Dimension." From *MathWorld*--A Wolfram Web Resource. <http://mathworld.wolfram.com/LebesgueCoveringDimension.html>

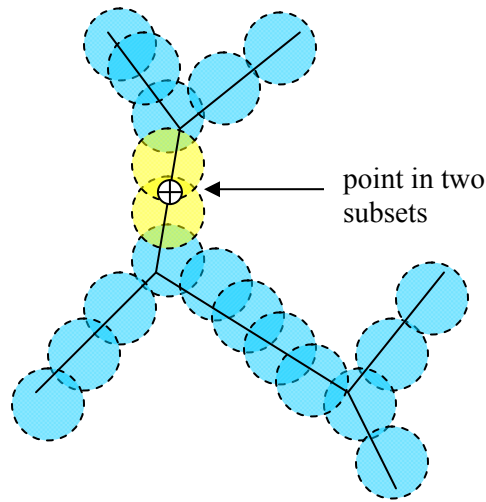


**Figure 2: The topological dimensionality of every edge-vertex graph is one**

*Notice that the solid circles entirely cover the graph. An individual point of the graph is at most a subset of two solid circles, and this means the topological dimensionality of the graph is one. All edge-vertex graphs behave similarly and have a topological dimensionality of one.*

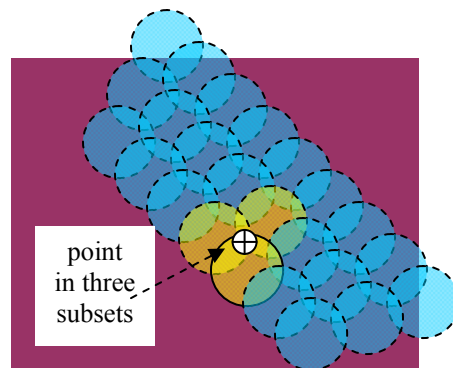


**Figure 3: The topological dimensionality of a solid rectangle is two**

*An individual point of the solid rectangle is at most a subset of three cover elements, and this means the topological dimensionality of the solid rectangle is two.*

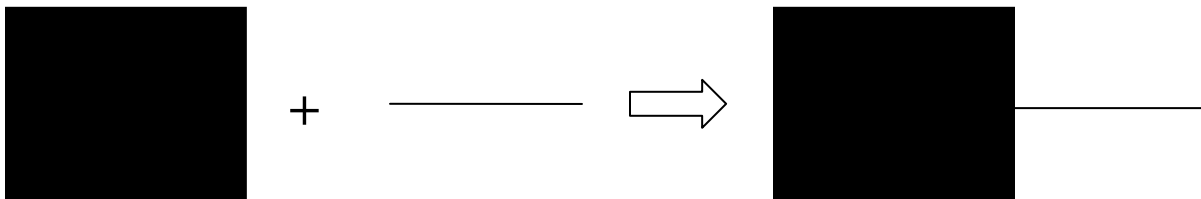


**Figure 4: The union of two topological spaces with different topological dimensionalities**

*On the right is shown a space that is formed by combining a 2-dimensional solid rectangle with a 1-dimensional line segment. Our intuition tells us that the combined space behaves as if it has different dimensionalities in different regions. However, the topological dimensionality refers only to a space as a whole and the space on the right has two topological dimensions. We would like to have a measure of dimensionality that tells us when a space is composed of pieces of different dimensionalities.*



## 1.4 The Manifold Covering Dimensionality

As explained in the previous section, the topological dimensionality does not capture the basic intuitions we have about the number of independent dimensions contained in edge-vertex graphs. A window screen with arbitrarily thin wires has the structure of a square lattice. Our intuition tells us that the square lattice is a 2-dimensional graph. We also imagine the structure of a perfect salt crystal. This structure can be represented by an edge-vertex graph by representing the center of each atom with a vertex and connecting adjacent atoms with an edge in the graph. Our intuition tells us that this is a 3-dimensional edge-vertex graph because (i) it represents a 3-dimensional crystal structure, (ii) it can be properly drawn in a 3-dimensional space, and (iii) it cannot be properly drawn in a 2-dimensional space.

We would like a means for computing the dimensionality of a space that conforms to these intuitions. We might begin by asking what minimum dimension smooth manifold is needed to properly draw the graph such that none of the edges intersect except at the vertices. The square lattice just described has a manifold covering dimensionality of 2 because it can be drawn in a 2-dimensional Euclidean space which is a type of 2-dimensional manifold. Any graph that can be properly drawn on the surface of a sphere, donut, or mobius strip also has a manifold covering dimensionality of 2 since these are 2-dimensional manifolds. The cubic lattice just described has a manifold covering dimensionality equal to 3 because it can be drawn in a 3-dimensional Euclidean space.

To clarify this definition we must specify what to do with graphs that are disconnected. The disconnected pieces are for all practical purposes separate graphs, each of which has its own manifold covering dimensionality. Consequently, the manifold covering dimensionality is defined for connected pieces of a graph.

**Definition 6:** The **manifold covering dimensionality** of a connected region of an edge-vertex graph is defined as the minimum topological dimensionality of a smooth manifold needed to properly draw the connected graph region. More generally, the manifold covering dimensionality  $\mathbb{M}$  of a connected space  $\mathbb{S}$  is defined as the minimum topological dimensionality of a smooth manifold needed to properly draw one space  $\mathbb{S}'$  that is topologically equivalent to  $\mathbb{S}$ . The manifold covering dimensionality is always a nonnegative integer and refers to the space  $\mathbb{S}$  as a whole.

Regardless of whether a connected space is discrete, continuous, or discrete-continuous dual its manifold covering dimensionality is defined as the smallest topological dimensionality of a smooth manifold that can properly embed a space topologically equivalent to the connected space. By properly embed, we mean that the connectivity of the embedded space is preserved. A smooth manifold does not intersect itself and must have a definable surface tangent. Therefore, a graph in the shape of a circle has a manifold covering dimensionality of 1, while a graph in the shape of a figure '8' has a manifold covering dimensionality of 2. A 1-dimensional figure '8' structure is not a smooth manifold because it doesn't have a defined surface tangent where the two loops join; therefore, we need a 2-dimensional smooth manifold like a plane in order to properly draw the figure '8' structure.

**Theorem 1:** The manifold covering dimensionality of a connected space  $\mathbb{S}$  is equal to or greater than its topological dimensionality:

$$\mathbb{T}[\mathbb{S}] \leq \mathbb{M}[\mathbb{S}]. \quad (4)$$

Proof: (1) According to the definition of the manifold covering dimensionality, the minimum topological dimensionality for a smooth manifold  $\mathbb{M}$  covering  $\mathbb{S}$  is

$$\mathbb{M}[\mathbb{S}] = \mathbb{T}[\mathbb{M}]. \quad (5)$$

(2) By definition of the topological dimensionality, the minimum topological dimensionality for a cover of  $\mathbb{S}$  is  $\mathbb{T}[\mathbb{S}]$ . Since  $\mathbb{M}$  covers  $\mathbb{S}$ , it follows that

$$T[\mathbb{S}] \leq T[\mathfrak{M}]. \quad (6)$$

(3) Together, equations (5) and (6) give (4).

### 1.5 The Euclidean Covering Dimensionality (n-Embeddable)

An n-dimensional Euclidean space is the set of all real n-tuples  $(x_1, x_2, \dots, x_n)$  and the associated invariant distance parameter  $\gamma$  defined by

$$(d\gamma)^2 = \sum_{i=1}^n (dx_i)^2. \quad (7)$$

A Euclidean n-space is denoted by the symbol  $\mathbb{E}^n$ , and the coordinates  $(x_1, x_2, \dots, x_n)$  specifying a location in this space are called Cartesian coordinates.

**Definition 7:** The **Euclidean covering dimensionality**  $\mathbb{D}$  of a connected space  $\mathbb{S}$  is formally defined as the minimum topological dimensionality of a Euclidean space needed to properly draw one space  $\mathbb{S}'$  that is topologically equivalent to  $\mathbb{S}$ . The Euclidean covering dimensionality is always a nonnegative integer and refers to the space  $\mathbb{S}$  as a whole.

In topology, the commonly used term n-embeddable refers to a space whose Euclidean covering dimensionality is n. For example, the surface of a sphere is a 2-dimensional manifold which requires a 3-dimensional Euclidean space to be properly drawn. Hence, the surface of the sphere has a manifold covering dimensionality  $\mathbb{M} = 2$ , a Euclidean covering dimensionality  $\mathbb{D} = 3$ , and is 3-embeddable. A spherical grid of latitude and longitude lines on the surface of the sphere forms a discrete edge-vertex graph which has a manifold covering dimensionality  $\mathbb{M} = 2$ , a Euclidean covering dimensionality  $\mathbb{D} = 3$ , and is 3-embeddable. An edge-vertex graph that can be properly drawn on a 2-dimensional plane but not a 1-dimensional line has a Euclidean covering dimensionality of 2.

What is the Euclidean covering dimensionality of the function  $y = \sin[x]$ ? To answer this question, we note the function  $y = \sin[x]$  is topologically equivalent to a straight line. Since a straight line is equivalent to a 1-dimensional Euclidean space, the Euclidean covering dimensionality of the function  $y = \sin[x]$  is one. Notice the importance of the words “needed to properly draw one space  $\mathbb{S}'$  that is topologically equivalent to  $\mathbb{S}$ ” in the definition of the Euclidean covering dimensionality. A sine wave cannot be properly drawn in 1-dimensional Euclidean space but a straight line that is topologically equivalent to a sine wave can be properly drawn in a 1-dimensional Euclidean space.

What is the Euclidean covering dimensionality of the function  $x^2 + y^2 = 1$ ? This function can be properly drawn on a plane but is not topologically equivalent to any function that can be properly drawn on a straight line; therefore, the Euclidean covering dimensionality of the function  $x^2 + y^2 = 1$  is two.

**Theorem 2:** The Euclidean covering dimensionality of a connected space  $\mathbb{S}$  is equal to or greater than its manifold covering dimensionality:

$$\mathbb{D}[\mathbb{S}] \geq \mathbb{M}[\mathbb{S}]. \quad (8)$$

Proof: (1) According to the definition of the Euclidean covering dimensionality, the minimum topological dimensionality for a Euclidean manifold  $\mathfrak{E}$  covering  $\mathbb{S}$  is

$$\mathbb{D}[\mathbb{S}] = T[\mathfrak{E}]. \quad (9)$$

(2) Since  $\mathfrak{E}$  is a type of smooth manifold covering  $\mathbb{S}$ , it follows that either  $\mathfrak{E}$  has the minimum number of topological dimensions for a smooth manifold  $\mathfrak{M}$  covering  $\mathbb{S}$  or else that some smooth manifold  $\mathfrak{M}$  covering  $\mathbb{S}$  has fewer topological dimensions than  $\mathfrak{E}$ :

$$\mathbb{T}[\mathfrak{E}] \geq \mathbb{T}[\mathfrak{M}]. \quad (10)$$

(3) Combining equations (5), (9), and (10) gives (8).

## 1.6 Fractal Dimensionalities

### 1.6.1 General Definition

**Definition 8:** The **fractal dimensionality** is “A number  $D$  associated with a fractal which satisfies the equation  $\eta = b^D$ , where  $b$  is the factor by which the length scale changes under a magnification in each step of a recursive procedure defining the object, and  $\eta$  is the factor by which the number of basic units increases in each such step.” (McGraw-Hill Dictionary of Scientific and Technical Terms, 1989)

Whereas the mathematical, topological, manifold covering, and Euclidean covering dimensionalities are nonnegative integers, the fractal dimensionality need not be integer. Because there are different ways to define the length scale  $b$  and the number of basic units, in practice there are a number of different kinds of fractal dimensionalities. A number of articles and books have been written that present a detailed treatment of how to compute various kinds of fractal dimensionalities. (For example, see Theiler, 1990; Corana, *et al.* 2004; Li, *et al.* 2004; Wang and Chen, 2001; Freeman, 1983; Cutler, 1994; Mandelbrot, 1985; Carr and Benzer, 1991.) Some of the more common fractal dimensionality measures are the Hausdorff dimensionality, capacity dimensionality, information dimensionality, correlation dimensionality, box-counting dimensionality, upper box (aka entropy, Kolmogorov, or upper Minkowski) dimensionality, lower box (aka lower Minkowski) dimensionality, pointwise dimensionality, packing dimensionality, Kaplan-Yorke dimensionality,  $q$ -dimensionality, Lyapunov dimensionality, Minkowski-Bouligand dimensionality, Rényi dimensionality of order  $\alpha$ , etc. In this section, we discuss two of these measures: the Hausdorff dimensionality and the box-counting dimensionality.

Stretching, bending, deforming, and/or rotating a space without changing its connectivity is called a homeomorphism. The term homeomorphism means specifically a continuous bijective (i.e. one-to-one in both directions) mapping from a first space to a second space. A property that remains unchanged during all homeomorphisms is called a topological property. Two spaces related by a homeomorphism are said to be topologically equivalent. Two edge-vertex graphs are topologically equivalent iff. they contain the same number of vertices, the same number of edges, and the connectivity of vertices in both graphs are identical. The mathematical, topological, manifold covering, and Euclidean covering dimensionalities are topological properties, because stretching, bending, deforming, and/or rotating a space without changing the space's connectivity does not change their values. On the other hand, the fractal dimensionality depends upon a defined length scale; stretching or deforming a space does not leave the length scale invariant so the fractal dimensionality is not a topological property. This why there is one unique measure each for the mathematical, topological, manifold covering, and Euclidean covering dimensionalities but a zoo of alternative measures for the fractal dimensionality.

### 1.6.2 Fractal Coastlines

Bob and Mary are vacationing in Florida for spring break. They are staying in two different hotels located next to the ocean. The shortest distance between the two hotels is 5 miles. They decide to walk from the first hotel to the second hotel by following the shoreline where the ocean touches the beach. Using a map of the beach, they estimate the walking distance along the shoreline between the two hotels will be about 7.5 miles. They happen to be on an exercise program that requires them to walk a certain distance each day, and for this purpose they wear a small digital device that records the actual distance they walk. When Bob and Mary walk precisely (without any sidetracking or backtracking) along the shoreline between the two hotels, the digital device records that they have walked an actual distance of 10 miles. Why does the map show a distance of 7.5 miles along the shoreline between the two hotels, but the digital device shows they have actually walked 10 miles?

The answer is that the shoreline is a fractal. For a fractal, the distance between two locations depends upon the size of the length scale used to measure distances. When Bob and Mary looked at the map of the coastline, they probably estimated the distance along the coastline between the two hotels using an effective length scale of several tenths of a mile. When they actually walked along the coastline, the digital device measured the distance along the coastline one step at a time, and this corresponds to a much smaller length scale.

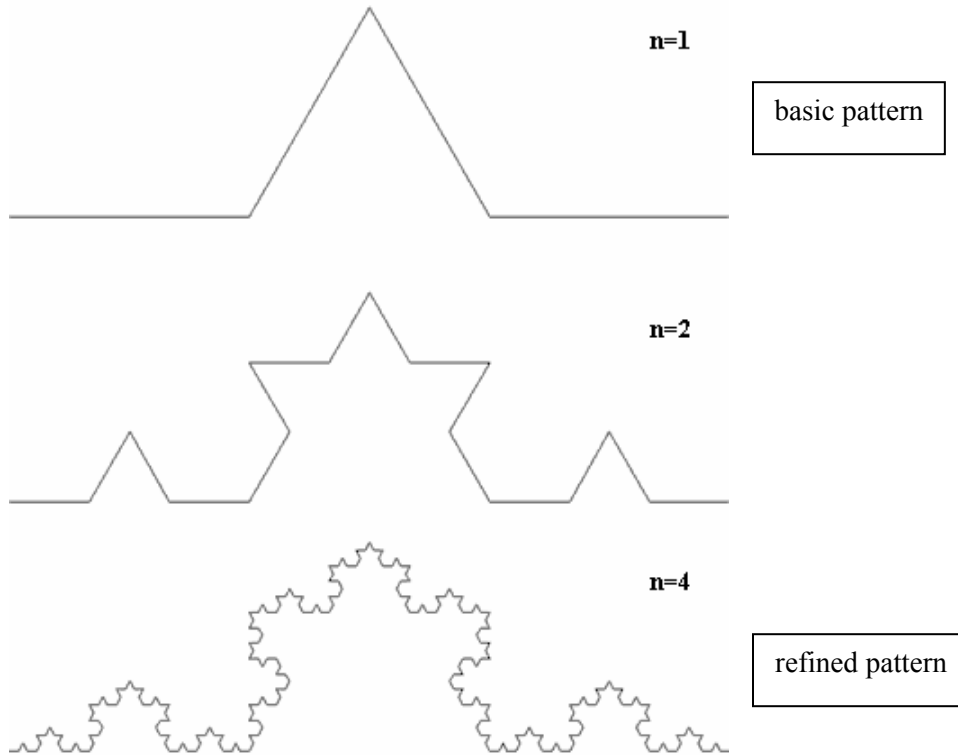


**Figure 5: Procedure for constructing the von Koch fractal<sup>2</sup>**

*The von Koch fractal is constructed by successively replacing straight line segments by the basic pattern.*

One traditional way to measure the fractal dimensionality of a coastline is to evaluate the limit

$$D_{fractal}[S_{AB}] \cong \lim_{\ell \rightarrow 0} - \frac{\ln[\eta[S_{AB}, \ell]]}{\ln \ell} \quad (\text{tentative definition}) \quad (11)$$

where  $\ell$  is the length of a straight ruler used to measure distance along the coastline  $S_{AB}$  and  $\eta[S_{AB}, \ell]$  is the number of times the ruler can be placed consecutively along the coastline between points A and B. Using this equation, the von Koch fractal shown in Figure 5 has a fractal dimensionality of  $\frac{2 \ln[2]}{\ln[3]} = 1.26...$ <sup>3</sup> (The mathematical, topological, and manifold covering dimensionalities of the von

Koch fractal are exactly one because it can be drawn as a crumpled line. The Euclidean covering dimensionality of the von Koch fractal is one if the ends are unjoined and two if the ends are joined together.)

<sup>2</sup> Image downloaded on 06/08/2008 from [http://commons.wikimedia.org/wiki/Image:Fractal\\_koch.png](http://commons.wikimedia.org/wiki/Image:Fractal_koch.png) and licensed under the terms of the **GNU Free Documentation license**, Version 1.2 or any later version published by the Free Software Foundation; with no Invariant Sections, no Front-Cover Texts, and no Back-Cover Texts.

<sup>3</sup> Eric W. Weisstein. "Koch Snowflake." From *MathWorld*--A Wolfram Web Resource. <http://mathworld.wolfram.com/KochSnowflake.html>

Equation (11) is not general enough for our purposes. If the space is unconnected, or if it branches, or if it has a topological dimensionality other than 1, then we cannot effectively use equation (11). In addition, the limit  $\ell \rightarrow 0$  is not appropriate for spaces that have a minimum distance scale due to discrete structure. In order to overcome these problems, equation (11) is replaced by the **box-counting dimensionality** defined by equation (16) of the next subsection. The box-counting dimensionality can be measured (a) for connected or unconnected spaces, (b) for branched or unbranched spaces, (c) for spaces having any possible value of the topological dimensionality, and (d) for discrete or continuous spaces. The box-counting dimensionality is very useful due to its generality and ease of implementation.

### 1.6.3 The Box-Counting Dimensionality

In order to compute the box-counting dimensionality of an object  $\mathbb{S}$ , we first determine whether it is possible to draw a representation of  $\mathbb{S}$  having correct distances between points as a subset of  $\mathbb{E}^Z$  for some nonnegative integer  $Z$ . The box-counting dimensionality is only applicable if it is possible to find at least one representation of the object and at least one value of  $Z$  for which distances are correct when the object's representation is embedded in  $\mathbb{E}^Z$ . (Informally, we seek a value of  $Z$  for which the object's shape can be correctly reproduced in  $\mathbb{E}^Z$ .) For convenience we could choose the smallest possible value for  $Z$ , but this is not strictly required. For example, the function  $y=\sin[x]$  can be represented as a subset of  $\mathbb{E}^Z$  with correct distances along this curve iff.  $Z \geq 2$ .

If an appropriate representation and value of  $Z$  can be identified, the box-counting dimensionality can be computed in the following manner. First, we fill the space  $\mathbb{E}^Z$  with  $Z$ -dimensional hypercubes of side length  $\varepsilon$  arranged in a regular lattice grid. (For  $\mathbb{E}^2$  this would be a square lattice; for  $\mathbb{E}^3$  this would be a cubic lattice.) We then count the number  $\eta[\mathbb{S}, \varepsilon]$  of  $Z$ -dimensional hypercubes of side length  $\varepsilon$  partially or fully occupied by the space  $\mathbb{S}$ . (A hypercube is partially occupied by the space  $\mathbb{S}$  if any part of  $\mathbb{S}$  is contained in the hypercube.) Then, the box-counting dimensionality of the space  $\mathbb{S}$  is commonly defined as

$$D_{\text{box-counting}}[\mathbb{S}] = \lim_{\varepsilon \rightarrow 0} \left[ -\frac{\ln[\eta[\mathbb{S}, \varepsilon]]}{\ln \varepsilon} \right]. \quad (\text{traditional definition}) \quad (12)$$

There is an obvious problem with the traditional definition of the box-counting dimensionality, equation (12). In a real situation, the number of boxes which one can explicitly count is finite and the edge length  $\varepsilon$  of each box is also finite. In addition, some spaces display a fractal scaling behavior over medium distance scales that is not operational at smaller distances. For a discrete space the fractal scaling necessary pertains to distances larger than the size of a single discrete element so that the limit should not be taken as  $\varepsilon \rightarrow 0$ . (In an edge-vertex graph, the fractal scaling necessarily pertains to distances larger than the edge length.) The traditional box-counting definition, equation (12), fails for these situations.

As an example, consider the fractal nature of a fern plant. (See [Figure 6](#).) What happens if we try to apply equation (12) to the real fern? Well, the fractal scaling of the plant is only operational down to some finite distance. This distance would probably be on the order of the size of a smallest leaf on the plant. Certainly, the fractal scaling of the plant would not be present at the size of a single atom. Consequently, we need to replace equation (12) with one that is valid for nonzero box size  $\varepsilon$ . We expect, and equation (12) is based on the idea, that the number of partially filled boxes for a fractal scales as

$$\eta[\mathbb{S}, \varepsilon] \cong K \varepsilon^{-D_{\text{box-counting}}} \quad (13)$$

where  $K$  is some constant. Taking the logarithm of both sides we obtain

$$\ln[\eta[\mathbb{S}, \varepsilon]] \cong \ln[K] - D_{\text{box-counting}} \ln[\varepsilon] \quad (14)$$

Since we do not want to compute the constant  $K$ , we will eliminate it. When the side length is doubled the number of partially filled boxes follows

$$\eta[\mathbb{S}, 2\varepsilon] \cong K (2\varepsilon)^{-D_{\text{box-counting}}} \quad \text{and} \quad \ln[\eta[\mathbb{S}, 2\varepsilon]] \cong \ln[K] - D_{\text{box-counting}} \ln[2\varepsilon]. \quad (15)$$



Combining equations (14) and (15) gives

$$D_{box-counting} \cong \frac{\ln[\eta[S, \varepsilon]] - \ln[\eta[S, 2\varepsilon]]}{\ln[2]}. \text{ (real-world definition)} \quad (16)$$



(a.) Barnsley's fern (a mathematical fractal resembling ferns)<sup>4</sup>



(b.) picture of a real fern plant<sup>5</sup>

**Figure 6: The fractal pattern of ferns**

*Ferns are an example of fractals. On top is shown a mathematical model of a fern fractal. We can readily see that this mathematical model has a structure similar to a real fern plant (bottom).*

<sup>4</sup> The image of Barnsley's fern was downloaded on 06/08/2008 from [http://commons.wikimedia.org/wiki/Image:Bransleys\\_fern.png](http://commons.wikimedia.org/wiki/Image:Bransleys_fern.png) and is licensed under the terms of the **GNU Free Documentation license**, Version 1.2 or any later version published by the Free Software Foundation; with no Invariant Sections, no Front-Cover Texts, and no Back-Cover Texts.

<sup>5</sup> Photo by Sanjay Ach of fern plants at Muir Woods, California distributed under the terms of the **GNU Free Documentation license**, Version 1.2 or any later version published by the Free Software Foundation; with no Invariant Sections, no Front-Cover Texts, and no Back-Cover Texts.



Note that equation (16) has form analogous to the definition of the fractal dimensionality  $\eta = b^D$  (see Definition 8 above). Equation (16) is useful for computing the fractal dimensionality of real-world fractals where the value of  $\varepsilon$  is chosen as some distance over which the real-world fractal displays the fractal scaling behavior. For example, one could use the following procedure to compute the fractal dimensionality of a real-world fern. For simplicity we neglect any time-dependence of the fern's shape. In the classical nonrelativistic approximation, the fern's shape can be drawn in a 3-dimensional Euclidean space. We then construct a cubic lattice where the grid size  $\varepsilon$  is a few inches and use equation (16) to compute the plant's fractal dimensionality.

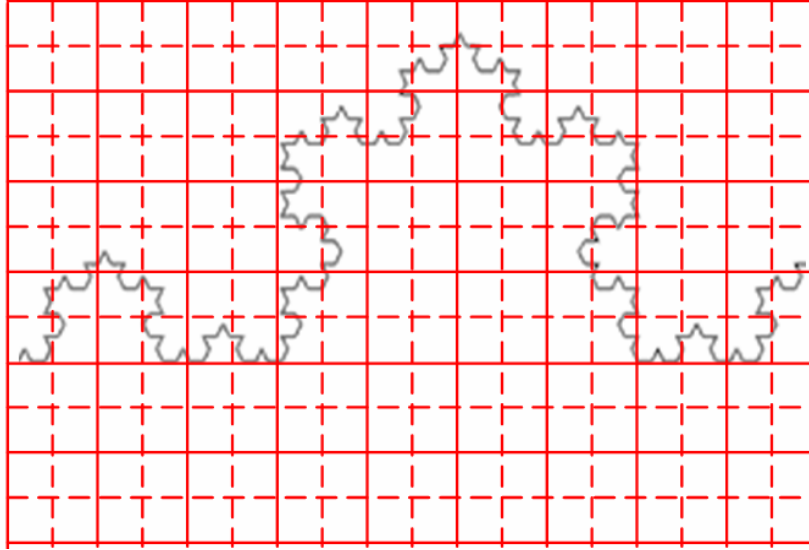


**Figure 7: Computing the fractal dimensionality of the von Koch fractal**

What is the box-counting dimensionality of the von Koch fractal? To compute this, we first note that the shape of the von Koch fractal can be correctly reproduced when the fractal is drawn on a 2-dimensional Euclidean space. (This 2-dimensional Euclidean space corresponds to the surface of a sheet of paper or the surface of an LCD computer monitor on which the fractal is displayed.) Consequently, we will need to construct a 2-dimensional square lattice to compute the fractal's box-counting dimensionality. Figure 7 shows a section of the von Koch fractal superimposed onto a square grid containing 54 squares with solid borders that have been subdivided into  $4 \times 54 = 216$  smaller squares with dashed borders. 18 of the larger squares are partially filled while 45 of the smaller squares are partially filled giving

$$D_{fractal} \cong D_{box-counting} \cong \frac{\ln[\eta[S, \varepsilon]] - \ln[\eta[S, 2\varepsilon]]}{\ln[2]} \cong \frac{\ln[45] - \ln[18]}{\ln[2]} = 1.32, \quad (17)$$

which is close to the exact fractal dimensionality of  $2 \ln[2]/\ln[3] = 1.26...$ <sup>6</sup> This example illustrates that using finite-sized boxes (hypercubes) we can achieve good estimates of a space's fractal dimensionality.

Now let's apply the same procedure to find the box-counting dimensionality of the Sierpiński gasket. To compute this, we first note that the shape of the Sierpiński gasket can be correctly reproduced when it is drawn on a 2-dimensional flat surface. Consequently, we will need to construct a 2-dimensional square lattice to compute its box-counting dimensionality. Figure 8 shows a section of Sierpiński gasket superimposed onto a square grid containing 54 squares with solid borders that have been subdivided into  $4 \times 54 = 216$  smaller squares with dashed borders. 26 of the larger squares are partially filled while 73 of the smaller squares are partially filled giving

<sup>6</sup> Weisstein, Eric W. "Koch Snowflake." From *MathWorld*--A Wolfram Web Resource. <http://mathworld.wolfram.com/KochSnowflake.html>

$$D_{fractal} \cong D_{box-counting} \cong \frac{\ln[\eta[\mathbb{S}, \varepsilon]] - \ln[\eta[\mathbb{S}, 2\varepsilon]]}{\ln[2]} \cong \frac{\ln[73] - \ln[26]}{\ln[2]} = 1.55, \quad (18)$$

which is fairly close to the exact fractal dimensionality of  $\frac{\ln[3]}{\ln[2]} = 1.58\dots$ <sup>7</sup>. This example also illustrates that using finite-sized boxes (hypercubes) we can achieve good estimates of a space's fractal dimensionality.

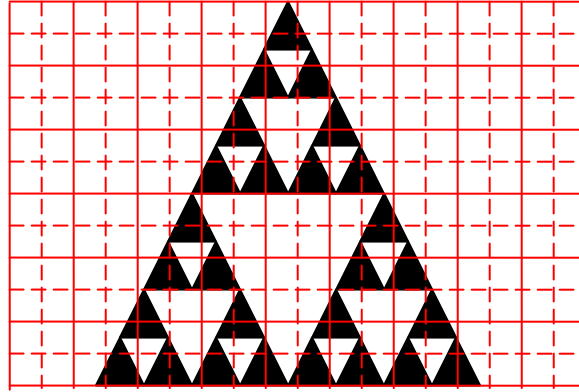


**Figure 8: Computing the fractal dimensionality of the Sierpiński gasket**

*Box counting is an extremely easy and useful way to estimate the fractal dimensionality. We first place a correctly shaped representation of the fractal inside a Euclidean space. We then construct hypercubic grids of different sizes in the Euclidean drawing space and count the number of hypercubes through which the fractal passes. This is used to compute the box-counting dimensionality via equation (16).*

The value of the box-counting dimensionality can depend upon the size of boxes because the fractal scaling displayed by an object can be different at different scales of magnification. Additionally, the box-counting dimensionality can be different for different regions within the same overall space.

#### 1.6.4 The Hausdorff Dimensionality

While the box-counting dimensionality is extremely useful and practical for real-world applications, it lacks the degree of rigor demanded by mathematicians. The Hausdorff dimensionality is a fractal dimensionality measure commonly used by mathematicians, but its definition is hard to understand:

“Formally, let  $\mathbf{A}$  be a subset of a metric space  $\mathbf{X}$ . Then the **Hausdorff dimension**  $\mathbf{D}[\mathbf{A}]$  of  $\mathbf{A}$  is the infimum of  $d \geq 0$  such that the  $d$ -dimensional Hausdorff measure of  $\mathbf{A}$  is 0 (which need not be an integer).”<sup>8</sup> “Let  $\mathbf{X}$  be a metric space,  $\mathbf{A}$  be a subset of  $\mathbf{X}$ , and  $\mathbf{d}$  a number  $\geq 0$ . The  $d$ -dimensional **Hausdorff measure** of  $\mathbf{A}$ ,  $\mathbf{H}^d[\mathbf{A}]$ , is the infimum of positive numbers  $\mathbf{y}$  such that for every  $r > 0$ ,  $\mathbf{A}$  can be covered by a countable family of closed sets, each of diameter less than  $\mathbf{r}$ , such that the sum of the  $d$ th powers of their diameters is less than  $\mathbf{y}$ . Note that  $\mathbf{H}^d[\mathbf{A}]$  may be infinite, and  $\mathbf{d}$  need not be an integer.”<sup>9</sup>

<sup>7</sup> Weisstein, Eric W. "Sierpinski Sieve." From *MathWorld*--A Wolfram Web Resource.

<http://mathworld.wolfram.com/SierpinskiSieve.html>

<sup>8</sup> Weisstein, Eric W. "Hausdorff Dimension." From *MathWorld*--A Wolfram Web Resource.

<http://mathworld.wolfram.com/HausdorffDimension.html>

<sup>9</sup> Weisstein, Eric W. "Hausdorff Measure." From *MathWorld*--A Wolfram Web Resource.

<http://mathworld.wolfram.com/HausdorffMeasure.html>

Can two topologically equivalent spaces with different distance metrics have different Hausdorff dimensionalities? This question needs further study. Consider pulling apart to infinite separation the two unjoined ends of the von Koch fractal to “stretch out” the fractal and form a straight line. If this stretching transformation is a homeomorphism then the von Koch fractal is topologically equivalent to a straight line. The Hausdorff dimensionality of the von Koch fractal is  $\ln[4]/\ln[3]$ , but the Hausdorff dimensionality of a straight line is 1. If the von Koch fractal and straight line are topologically equivalent, then the Hausdorff dimensionality is not topologically invariant.

### 1.6.5 Multiple Fractals and Nonfractals in the Same Space

A particularly important point is that a single space often embeds many different fractals simultaneously. Each of these fractals has its own fractal dimensionality. The fractal scaling of different fractals may be operational at either the same or different length scales. Because a space can simultaneously embed many fractals and many objects that are not fractals (‘nonfractals’), it is best to think of fractals as objects occurring in spaces rather than the space itself being fractal or not. In other words, think of a space as a container that holds fractals and/or nonfractals simultaneously. Accordingly, the question “Is physical space a fractal?” is ill-posed, because physical space contains a multitude of both fractals and nonfractals. Consider a very long piece of string. We could arrange the string in the shape of a random walk (a type of fractal) or in the shape of a function like  $f[x] = \sin[x]$  (a type of nonfractal). We could also superimpose these two curves to produce a string that behaves like the sum of a curve  $f[x] = \sin[x]$  and a random walk fractal. In this case, it is useless to say the string is a fractal or nonfractal because it includes both. We could even add more functions, both fractal and nonfractal, to the string to produce a superposition of many fractals and nonfractals. The string functions merely as a container to hold these fractals and nonfractals.

## **1.7 The Need for a New Type of Dimensionality Measure**

The topological dimensionality, manifold covering dimensionality, Euclidean covering dimensionality, and the mathematical dimensionality (where defined) are all overall properties of a space. They each assign a scalar value to the space as a whole. Our intuition tells us that the dimensionality of a space can change as a function of position. For example, in the space of Figure 4 part of the space is 1-dimensional and part of the space is 2-dimensional; however, none of the four dimensionality measures just mentioned are capable of describing these changes. It would be advantageous to have a dimensionality field that measures the number of independent directions as a function of location in space. Because the local number of independent directions depends only on a space’s connectivity and is independent of the method used to measure distances, such a dimensionality measure would be topologically invariant. I am not aware of any existing dimensionality measures that satisfy these basic criteria. The term ‘connectivity dimensionality field’ will be used, because a dimensionality measure of this type depends only on a space’s connectivity.

**Definition 9:** In a space, the **connectivity dimensionality field**  $N[\odot]$  is an effective and smooth measure of the number of linearly independent directions in the vicinity of location  $\odot$ .

The connectivity dimensionality field measures the *effective* number of independent directions passing through a local region of space. Consider the equation  $x \in \{\text{prime numbers}\}$ . We could represent the first prime number as  $P_1$ , the second prime number as  $P_2$ , and in general the  $i$ th prime number as  $P_i$  for  $i = 1, 2, \dots$ . Since  $i$  is not a continuous variable, the mathematical dimensionality is zero and the quartropy is infinite for the set of prime numbers. Intuitively, we think of the set of prime numbers as being located at points on a 1-dimensional number line with smaller prime numbers on the

left and larger prime numbers to the right. When scanning through the set of prime numbers from smaller to higher values we think of traveling along a direction. Since all prime numbers are located along this one direction, we can think of the set of prime numbers as being effectively one-dimensional. We can represent each prime number by a vertex and connect two vertices with an edge if the corresponding prime numbers are adjacent (e.g. the prime number 11 is adjacent to the prime numbers 7 and 13). Because this graph is a linear vertex-labeled graph, the set of prime numbers has a connectivity dimensionality of one.

The connectivity dimensionality field of a manifold is a nonnegative integer equal to the manifold's topological dimensionality. Thus, a circle has a connectivity dimensionality equal to 1, while a sphere has a connectivity dimensionality equal to two. An n-dimensional Euclidean space has a connectivity dimensionality equal to n.

The following example illustrates a key difference between the fractal and connectivity dimensionalities. Consider an arbitrarily thin sheet of paper. Suppose the paper is initially lying flat, but then we slightly crumple it. If the paper is only slightly crumpled, no points will be touching in the crumpled paper that were not touching in the flat paper. On the other hand, if we wadded the paper into a ball, points will be touching in the wadded ball that were not touching in the flat paper. The connectivity of the slightly crumpled paper is the same as the flat paper, but the wadded paper has a different connectivity than the flat paper. It follows that the connectivity dimensionality field of the flat versus slightly crumpled paper is the same, while the connectivity dimensionality field of the wadded paper is different. Since the addition of new connections increases the number of independent directions one can move along the paper, the process of wadding increases the connectivity dimensionality field of the paper. In the extreme case, when the paper is tightly wadded into a ball, the connectivity dimensionality field of the paper approaches 3. The fractal dimensionality is a measure of the crumpledness of the paper. The wadded paper has the highest fractal dimensionality while the flat paper has the lowest fractal dimensionality. The fractal dimensionality of the slightly crumpled paper is larger than for the flat paper and lower than for the wadded paper. Although the fractal dimensionality and connectivity dimensionality of the flat paper are equal, the fractal dimensionality of the slightly crumpled paper is necessarily higher than its connectivity dimensionality.

## 2. THE CONNECTIVITY DIMENSIONALITY FIELD DEFINED

### 2.1 Hyperspheres

In Euclidean spaces, a hypersphere is a collection of all points the same distance from a central point. A hypersphere in two-dimensional Euclidean space is a circle whereas a hypersphere in three-dimensional Euclidean space is an ordinary sphere. The equation for a hypersphere of radius R centered about the point  $(y_1, y_2, \dots, y_n)$  is

$$\sum_{i=1}^n (x_i - y_i)^2 = R^2. \quad (19)$$

The hypersphere of radius R in Euclidean n-space has an enclosed hypervolume and hyperarea (Sommerville, 1958) of

$$V[n, R] = \frac{2 \cdot \pi^{n/2}}{n \cdot \Gamma[n/2]} \cdot R^n \quad (20)$$

and

$$S[n, R] = \frac{dV[n, R]}{dR} = \frac{2 \cdot \pi^{n/2}}{\Gamma[n/2]} \cdot R^{n-1}. \quad (21)$$

Suppose we have two hyperspheres of radius  $R_1$  and  $R_2$ . The ratio of their hypervolumes is

$$\frac{V_2}{V_1} = \frac{V[n, R_2]}{V[n, R_1]} = \left(\frac{R_2}{R_1}\right)^n. \quad (22)$$

Taking the logarithm of both sides, we obtain

$$n = \frac{\ln[V_2] - \ln[V_1]}{\ln[R_2] - \ln[R_1]}. \quad (23)$$

Using equation (23), we can compute the dimensionality  $n$  for a space by comparing the hypervolumes enclosed in hyperspheres of different radii. This method for computing dimensionality is superior to counting independent variables because it applies equally well to spaces of noninteger dimensionality. For example, in a 2.5-dimensional space, the enclosed hypervolume of a hypersphere scales as  $R^{2.5}$ .

One drawback of equations (20) - (23) is that they apply only to homogeneous and isotropic spaces having constant dimensionality, density, and metric. The following sections consider the problem of how to compute the dimensionality in spaces that are not necessarily homogeneous or isotropic and which may have variable dimensionality, density, and metric.

## 2.2 General Method for Computing the Connectivity Dimensionality

How can the connectivity dimensionality field be generally defined and measured in a space? In particular, we need a general method that applies to both abstract or physical spaces and discrete, continuous, or discrete-continuous dual spaces. Recall that the connectivity dimensionality at a location  $\odot$  in space is a measure of the effective number of independent directions in a compact region of space enclosing  $\odot$ . Because the number of independent directions in a space depends only upon the connectivity of points in that space, the connectivity dimensionality depends only on adjacency relationships in the set of independent locations  $\{\odot\}$  comprising a space.

Consider a connected path  $\widehat{\Upsilon}$  between two locations  $x$  and  $y$  and a connected path  $\widehat{\Psi}$  between locations  $y$  and  $z$ .<sup>10</sup> Suppose we construct some travel progress measure  $\kappa$  along paths in the space. We require  $\kappa > 0$  for any path connecting different locations, while  $\kappa = 0$  for a single location. For a travel path  $\widehat{\Omega}$  from  $x$  to  $y$  along  $\widehat{\Upsilon}$  followed by  $y$  to  $z$  along  $\widehat{\Psi}$ , we have

$$\widehat{\Upsilon} = \widehat{xy}, \widehat{\Psi} = \widehat{yz}, \text{ and} \quad (24)$$

$$\widehat{\Omega} = \widehat{\Upsilon} + \widehat{\Psi} = \widehat{xyz}. \quad (25)$$

A travel progress measure  $\kappa$  satisfying the property

$$\kappa[\widehat{\Omega}] = \kappa[\widehat{\Upsilon}] + \kappa[\widehat{\Psi}]. \quad (26)$$

is said to be additive because the travel progress along a summed path equals the sum of travel progresses along the path parts. A travel progress measure  $\kappa$  satisfying the property

$$\kappa[\widehat{\Upsilon}] = \kappa[-\widehat{\Upsilon}] \quad (27)$$

is said to be reversible where  $-\widehat{\Upsilon}$  is the same path of travel as  $\widehat{\Upsilon}$  except that the direction of travel has been reversed.

For a reversible, additive travel progress measure  $\kappa$ , we define the invariant distance function  $d_\kappa[x, y]$  between two locations  $x$  and  $y$  in the space as the minimum travel progress for a path connecting  $x$  and  $y$ :

$$d_\kappa[x, y] = \min \left\{ \kappa[\widehat{xy}] \right\}. \quad (28)$$

<sup>10</sup> We use the symbol  $\widehat{\phantom{x}}$  to denote a path.  $\widehat{\Upsilon} = \widehat{xy}$  denotes a path that starts at  $x$  and ends at  $y$ .  $\widehat{\Omega} = \widehat{xyz}$  denotes a path that starts at  $x$ , passes through  $y$ , and ends at  $z$ .

(The invariant distance  $d_\kappa[x, y]$  is the distance along a shortest path connecting  $x$  to  $y$ .) This distance function satisfies several basic properties. First, the distance between a location and itself is zero:  $d_\kappa[x, x] = 0$ . Second, the distance from any location to a different location is positive:  $d_\kappa[x, y] > 0$  if  $x \neq y$ . Third, the distance from location  $x$  to  $y$  is the same as the distance from location  $y$  to  $x$ :  $d_\kappa[x, y] = d_\kappa[y, x]$ . For any location  $q$  on a shortest path from  $x$  to  $y$ , we have  $d_\kappa[x, y] = d_\kappa[x, q] + d_\kappa[q, y]$ . On the other hand, if  $q$  is not on a shortest path from  $x$  to  $y$ , we have  $d_\kappa[x, y] < d_\kappa[x, q] + d_\kappa[q, y]$ .

Suppose that we construct some function  $\Gamma[\mathcal{R}]$  that is an additive property of the independent locations contained within the region  $\mathcal{R}$ . This means that  $\Gamma[\mathcal{R}] = \Gamma[\mathcal{R}_A] + \Gamma[\mathcal{R}_B]$  where the region  $\mathcal{R}$  can be subdivided into two nonoverlapping regions  $\mathcal{R}_A$  and  $\mathcal{R}_B$  (i.e.  $\mathcal{R}_A \cup \mathcal{R}_B = \mathcal{R}$  and  $\mathcal{R}_A \cap \mathcal{R}_B = \emptyset$ ). Suppose we further require that for any region  $\Gamma[\mathcal{R}]$  be a positive real number:

$$\Gamma[\mathcal{R}] > 0 \text{ if } \mathcal{R} \neq \emptyset. \quad (29)$$

A measure  $\Gamma[\mathcal{R}]$  of this type is called a **nonnegative extensive property**.

**Definition 10:** A **nonnegative extensive property** is a property that is zero for the null set, positive for any region of space with positive hypervolume, and for which the property value of the union of two nonintersecting regions equals the sum of property values for those two regions.

We can choose some region  $\mathcal{B}_\lambda$  around a desired location  $x$  as the set of all locations  $y$  for which  $d_\kappa[x, y] \leq \lambda$ :

$$\mathcal{B}_\lambda = \{y; d_\kappa[x, y] \leq \lambda\}. \quad (30)$$

If the properties of the space are identical at all locations within this enclosed region, then since  $\Gamma[\mathcal{B}_\lambda]$  is an extensive property it scales proportional to  $\lambda^N$  where  $N$  is the dimensionality at locations within region  $\mathcal{B}_\lambda$ . Alas life cannot be so simple, for the properties of the space may vary as functions of position within the region  $\mathcal{B}_\lambda$ . We now have a formidable challenge on our hands. Namely, how can we develop a general method for computing the connectivity dimensionality when we don't know how in particular the properties of the space may vary as functions of location?

If the functions  $d_\kappa[x, y]$  and  $\Gamma[\mathcal{B}_\lambda]$  were smooth and differentiable, we could try to determine the scaling of  $\Gamma[\mathcal{B}_\lambda]$  as  $\lambda$  approaches a differentially small positive number. This would allow us to estimate the dimensionality  $N$  for a differentially small region of the space. However, for many types of spaces the functions  $d_\kappa[x, y]$  and  $\Gamma[\mathcal{B}_\lambda]$  are not smooth or differentiable. To meet this challenge, we asymptotically match the distance measure  $d_\kappa[x, y]$  and the extensive property  $\Gamma[\mathcal{B}_\lambda]$  of the space to smooth functions. We shall use the brackets  $\llbracket \ ]$  to denote asymptotic matching; the brackets  $\llbracket \ ]_E$  will denote an average over some ensemble  $E$ ; the brackets  $\langle \ \rangle$  will denote the expectation value; the brackets  $\{ \}$  will enclose a set, the brackets  $[ \ ]$  will enclose the argument of a function; and the parentheses  $( \ )$  will enclose algebraic terms in a product, sum, array, or exponent. To asymptotically



match some function  $F$  to the smooth function  $\lfloor F \rfloor$ , we choose a smooth well-behaved function  $\lfloor F \rfloor$  continuously differentiable such that the rms difference  $(\lfloor F \rfloor - F)^2$  is small. For nonnegative extensive properties like  $\Gamma[\mathcal{R}_\lambda]$ , the rms deviation  $\left\langle \sqrt{(\lfloor \Gamma \rfloor - \Gamma)^2} \right\rangle$  usually grows much slower than the value of the extensive property itself as the size of the region  $\mathcal{R}_\lambda$  increases.

Let  $\widehat{P}_x$  be a point asymptotically matched to location  $x$ . Let  $\mathcal{L}[\lambda, \widehat{P}_x]$  be a smooth extensive continuous function that is asymptotically matched to the extensive property  $\Gamma[\mathcal{R}_\lambda]$ :

$$\mathcal{L}[\lambda, \widehat{P}_x] = \lfloor \Gamma[\mathcal{R}_\lambda] \rfloor. \quad (31)$$

In practice, the extensive property  $\Gamma[\mathcal{R}_\lambda]$  is evaluated at a subset of discrete values  $\{\lambda_i\}$  of the continuous parameter  $\{\lambda\}$ , where  $i=1,2,3,\dots$ . To perform the asymptotic matching, a smooth curve is fit to the data  $\{(\lambda_i, \Gamma[\mathcal{R}_{\lambda_i}])\}$ . In general, we can associate with the extensive function  $\mathcal{L}[\lambda, \widehat{P}_x]$  the density  $\rho_{\mathcal{L}}[\lambda, \widehat{P}_x]$  such that  $\mathcal{L}[\lambda, \widehat{P}_x]$  equals  $\rho_{\mathcal{L}}[\lambda, \widehat{P}_x]$  times the number of independent locations  $\Upsilon[\lambda, \widehat{P}_x]$  contained in the region of interest:

$$\Upsilon[\lambda, \widehat{P}_x] = \mathcal{L}[\lambda, \widehat{P}_x] / \rho_{\mathcal{L}}[\lambda, \widehat{P}_x]. \quad (32)$$

Suppose the connectivity dimensionality is not constant within the space of interest. Note that

$$\left\| N[\lambda, \widehat{P}_x] \right\|_{\mathcal{S}} = \frac{d \ln \left[ \Upsilon[\lambda, \widehat{P}_x] \right]}{d \ln [\lambda]} = \frac{d \ln \left[ \mathcal{L}[\lambda, \widehat{P}_x] \right]}{d \ln [\lambda]} - \frac{d \ln \left[ \rho_{\mathcal{L}}[\lambda, \widehat{P}_x] \right]}{d \ln [\lambda]} \quad (33)$$

gives an asymptotically matched connectivity dimensionality averaged over the set  $\mathcal{S}$  of asymptotically matched locations a distance  $\lambda$  from  $\widehat{P}_x$ . Expanding the average connectivity dimensionality  $\left\| N[\lambda, \widehat{P}_x] \right\|_{\mathcal{S}}$  as a Taylor series in  $\lambda$  gives

$$\left\| N[\lambda, \widehat{P}_x] \right\|_{\mathcal{S}} = a_0[\widehat{P}_x] + a_1[\widehat{P}_x] \cdot \lambda + \frac{1}{2} a_2[\widehat{P}_x] \cdot \lambda^2 + \dots \quad (34)$$

Note that in the limit  $\lambda \rightarrow 0$ , the hypersurface  $\mathcal{S}$  becomes the point  $\widehat{P}_x$  and hence

$$\lim_{\lambda \rightarrow 0} \left\| N[\lambda, \widehat{P}_x] \right\|_{\mathcal{S}} = a_0[\widehat{P}_x] = N[\widehat{P}_x]. \quad (35)$$

Therefore the way to recover  $N[\widehat{P}_x]$  is by taking the limit

$$N[\widehat{P}_x] = \lim_{\lambda \rightarrow 0} \left\| N[\lambda, \widehat{P}_x] \right\|_{\mathcal{S}} = \lim_{\lambda \rightarrow 0} \frac{d \ln \left[ \Upsilon[\lambda, \widehat{P}_x] \right]}{d \ln [\lambda]}. \quad (36)$$

For an arbitrary point  $\widehat{P}$  this gives

$$N[\widehat{P}] = \lim_{\lambda \rightarrow 0} \left\| N[\lambda, \widehat{P}] \right\|_{\mathcal{S}} = \lim_{\lambda \rightarrow 0} \frac{d \ln \left[ \Upsilon[\lambda, \widehat{P}] \right]}{d \ln [\lambda]}. \quad (37)$$

Equation (37) gives the general method for determining the connectivity dimensionality field in spaces. This definition is completely based on first-principle scaling arguments. Because the connectivity dimensionality field is obtained by asymptotic matching to continuous smooth functions, the connectivity dimensionality field is a continuous and differentiable function of position.

Let's review the basic criteria that a space must satisfy in order to have a connectivity dimensionality field. First, the space must contain at least one location and some adjacency relationships between locations in the space.<sup>11</sup> Second, it must be possible to define an additive invariant distance function  $\mathcal{A}_g[x, y]$  and nonnegative extensive property  $\Gamma[\mathcal{R}]$  for the space. Third, it must be possible to asymptotically match  $\Gamma[\mathcal{R}_\lambda]$  to a smooth, continuously differentiable function  $\mathcal{L}[\lambda, \widehat{P}_x]$ . Fourth, we

must be able to determine the relationship between the extensive property  $\mathcal{L}[\lambda, \widehat{P}_x]$  and the number of independent locations  $\Upsilon[\lambda, \widehat{P}_x]$ . Fifth, the limit  $N[\widehat{P}] = \lim_{\lambda \rightarrow 0} \frac{d \ln[\Upsilon[\lambda, \widehat{P}]]}{d \ln[\lambda]}$  must exist and be reasonably well defined.<sup>12</sup> For any space that satisfies these criteria, we can compute the connectivity dimensionality field.

### 2.3 The Connectivity Dimensionality Field is Nonnegative and Real-valued

#### Theorem 3:

The connectivity dimensionality field is everywhere nonnegative and real-valued.

#### Proof:

1. The connectivity dimensionality is provided by the above definition:

$$N[\widehat{P}] = \lim_{\lambda \rightarrow 0} \frac{d \ln[\Upsilon[\lambda, \widehat{P}]]}{d \ln[\lambda]} \text{ where } \Upsilon[\lambda, \widehat{P}_x] \text{ is a nonnegative extensive real property and } \lambda \text{ is a continuous nonnegative real parameter.}$$

$$2. \text{ Expand: } \frac{d \ln[\Upsilon[\lambda, \widehat{P}_x]]}{d \ln[\lambda]} = \frac{\lambda}{\Upsilon[\lambda, \widehat{P}_x]} \frac{d[\Upsilon[\lambda, \widehat{P}_x]]}{d[\lambda]}.$$

3. Since  $\Upsilon[\lambda, \widehat{P}_x]$  is a nonnegative real property and  $\lambda$  is nonnegative, it follows that

$$\frac{\lambda}{\Upsilon[\lambda, \widehat{P}_x]} \geq 0.$$

4. Consider the definition of derivative:  $\frac{d[\Upsilon[\lambda, \widehat{P}_x]]}{d[\lambda]} = \lim_{|\varepsilon| \rightarrow 0} \frac{\Upsilon[\lambda + |\varepsilon|, \widehat{P}_x] - \Upsilon[\lambda, \widehat{P}_x]}{|\varepsilon|}$ . Since

$$\Upsilon \text{ is an extensive property, } \Upsilon[\lambda + |\varepsilon|, \widehat{P}_x] - \Upsilon[\lambda, \widehat{P}_x] = \Upsilon[\mathcal{R}_{\lambda+|\varepsilon|} - \mathcal{R}_\lambda] = \Upsilon[\Delta \mathcal{R}].$$

Clearly  $\mathcal{R}_{\lambda+|\varepsilon|}$  includes  $\mathcal{R}_\lambda$  so  $\Delta \mathcal{R}$  is a well-posed region. Since  $\Upsilon$  is a nonnegative

<sup>11</sup> Please keep in mind the distinction between points and locations. In general, a point is a location of infinitesimally small size. For example: New York is a location, but New York is not a point.

<sup>12</sup> Here, "reasonably well defined" means defined but may include some uncertainty.

extensive property:  $\Upsilon[\Delta(\mathcal{R})] \geq 0$ . Since  $|\varepsilon| > 0$ , we have

$$\frac{d[\Upsilon[\lambda, \widehat{P}_x]]}{d[\lambda]} = \lim_{|\varepsilon| \rightarrow 0} \frac{\Upsilon[\lambda + |\varepsilon|, \widehat{P}_x] - \Upsilon[\lambda, \widehat{P}_x]}{|\varepsilon|} \geq 0.$$

5. Putting # 3 and #4 back into #2 gives:  $\frac{d \ln[\Upsilon[\lambda, \widehat{P}_x]]}{d \ln[\lambda]} \geq 0$ . Putting this back into # 1 gives:

$$N[\widehat{P}_x] = \lim_{\lambda \rightarrow 0} \frac{d \ln[\Upsilon[\lambda, \widehat{P}_x]]}{d \ln[\lambda]} \geq 0. \text{ Thus it is proven the connectivity dimensionality field is everywhere nonnegative.}$$

6. In order for  $N[\widehat{P}] = \lim_{\lambda \rightarrow 0} \frac{d \ln[\Upsilon[\lambda, \widehat{P}]]}{d \ln[\lambda]}$  to be complex-valued either  $d \ln[\Upsilon[\lambda, \widehat{P}_x]]$  or  $d \ln[\lambda]$  must be complex-valued. Because  $\Upsilon[\lambda, \widehat{P}_x]$  is nonnegative and real, it follows that  $d \ln[\Upsilon[\lambda, \widehat{P}_x]]$  is also real. Because  $\lambda$  is nonnegative and real, it follows that  $d \ln[\lambda]$  is also real. Because both  $d \ln[\Upsilon[\lambda, \widehat{P}_x]]$  and  $d \ln[\lambda]$  are real-valued, it follows that

$$N[\widehat{P}_x] = \lim_{\lambda \rightarrow 0} \frac{d \ln[\Upsilon[\lambda, \widehat{P}_x]]}{d \ln[\lambda]} \geq 0 \text{ is also real-valued.}$$

7. From # 5 and # 6, it follows that the connectivity dimensionality field is everywhere nonnegative and real-valued.

## 2.4 The Connectivity Distance, Connectivity Radius, and Count Function

To compute the connectivity dimensionality fields of edge-vertex graphs, we must first select an appropriate invariant distance measure and an appropriate nonnegative extensive property. Because the connectivity dimensionality depends only on the connectivity of a space, the correct distance measure and nonnegative extensive property must depend only on the graph's connectivity. In an edge-vertex graph, the distinguishable locations are the graph vertices. The proper distance function for computing the connectivity dimensionality of an edge-vertex graph is the connectivity distance function. The proper nonnegative extensive property for computing the connectivity dimensionality of an edge-vertex graph is the count function.

The **connectivity distance**, a commonly used distance measure in graph theory, is defined as the minimum number of edges for a path connecting two vertices  $x$  and  $y$  in an edge-vertex graph:

$$d_{\text{connectivity}}[x, y] = \text{minimum \# of edges for a path connecting vertices } x \text{ and } y. \quad (38)$$

Clearly, the connectivity distance also equals the minimum number of vertices minus one for a path connecting vertices  $x$  and  $y$ . The connectivity distance satisfies the four basis properties of a metric:

$$(1.) \quad d_{\text{connectivity}}[x, x] = 0, \quad (39)$$

$$(2.) \quad d_{\text{connectivity}}[x, y] + d_{\text{connectivity}}[y, z] \geq d_{\text{connectivity}}[x, z], \quad (40)$$

$$(3.) \quad d_{\text{connectivity}}[x, y] = d_{\text{connectivity}}[y, x], \quad (41)$$

$$(4.) \quad d_{\text{connectivity}}[x, y] > 0 \text{ for } x \neq y. \quad (42)$$

Moreover, the connectivity distance is an additive distance measure:

$$d_{\text{connectivity}}[x, y] + d_{\text{connectivity}}[y, z] = d_{\text{connectivity}}[x, z] \quad (43)$$

for any vertex  $y$  on a shortest connectivity path from  $x$  to  $z$ .

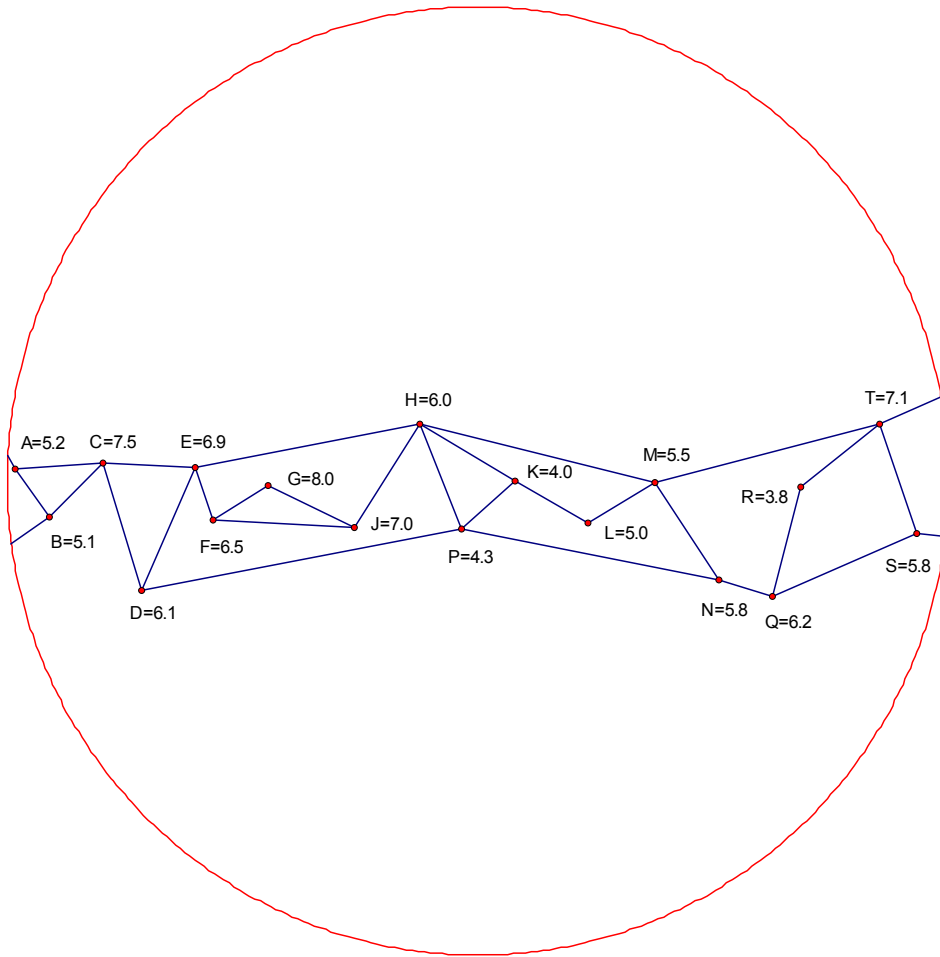


**Figure 9: Vertex-labeled graph used to illustrate the connectivity distance function**

*As explained in section 5.3, the vertex P in this graph has a connectivity dimensionality of about 1.5.*

**Example 1:** What is the connectivity distance between vertices **A** and **S** in the graph of Figure 9? What are the shortest paths associated with this distance?

**Hint:** In order to solve this problem, we need to try various possible routes between vertices **A** and **S** and find the shortest paths.

**Solution:** It is easy to see that there are two shortest paths (ACEHMTS and ACDPNQS) which are six edges long, so the connectivity distance is 6.

**Example 2:** What is the connectivity distance between vertices **C** and **Q** in the graph of Figure 9? What are the shortest paths associated with this distance?

**Solution:** It is easy to see that there is one shortest path (CDPNQ) which is four edges long, so the connectivity distance is 4.

The most common measure of hypervolume for a region of space in an edge-vertex graph is to simply count the number of vertices contained in that region. This count function is a nonnegative extensive property.

**Definition 11:** The **count function**  $\text{Count}[\mathcal{R}]$  is defined as the number of vertices contained in region  $\mathcal{R}$ .

**Definition 12:** The **connectivity radius** is a radius-like quantity based on the connectivity distance. The connectivity radius is used to specify a collection of positions that are the same connectivity distance away from a chosen position. The connectivity radius can take on the value of any nonnegative real number.

The count function  $C[\zeta, \mathbf{A}]$  for a **connectivity radius**  $\zeta$  about the vertex  $\mathbf{A}$  is defined as

$$C[\zeta, \mathbf{A}] = \sum_{\mathbf{B}} \text{if} \left[ d_{\text{connectivity}}[\mathbf{A}, \mathbf{B}] \leq \zeta \right], \quad (44)$$

where the sum is carried out over all vertices in the graph and the  $\text{if}[\_]$  function has a value of 1 if its argument is true and a value of 0 if its argument is false. The count function  $C[\zeta, \mathbf{A}]$  is simply the number of vertices contained in a region of space whose connectivity distance from vertex  $\mathbf{A}$  is less than or equal to  $\zeta$ .

Whereas the count functions  $\text{Count}[\mathcal{R}]$  and  $C[\zeta, \mathbf{A}]$  are discrete functions, we can asymptotically match them to continuous functions of continuous positions. Let  $\{\widehat{P}\}$  be a set of continuously interpolated points in the matched continuous space  $\mathcal{C}$ . Each vertex in the discrete space  $\mathcal{D}$  has unit hypervolume and is asymptotically matched to a unit hypervolume region of continuous points in the continuous space  $\mathcal{C}$ . For a vertex  $\mathbf{A}$  residing in  $\mathcal{D}$ , let the matched region of unit hypervolume in  $\mathcal{C}$  be called the **elementary vertexal compartment** for vertex  $\mathbf{A}$ . In all discrete-continuous dual spaces, each vertex in  $\mathcal{D}$  has an associated elementary vertexal compartment in the matched continuous space  $\mathcal{C}$ . For an asymptotically discrete-continuous dual space, there exists at least one pair of adjacent vertices in the discrete graph that gives rise to nonadjacent elementary vertexal compartments in the continuous space. For a strictly discrete-continuous dual space, every pair of adjacent vertices in the discrete graph gives rise to adjacent elementary vertexal compartments in the continuous space.

Let  $\widehat{a}$  be any point within the elementary vertexal compartment for vertex  $\mathbf{A}$ , then let us define a differentiable asymptotically matched continuous function  $\mathcal{F}_{\text{vertexal}}[\zeta, \widehat{a}]$  for a connectivity radius of  $\zeta$  about the continuous point  $\widehat{a}$ :

$$\mathcal{F}_{\text{vertexal}}[\zeta, \widehat{a}] = \left\lfloor C[\zeta, \mathbf{A}] \right\rfloor. \quad (45)$$

For a connectivity distance  $\zeta = 0$ , we have

$$C[\zeta = 0, \mathbf{A}] = 1 \quad (46)$$

because the only vertex located at zero connectivity distance from vertex  $\mathbf{A}$  is the vertex  $\mathbf{A}$  itself. On the other hand, since the continuous space contains an infinite number of continuous positions in the elementary vertexal compartment for  $\mathbf{A}$ , the probability of randomly selecting  $\widehat{a}$  to be the vertex  $\mathbf{A}$  is zero unless the space consists of the single point  $\mathbf{A}$ . Since the distance between vertex  $\mathbf{A}$  and any other point in the set of continuous positions  $\{\widehat{P}\}$  is positive definite, we have no vertices within zero connectivity radius of the randomly selected continuous position  $\widehat{a}$ :

$$\mathcal{F}_{\text{vertexal}} \left[ \zeta = 0, \widehat{a} \right] = 0 \quad (47)$$

unless the entire space consists of the single point  $\mathbf{A}$  in which case  $\widehat{a} = \mathbf{A}$  and  $\mathcal{F}_{\text{vertexal}} \left[ \zeta = 0, \widehat{a} \right] = 1$ .

**Table 1** below shows the correspondence between the functions for a generic space and those functions specifically adapted to edge-vertex graphs. Of particular interest, the independent locations in an edge-vertex graph are the vertices. Since the count function is the number of vertices, this gives rise to a unit density of independent locations for the count function. For an edge-vertex graph, we use the connectivity radius  $\zeta$  to denote both a discrete distance radius and a smooth continuous distance radius.

For example,  $\zeta_i = \frac{1}{2}, \frac{3}{2}, \frac{5}{2}, \dots$  denotes a discrete distance radius while  $\zeta = \text{any nonnegative real number}$  represents the smoothed continuous distance radius.

**Table 1: Correspondence between generic and edge-vertex graph functions**

Generic Function	Graph Function	Comments
$d_{\kappa}[x, y]$	$d_{\text{connectivity}}[\mathbf{A}, \mathbf{B}]$	distance function
$\Gamma[\mathcal{R}]$	$\text{Count}[\mathcal{R}]$	nonnegative extensive property
$\lambda_i$	$\zeta_i$	discrete distance radius
$\lambda$	$\zeta$	smoothed continuous distance radius
$\Gamma[\mathcal{R}_{\lambda}]$	$C[\zeta, \mathbf{A}]$	nonnegative extensive property for a given distance radius
$\mathcal{L}[\lambda, \widehat{P}_x]$	$\mathcal{F}_{\text{vertexal}}[\zeta, \widehat{a}]$	asymptotically matched smooth nonnegative extensive property for a given distance radius
$\Upsilon[\lambda, \widehat{P}_x]$	$\mathcal{F}_{\text{vertexal}}[\zeta, \widehat{a}]$	number of independent locations contained within a given distance radius
$\rho_{\mathcal{L}}[\lambda, \widehat{P}_x]$	1	density of independent locations

## 2.5 Efficient Computational Algorithms

A vertex-labeled graph is a set of information consisting of: (i.) a set of points called vertices (i.e. the vertices), (ii.) the connectivity (adjacency relationships) between those vertices in the form of line segments called edges, and (iii.) scalar values at those vertices. Suppose we select one of the vertices in the graph and call this vertex 1. Then, we select one of the vertices adjacent to vertex 1 and call this vertex 2. Then, we select one of the other vertices adjacent to either vertex 1 or 2 and call this vertex 3. Let this process be continued such that at each step we select a new vertex (i.e. one that has not been previously selected) adjacent to one of the previously selected vertices. For example, selecting vertex 10 requires us to find a vertex in the graph adjacent to at least one of the previously nine selected vertices, and such that vertex 10 has not been previously selected. This process is continued until all of the vertices in the graph have been selected and given an index. Next, we construct a table such that the vertex index is in the first column and the indices of the adjacent vertices are in the remaining columns. The adjacent vertices are listed with smaller indices appearing to the left of larger indices. Table 2 below gives a table representation of the graph of [Figure 9](#). Vertex scalar values can be stored in a second array (not shown).



**Table 2: A table representation of the edge-vertex graph shown in Figure 9**

1	2	3			
2	1	3			
3	1	2	4	5	
4	3	5	10		
5	3	4	6	8	
6	5	7	9		
7	6	9			
8	5	9	10	11	13
9	6	7	8		
10	4	8	11	14	
11	8	10	12		
12	11	13			
13	8	12	14	18	
14	10	13	15		
15	14	16	17		
16	15	18			
17	15	18			
18	13	16	17		

For this method of storing a graph, the memory requirements scale proportional to the number of vertices in the graph times the average number of edges per vertex. This storage algorithm also provides important advantages related to redrawing the graph. In order to draw the graph from the table, we start in the first row, draw the first vertex, and label its scalar value. Then we draw the second vertex, the edge between vertices 1 and 2, and label the scalar value of vertex 2. Then, we go to the third line of the table and identify the adjacent vertex with the lowest index (this will be either vertex 1 or 2), draw vertex 3 and the corresponding edge, and label the scalar value at vertex 3. In general, we continue this process going down the table row by row. At each row, we draw the new vertex, any edges connecting it to vertices of lower index (i.e. the vertices already drawn), and label its scalar value. The edges to higher index vertices (vertices not yet drawn) are not drawn; these edges are drawn later when the row corresponding to the higher index vertex is read and the edge becomes an edge to a vertex of lower index. In this manner, by reading down the table row by row, the graph can be drawn in a most efficient manner.

The table storage algorithm also has advantages when it comes to finding the vertices within a given distance of a chosen vertex. For example, suppose that we want to count how many vertices are within 10.5 edges of vertex 6. In order to compute this count function, we first construct a list. We put vertex 6 at the beginning of this list. Then, we go to table row 6 and read in the adjacent vertices. These are added to our list. Then, we go to the table rows corresponding to those vertices and read in all of their adjacent vertices and add these to the list (if they do not already appear in the list). Then, we go to the table row corresponding to each of those additional vertices, read in their adjacent vertices, and add these to the list (if they do not already appear in the list). In addition to listing the new vertices, at each step we keep track of the vertex from the previous step that led to the new vertex. (If there are multiple vertices in the previous step connected to the new vertex, we note any one of them and ignore the others.) This process is repeated a total of 10 times, to give the set of all vertices within a distance of 10.5 edges of vertex 6. The number of distinct vertices in the list is the count function  $C[\zeta, \mathbf{A}]$  for a distance of 10.5 edges around vertex 6.

We can find the shortest connectivity distance between any two vertices  $\mathbf{A}$  and  $\mathbf{B}$  in the graph using this method. First we start with vertex  $\mathbf{A}$  and using the above method we construct the list of vertices within a connectivity distance  $\zeta_i$  of vertex  $\mathbf{A}$  for  $\zeta_i = \frac{1}{2}, 1\frac{1}{2}, 2\frac{1}{2}, \dots$ . We stop this process as soon as vertex  $\mathbf{B}$  is reached, and the connectivity distance between  $\mathbf{A}$  and  $\mathbf{B}$  is the largest integer less than or equal

to  $\zeta_i$ . Furthermore, a path with the fewest number of edges between **A** and **B** is the sequence of adjacent vertices that led to the appearance of vertex **B** in the list. To find this sequence, we locate vertex **B** in the list and identify the vertex which generated it from the previous step. We then look up that vertex in the list and in turn identify the vertex that generated it from the prior step. This process is repeated until we arrive back at vertex **A**, and the sequence of vertices so identified is a path with the fewest edges connecting vertices **A** and **B**. (Although it may be possible for other paths to tie with this distance, none are shorter.)

**Example 3:** For the graph of Table 2, compute the connectivity distance from vertex 2 to 6 and the associated shortest path.

**Solution:**

- (1.) Go to row corresponding to vertex 2 and identify adjacent vertices 1(2) and 3(2). (The number in parentheses is the vertex that generated the new adjacent vertex.)
- (2.) Go to rows corresponding to vertices 1 and 3 and identify new adjacent vertices 4(3) and 5(3).
- (3.) Go to rows corresponding to vertices 4 and 5 and identify new adjacent vertices 10(4), 6(5), and 8(5).

Note that vertex 6 appears in the list at step 3. Hence the connectivity distance from vertex 2 to vertex 6 is 3. To find a shortest path we start with vertex 6 and work backwards: vertex 6 was generated by vertex 5 which was generated by vertex 3 which was generated by vertex 2. Hence, a shortest connectivity distance path is vertex 2  $\rightarrow$  vertex 3  $\rightarrow$  vertex 5  $\rightarrow$  vertex 6.

**Example 4:** For the graph of Table 2, compute the count function for a  $\zeta_i = 3.5$  neighborhood around vertex 2.

**Solution:** For a  $\zeta_i = 3.5$  neighborhood around vertex 2, the maximum connectivity distance is the largest integer less than or equal to 3.5. In example 1, we already computed the list of vertices within 3 edges of vertex 2. All we have to do is count the number of different vertices appearing in that list. From step 0, we have vertex 2. From step 1 we have vertices 1 and 3. From step 2 we have vertices 4 and 5. From step 3 we have vertices 6, 8, and 10. This gives a total count of 8 for a  $\zeta_i = 3.5$  neighborhood around vertex 2:  $C[3.5, \text{vertex \#2}] = 8$ .

The computational algorithms described in this section can be easily and efficiently programmed into computers. The algorithms for computing connectivity distance  $d_{\text{connectivity}}[\mathbf{A}, \mathbf{B}]$  and the count function  $C[\zeta, \mathbf{A}]$  both scale in polynomial time with respect to increasing connectivity distance as long as the count function itself scales polynomially in  $\zeta$ . This means the time required to compute these functions scales reasonably well as the connectivity radius increases.

### 3. DISCRETE-CONTINUOUS DUALITY

#### 3.1 Overview

Mathematics is one of the tools people use to describe different aspects of nature. Some aspects of nature are discrete while others are continuous. To describe discrete aspects of nature, we use discrete spaces. To describe continuous aspects of nature, we use continuous spaces.

**Definition 13:** A **continuous space** is a space in which positions can be varied differentially.

**Definition 14:** A **discrete space** is a space in which positions cannot be varied differentially.

For example, on my brief case are six dials. Each of the dials can be turned to display one of the numbers 0, 1, 2, 3, 4, 5, 6, 7, 8, or 9. Opening the brief case requires that all of the dials are turned to display the correct combination. Because each of the dials has ten choices, the total number of possible combinations is  $10^6 = 1$  million. The set of possible combinations is a purely discrete space. A discrete space is a space comprised of countable units. In this case, the countable units are the possible numbers for each dial.

Another example of a discrete space is the game of Yahtzee<sup>®</sup> discussed earlier. In this game, five indistinguishable dice are rolled to produce a set of numbers. With each roll of the five dice there are 117 possible outcomes. Another example of a discrete space is the set of telephone numbers. In each of these examples, positions cannot be varied differentially.

Now let us consider some examples of continuous spaces. The set of real numbers is a one-dimensional continuous space. The complex number plane is a two-dimensional continuous space. Another example of a continuous space is the surface of a perfect sphere. For each of these spaces, positions can be varied differentially.

At one time in history, scientists thought that every motion was either a particle or a wave. Scientists became confused when some motions displayed properties of both particles and waves. As soon as the scientists decided to call the motion a particle, that motion displayed wave properties. On the other hand, as soon as scientists decided to call the motion a wave, that motion displayed particle properties. Finally, scientists were forced to invent the concept of wave-particle duality. According to the notion of wave-particle duality, a motion can be both a particle and a wave; that is, the motion can be a wave-particle. Wave-particle duality has been beautifully and unequivocally demonstrated in a variety of multi-slit diffraction experiments even with large molecules (Nairz, *et al.* 2003).

In the early 20<sup>th</sup> century, Niels Bohr proposed that **complementarity** applies to physical systems exhibiting quantum mechanics.

**Definition 15: Complementarity** is “The concept that the underlying properties of entities (especially subatomic particles) may manifest themselves in contradictory forms at different times, depending on the conditions of observation; thus, any physical model of an entity exclusively in terms of one form or the other will be necessarily incomplete.” (American Heritage Science Dictionary, 2005)

The American Heritage Science Dictionary (2005) goes on to give the following example of complementarity: “For example, although a unified quantum mechanical understanding of such phenomena as light has been developed, light sometimes exhibits properties of waves and sometimes properties of particles (an example of wave-particle duality). See also uncertainty principle.”

One of the central themes of this paper is that complementarity also applies to special kinds of spaces which we shall call **discrete-continuous dual spaces**. The central idea of discrete-continuous duality is that the properties of some spaces may manifest themselves in contradictory forms at times depending on the conditions of observation. At times a particular space may manifest its discreteness while at other times that same space may manifest its continuity. Consequently, both a purely discrete and a purely continuous description of that space fall short of an adequate representation of its properties. To describe such spaces, one must consider simultaneously the discrete and continuous aspects of the space; that is, the properties of the space can be properly understood only by considering it a discrete-continuous dual entity.

Just as wave-particle duality produced a new way of looking at the physical world which could not be understood as a simple combination of particle and wave mechanics, so also discrete-continuous duality produces a new way of looking at the mathematical world which cannot be understood as a simple

combination of discrete and continuous mathematics. Wave-particle duality in the field of physics is known to be related to a momentum-position uncertainty principle first formulated by Werner Heisenberg around 1926. This article shows that discrete-continuous duality produces uncertainty principles governing the connectivity dimensionality field. In both physics and mathematics, these uncertainty principles arise from complementarity.

The opening of this section stated “*Some aspects of nature are discrete while others are continuous. To describe discrete aspects of nature, we use discrete spaces. To describe continuous aspects of nature, we use continuous spaces.*” Now we understand this paragraph should be revised to give “*Some aspects of nature are discrete, some aspects of nature are continuous, and some aspects of nature are discrete-continuous dual. To describe discrete aspects of nature, we use discrete spaces. To describe continuous aspects of nature, we use continuous spaces. To describe discrete-continuous dual aspects of nature we use discrete-continuous dual spaces. In **continuous spaces**, positions can be varied differentially. In **discrete spaces**, positions cannot be varied differentially. In **discrete-continuous dual spaces** there are two complementary representations: one in which positions can be varied differentially and one in which positions cannot be varied differentially.*”

As explained in the following sections, there are two basic types of discrete-continuous duality: (a.) strict discrete-continuous duality and (b.) asymptotic discrete-continuous duality. A comment on terminology may be in order. One speaks of *strict* or *asymptotic* discrete-continuous *duality*, but one speaks of *strictly* or *asymptotically* discrete-continuous *dual spaces*. In the first case, the adjectives *strict* and *asymptotic* modify the noun *duality*; in the second case, the adverbs *strictly* and *asymptotically* modify the adjective *dual*.

### 3.2 Strictly Discrete-Continuous Dual Space Defined

**Definition 16:** A strictly discrete-continuous dual space is defined as a set  $\{\mathcal{D}, \mathcal{C}\}$  containing a discrete space  $\mathcal{D}$  and a continuous space  $\mathcal{C}$  that satisfy the following properties:

1. Both  $\mathcal{D}$  and  $\mathcal{C}$  are connected spaces. (There exists a connected path from any location in  $\mathcal{D}$  to any other location in  $\mathcal{D}$  without leaving  $\mathcal{D}$ . There exists a connected path from any location in  $\mathcal{C}$  to any other location in  $\mathcal{C}$  without leaving  $\mathcal{C}$ .)
2. The discrete space  $\mathcal{D}$  can be represented by a set of compact continuous spaces that have been glued together. For example, if  $\mathcal{D}$  is representable by an edge-vertex graph, then the glued compact continuous spaces are the 1-dimensional edges.
3. The number of points per unit hypervolume in  $\mathcal{C}$  is infinite.
4. Each location in  $\mathcal{D}$  is matched to some corresponding location in  $\mathcal{C}$ .
5. There exists (at least one) discrete distance function in  $\mathcal{D}$  and a corresponding asymptotically matched continuous distance function in  $\mathcal{C}$ . Consequently, positions close together in  $\mathcal{D}$  have matched positions which are close together in  $\mathcal{C}$  and positions far apart in  $\mathcal{D}$  have matched positions which are far apart in  $\mathcal{C}$ .
6. The connectivity dimensionality is relatively well defined in  $\mathcal{D}$  and varies relatively smoothly throughout  $\mathcal{D}$ . The connectivity dimensionality is relatively well defined in  $\mathcal{C}$  and varies continuously and smoothly throughout  $\mathcal{C}$ . For each location in  $\mathcal{D}$  the connectivity dimensionality (over a scale larger than a discrete element) asymptotically matches the connectivity dimensionality (over a similar scale) of the corresponding location in  $\mathcal{C}$ . If present, compact dimensions in  $\mathcal{D}$  are asymptotically matched to compact dimensions in  $\mathcal{C}$ .

7.  $\mathbb{C}$  is a continuous Hausdorff space. (A Hausdorff space is a space with disjoint neighborhoods (Hausdorff 1914).)  $\mathbb{D}$  is large-world; that is,  $\mathbb{D}$  contains some positions which are very far apart.
8. The continuous space  $\mathbb{C}$  spans just enough space to incorporate all of the elements in  $\mathbb{D}$  and their continuously interpolated points. Consequently, hyperbubbles in  $\mathbb{D}$  larger than the scale of a discrete element have corresponding hyperbubbles in  $\mathbb{C}$ .<sup>13</sup> Regions in  $\mathbb{D}$  the size of a discrete element are filled in via interpolation to give populated regions in  $\mathbb{C}$  because matching a discrete space to a continuous space requires smoothing over the size of a discrete element.
9. All edges and other structural features in  $\mathbb{C}$  must be relatively smooth. This means each distinct structural feature in  $\mathbb{C}$  is asymptotically comprised of *many* discrete elements from  $\mathbb{D}$ .
10. Distinguishable elements not intersecting in  $\mathbb{D}$  do not intersect in  $\mathbb{C}$ ; distinguishable elements intersecting in  $\mathbb{D}$  also intersect in  $\mathbb{C}$ . This condition is equivalent to requiring that the discrete space  $\mathbb{D}$  can be properly drawn in the continuous space  $\mathbb{C}$ .

For obvious reasons, disconnected spaces and spaces without a defined connectivity dimensionality field cannot be discrete-continuous dual. Interestingly, all small-world networks cannot be discrete-continuous dual.

**Definition 17:** A **small-world network** is a network comprised of many vertices connected in such a way that the connectivity distance between any two vertices is small.

For example, there are about 6 billion people living on earth now. If one were to represent each person by a vertex and connect two vertices together if these people know each other, the result would be a small-world network (Travers and Milgram, 1969). Consider arbitrarily picking two of these six billion people. It is statistically likely that the first person would know someone who knows someone who knows someone who knows someone who knows the second person.

**Definition 18:** A **large-world network** is a network comprised of many vertices connected in such a way that the connectivity distance between most pairs of vertices is large.

Many large-world networks have either strict or asymptotic discrete-continuous duality.

### 3.3 Examples of Strictly Discrete-Continuous Dual Spaces

Crystal structures are a common example of strictly discrete-continuous dual spaces. The equilibrium positions of the atomic centers in a sodium chloride crystal form a cubic lattice. This lattice structure can be represented by a simple graph in which the vertices mark the (equilibrium) positions of the atomic centers. Two vertices in the graph are connected by an edge if the corresponding atoms are adjacent to each other in the crystal. The crystal exists in a continuous-like space. In particular, one can irradiate the crystal causing the atomic centers to vibrate. When the atomic centers vibrate, the connectivity of the associated simple graph is completely unchanged but the positions of the atoms in the associated continuous space does change. Moreover, a continuous beam of x-rays will diffract off of the crystals to produce an x-ray diffraction pattern. These x-rays are waves moving in a continuous-like space, yet the diffraction pattern they produce is because of the discrete structure of the lattice. To understand how radiation interacts with the crystal one must envision the crystal as composed of a discrete lattice

<sup>13</sup> Hyperbubbles are explained in section 5.6.

immersed in a continuous space. Neither a purely discrete nor a purely continuous representation of the crystal is adequate to explain its properties. Only by considering the crystal to be discrete-continuous dual can its fundamental properties be understood.

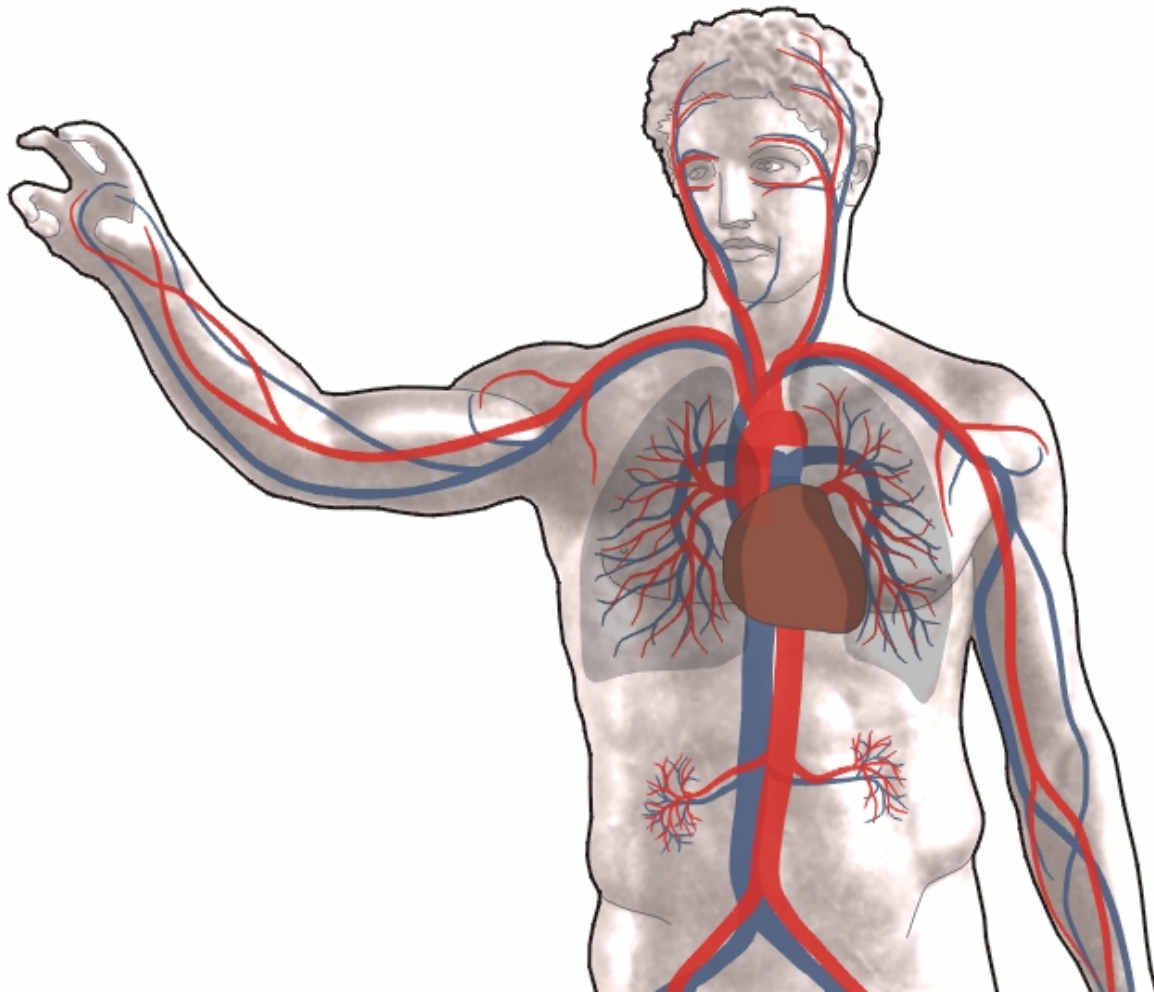


**Figure 10: The human circulatory system is an example of a strictly discrete-continuous dual network<sup>14</sup>**

Continuous spaces equipped with coordinate grids are another example of strictly discrete-continuous dual spaces. Graph paper (i.e. paper covered with a square grid of lines) is an example of a continuous space equipped with a coordinate grid. The continuous surface of the paper is the continuous space representation while the square grid of lines is the discrete representation. Together, the surface of the graph paper and the coordinate grid printed on it form a discrete-continuous dual space. Graph paper forms a strictly discrete-continuous dual network because (i) the grid lines can be properly drawn on the paper, (ii) the grid lines reach into every major part of the paper's surface, and (iii) the continuous surface of the paper strictly interpolates positions between the grid lines. It is easy to imagine what will happen upon removal of either the discrete or continuous representations. To remove the discrete representation, one erases the coordinate grid giving a blank sheet of paper. The grid lines allow sketches to be drawn to scale without using a ruler. Once the lines are erased, the graph paper ceases being graph paper and just becomes paper. We can also imagine what happens upon removal of the continuous space. To remove the continuous space, one cuts out all of the surface of the paper which isn't covered by the grid lines giving a

<sup>14</sup> This image was downloaded from <http://en.wikipedia.org/wiki/Image:Blutkreislauf.png> 12/22/06 and is licensed under the Creative Commons Attribution ShareAlike 2.5 License.



window-screen-like structure that contains many square holes. The resulting paper window screen is useless to draw sketches on. In summary, the graph paper can only perform its function by being a strictly discrete-continuous dual space composed of complementary discrete and continuous representations.

The human circulatory system can be approximately modeled by a discrete-continuous dual space. A 3-dimensional continuous space can be used to represent all of the living tissue in the body that consumes oxygen for survival. A discrete network of lines can be used to represent the central axes of the blood vessels such that two lines intersect where two blood vessels join; the discrete set of paths represents the set of blood vessels which transport blood throughout the body. In a strictly discrete-continuous dual space, the discrete set of paths is a subset of a corresponding continuous space and the discrete set of paths also extends into every significantly sized region of the corresponding continuous space. If the circulatory system of a person were not strictly discrete-continuous dual, then this means either: (1.) some of the person's tissue is not close to blood vessels and thus is not supplied oxygen by the circulatory system (i.e. the discrete network doesn't reach into all major areas of the continuous space) or (2.) some of the person's blood vessels stick out in the open and are not surrounded by a region of living tissue (i.e. the discrete set of paths is not a subset of the corresponding continuous space). In case (1.) some of the living tissue would die due to oxygen starvation and in case (2.) the exposed blood vessels would be in danger of being injured or ruptured which could lead to blood loss and death. Therefore, if a person's circulatory network were not strictly discrete-continuous dual some part of them would likely die. To avoid these problems, the blood vessels do not extend outside of the body and all living tissue in the body is nearby to a blood vessel, giving the human circulatory system a strictly discrete-continuous dual structure. The human circulatory system forms a strictly discrete-continuous dual space because this is the particular arrangement which is best suited for supplying oxygen and other nutrients to living tissues in large organisms, for removing metabolic by-products and wastes from those same tissues, and for protecting blood vessels from injury.

### 3.4 Asymptotically Discrete-Continuous Dual Space Defined

In an asymptotically discrete-continuous dual space, small (i.e. short-range) mismatches in connectivity are tolerated between the discrete space and the associated continuous space. Due to these short-range connectivity mismatches, the discrete space cannot be properly drawn in the associated continuous space it services.

**Definition 19:** An **asymptotically discrete-continuous dual space** is defined as a set  $\{\mathcal{D}, \mathcal{C}\}$  containing a discrete network  $\mathcal{D}$  and a continuous space  $\mathcal{C}$  that satisfy the following properties:

1. Both  $\mathcal{D}$  and  $\mathcal{C}$  are connected spaces. (There exists a connected path from any location in  $\mathcal{D}$  to any other location in  $\mathcal{D}$  without leaving  $\mathcal{D}$ . There exists a connected path from any location in  $\mathcal{C}$  to any other location in  $\mathcal{C}$  without leaving  $\mathcal{C}$ .)
2. The discrete space  $\mathcal{D}$  can be represented by a set of compact continuous spaces that have been glued together. For example, if  $\mathcal{D}$  is representable by an edge-vertex graph, then the glued compact continuous spaces are the 1-dimensional edges.
3. The number of points per unit hypervolume in  $\mathcal{C}$  is infinite.
4. Positions in  $\mathcal{D}$  are asymptotically matched to positions in  $\mathcal{C}$ .
5. There exists (at least one) discrete distance function in  $\mathcal{D}$  and a corresponding asymptotically matched continuous distance function in  $\mathcal{C}$ . Consequently, positions close together in  $\mathcal{D}$  have asymptotically matched positions which are close together in  $\mathcal{C}$  and positions far apart in  $\mathcal{D}$  have asymptotically matched positions which are far apart in  $\mathcal{C}$ .

6. The connectivity dimensionality is relatively well defined in  $\mathcal{D}$  and varies relatively smoothly throughout  $\mathcal{D}$ . The connectivity dimensionality is relatively well defined in  $\mathcal{C}$  and varies continuously and smoothly throughout  $\mathcal{C}$ . The connectivity dimensionality field of  $\mathcal{D}$  is asymptotically matched to the connectivity dimensionality field of  $\mathcal{C}$ . If present, compact dimensions in  $\mathcal{D}$  are asymptotically matched to compact dimensions in  $\mathcal{C}$ .
7.  $\mathcal{C}$  is a continuous Hausdorff space.  $\mathcal{D}$  is large-world; that is,  $\mathcal{D}$  contains some positions which are very far apart.
8. The asymptotically matched continuous space  $\mathcal{C}$  spans just enough space to incorporate all of the elements in  $\mathcal{D}$  and their continuously interpolated points. Consequently, hyperbubbles in  $\mathcal{D}$  much larger than the scale of a discrete element have corresponding hyperbubbles in  $\mathcal{C}$ . Regions in  $\mathcal{D}$  the size of a discrete element are filled in via interpolation to give populated regions in  $\mathcal{C}$ .
9. All edges and other structural features in  $\mathcal{C}$  must be relatively smooth. This means each distinct structural feature in  $\mathcal{C}$  is asymptotically comprised of *many* discrete elements from  $\mathcal{D}$ .
10. The discrete space  $\mathcal{D}$  cannot be properly drawn in the continuous space  $\mathcal{C}$ .

### 3.5 Example of an Asymptotically Discrete-Continuous Dual Space

Some types of supply networks naturally evolve into asymptotically discrete-continuous dual spaces. Modern society needs supply routes to function, and roads are an efficient means of transporting supplies. Thus, people will build roads to where they live and where they cannot build roads they will not build large cities. Some mountainous regions, deserts, and bodies of water do not contain any roads, and these same regions usually will not contain large cities.

The roads can be represented by a discrete network. The land and real estate where people can live and work can be represented as a continuous space. The real estate is approximately but not exactly two dimensional. In moderately populated regions where land is readily available, building vertically is more expensive than building horizontally and so the real estate is 2-dimensional. However, in densely populated regions land is scarce and building vertically becomes necessary; in this case the real estate is partly 3-dimensional. In extremely remote regions, the real estate may become one-dimensional where all buildings are located close to a principle highway that traverses otherwise barren land. The discrete network of roads together with the real estate form an asymptotically discrete-continuous dual space.

A map is a drawing or representation of this discrete-continuous dual space. (See Figure 11.) A closer analysis shows that there is a fundamental difference between the network of supply roads and the circulatory system of the human body. In the human body one does not find two nonintersecting veins or arteries which get projected onto the same point of the continuous space; that is, the discrete network can be properly drawn in the associated continuous space. However, in the case of roads, two nonintersecting roads can get projected onto the same point of the continuous space. This occurs where one road passes over the top of another road and there are no exit ramps from one road to the other. In this case, the one road must be drawn as a broken line to indicate it passes underneath the other road; however, the road itself does not have an actual break in it. Because the drawing shows the road as a broken line but the real road is not broken, the network of roads cannot be properly drawn on the 2-dimensional map. This is why the network of roads is asymptotically discrete-continuous dual and not strictly discrete-continuous dual.

Spaces with wormholes that that connect otherwise remote regions are not asymptotically or strictly discrete-continuous dual because the distance functions in the discrete and continuous representations are *grossly* mismatched when wormholes are present. For example, one would not expect to find a road from Ohio to California that was only 3 miles long when on a 2-dimensional atlas the shortest possible distance between them appears to be at least a thousand miles. (Such a shortcut would be a wormhole.) When two roads in an atlas appear to cross each other but don't intersect, one would expect to be able to find a

*reasonably short* path between the two roads. An asymptotically discrete-continuous dual network tolerates small (i.e. short-range) mismatches in connectivity between the discrete network and the associated continuous space. When these conditions are satisfied, distances in the continuous representation and discrete network are *approximately* matched and the network is asymptotically discrete-continuous dual.



**Figure 11: A system of roads is an example of an asymptotically discrete-continuous dual network<sup>15</sup>**  
*In an asymptotically discrete-continuous dual network, the discrete set of paths is not strictly a subset of the corresponding continuous space to which it is asymptotically matched. Distance functions in the discrete space and the corresponding asymptotically matched continuous space are approximately but not perfectly matched. An example of a mismatch between the system of roads (a discrete network) and the 2-dimensional map onto which they are projected (an asymptotically matched continuous space) is shown in the blue circle above where some of the roads appear to cross but there is no actual intersection of the roads. This is indicated on the map by drawing one road as an unbroken line passing through a broken representation of the other road. Roads which have direct intersections (as shown in the blue square) behave identically in the discrete network and the asymptotically matched continuous space. Roads which have short exit ramps connecting them (as shown by the blue arrow) are very closely but not exactly represented in the asymptotically matched continuous space. Since the mismatch is slight, the system of roads shown above is asymptotically discrete-continuous dual.*

### 3.6 Method for Determining Whether an Edge-Vertex Graph is Discrete-Continuous Dual

In this section, we consider the general problem of how to determine whether an edge-vertex graph is discrete-continuous dual. In this case, the discrete distance function chosen is the connectivity distance. The following procedure is suggested as a guide:

1. Check to see whether the edge-vertex graph is connected.
2. Check to see whether the graph is large-world (i.e. has many vertices far apart).

<sup>15</sup> The underlying map (Public Domain) showing a section of roads in Columbus, Ohio was obtained from the Tiger Map Server located at tiger.census.gov.

3. Check to see whether the graph has a relatively well-defined connectivity dimensionality field that varies relatively smoothly with position. (A method for computing the connectivity dimensionality field is presented later in this article.)
4. Check to see whether interpolation of positions forms an approximately smooth continuous Hausdorff space with an approximately smooth and well-defined connectivity dimensionality field asymptotically matching the connectivity dimensionality field of the graph. If there are any compact dimensions, make sure they are also asymptotically (or strictly) matched between the discrete and continuous spaces. (Specific procedures for discrete-continuous dual matching are presented later in this article.)
5. Check to see whether there are no wormhole edges. A wormhole edge connects two adjacent vertices in the graph that are asymptotically matched to remote (very far apart) locations in the matched continuous space. A space is not discrete-continuous dual if it has wormhole edges, because a wormhole edge indicates a gross mismatch in connectivity between the discrete and continuous spaces.
6. Check to see whether the graph can be properly drawn in the smooth, matched continuous space.
7. The space is strictly discrete-continuous dual iff. conditions 1-6 are satisfied.
8. Iff. conditions 1-5 are satisfied but not 6, the space is asymptotically discrete-continuous dual.
9. Iff. any of conditions 1-5 are not satisfied, the space is not discrete-continuous dual.

We can construct a false-crossing distribution by drawing the discrete space  $\mathcal{D}$  in the matched continuous space  $\mathcal{C}$ . A false crossing occurs when two edges in the drawing appear to cross but there is no actual vertex at the apparent crossing. Let  $P_k[\mathcal{D}, \mathcal{C}] \geq 0$  be the probability that an edge selected at random from the graph  $\mathcal{D}$  has  $k$  false crossings. Then,

$$\sum_{k=0}^{\infty} P_k[\mathcal{D}, \mathcal{C}] = 1. \quad (48)$$

If  $\mathcal{D}$  is strictly discrete-continuous dual to  $\mathcal{C}$ , then

$$P_k[\mathcal{D}, \mathcal{C}] = 0 \text{ for } k > 0 \text{ and } P_0[\mathcal{D}, \mathcal{C}] = 1. \quad (49)$$

If  $\mathcal{D}$  is asymptotically discrete-continuous dual to  $\mathcal{C}$ , then

$$P_k[\mathcal{D}, \mathcal{C}] = 0 \text{ for } k > \delta \quad (50)$$

where  $\delta$  is the maximum number of false crossings permitted for a edge. The moments of this distribution provide useful information. For example, the average number of false crossings per edge is given by the first moment:

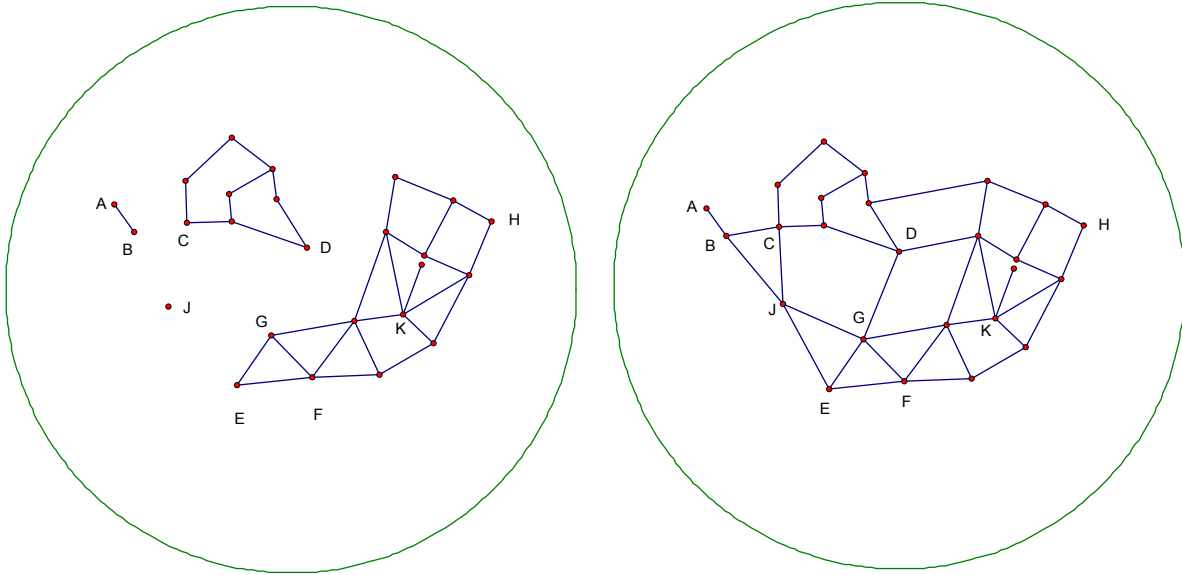
$$\llbracket k \rrbracket = \sum_{k=0}^{\infty} k (P_k[\mathcal{D}, \mathcal{C}]). \quad (51)$$

The average number of false crossings per edge for edges with at least one false crossing is given by

$$\llbracket f \rrbracket = \frac{\sum_{k=1}^{\infty} k (P_k[\mathcal{D}, \mathcal{C}])}{\sum_{k=1}^{\infty} P_k[\mathcal{D}, \mathcal{C}]} \quad (52)$$

The rms number of false crossings per edge is given by the square root of the second moment:

$$k_{rms} = \sqrt{\llbracket k^2 \rrbracket} = \sqrt{\sum_{k=0}^{\infty} k^2 (P_k[\mathcal{D}, \mathcal{C}])}. \quad (53)$$



(a.) unconnected

(b.) connected

**Figure 12: Examples of (a.) unconnected and (b.) connected graphs**

*For the unconnected graph on the left, there is no path between vertices A and F. For the connected graph on the right there is a path between all possible pairs of vertices.*

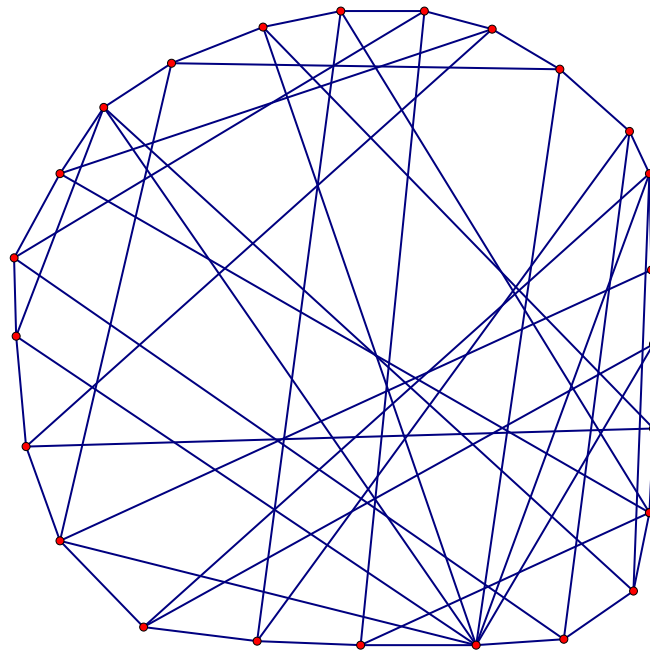


**Figure 13: A graph that is not discrete-continuous dual because it is small-world**

*Shown here is a small world graph. Notice that every pair of vertices is connected by a short path. Graphs of this type are not discrete-continuous dual.*

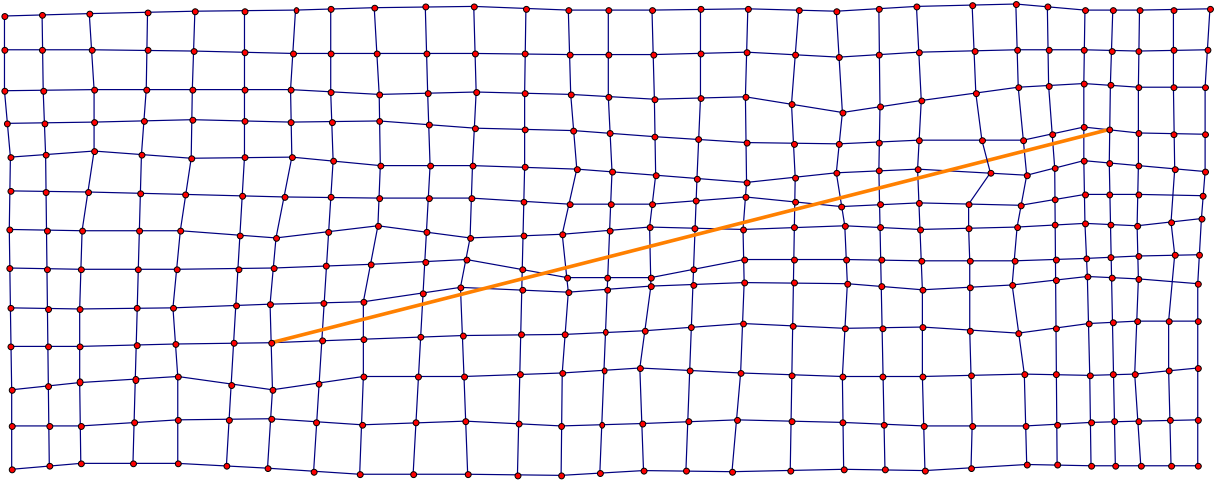


**Figure 14: Example of a worm-hole edge**

*Without the worm-hole edge (colored in orange), the discrete space (presumed to extend beyond the four edges shown) would be dual to a two-dimensional Euclidean space. The worm-hole edge provides a shortcut between otherwise remote positions, and this destroys the discrete-continuous duality.*

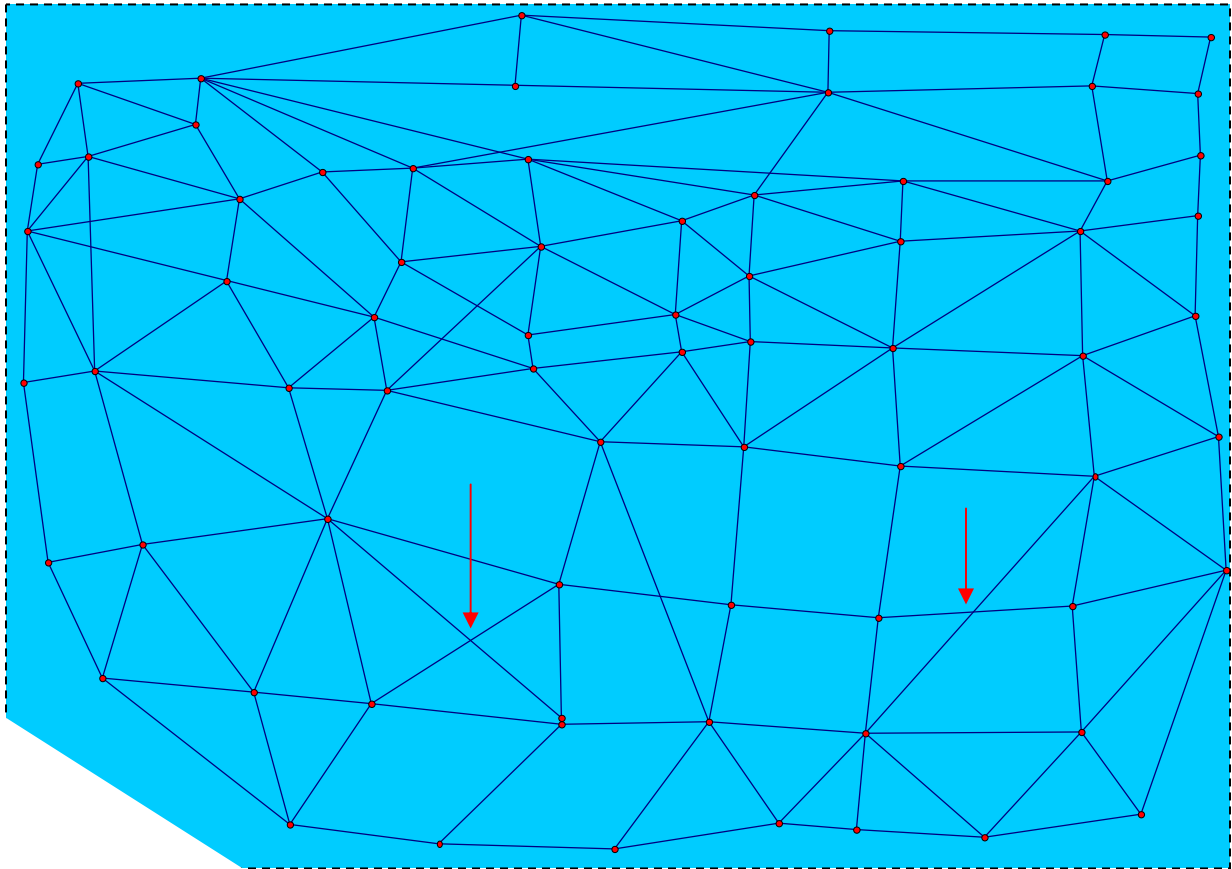


**Figure 15: Example of an asymptotically discrete-continuous dual graph**

*This graph is asymptotically discrete-continuous dual to the 2-dimensional continuous space colored in light blue. Near the red arrows some of the edges appear to cross where they actually do not cross; consequently, the graph cannot be properly drawn in the matched continuous space. Because there are no worm-hole edges connecting remote regions of the space to each other, distances in the graph can be asymptotically matched to those in the continuous space.*



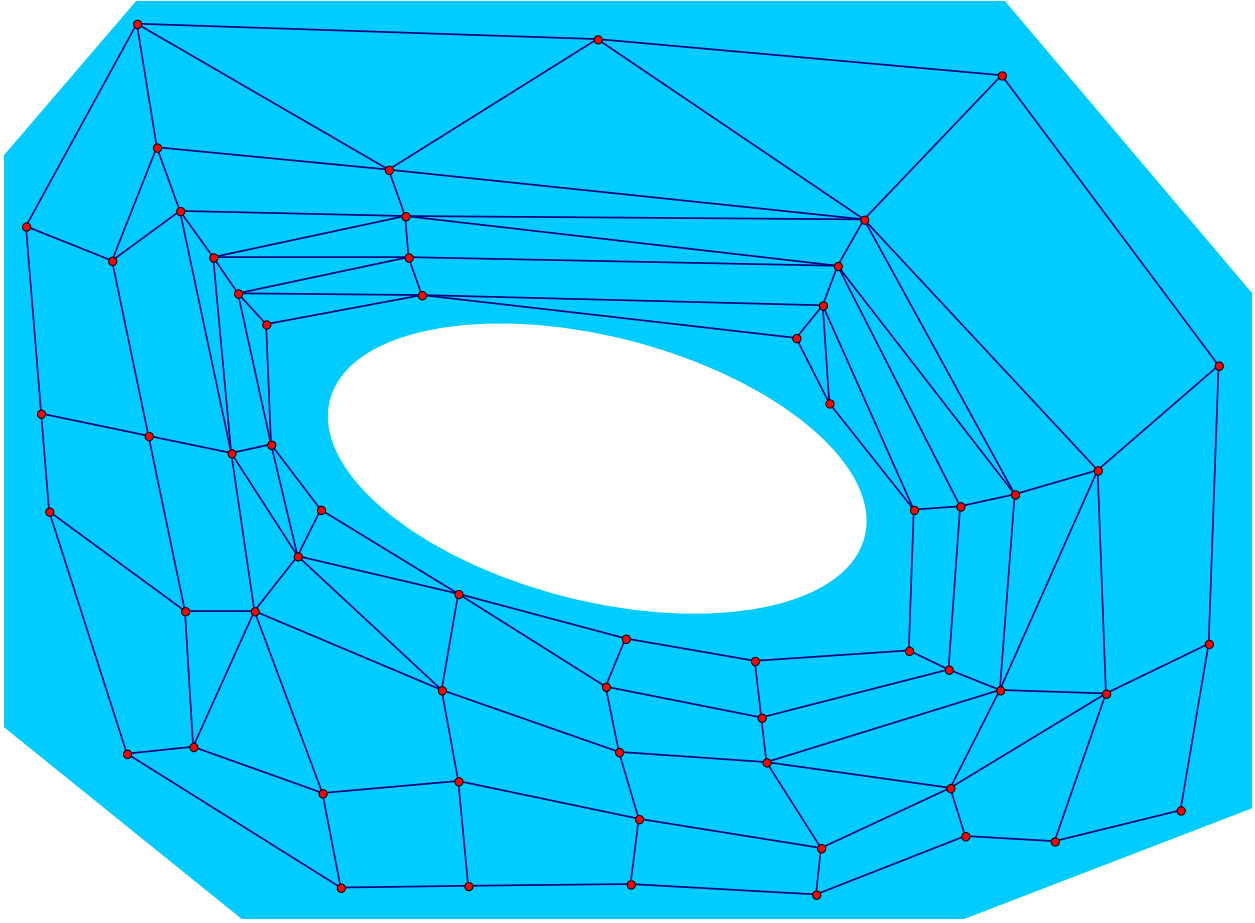


**Figure 16: Example of a strictly discrete-continuous dual graph**

*This graph is strictly discrete-continuous dual to the 2-dimensional continuous space colored in light blue containing a hole. Notice that the graph can be properly drawn in the matched continuous space.*

Consider the small-world network in Figure 13 above. A random sample of four edges gave the following number of false crossings: 16, 0, 6, and 11. The mean of these four values is 8.25 while the standard deviation is 6.85. The standard deviation of the mean can be approximated by:

$$\frac{\sigma}{\sqrt{n-1}} = \frac{6.85}{\sqrt{4-1}} \cong 4. \text{ From this we infer that the average number of false crossings per edge is}$$

approximately  $8 \pm 4$ . Because this number is unacceptably high, the graph is not discrete-continuous dual.

Now let's consider the graph of Figure 14. In this case, the average number of false crossings per edge is very low; however, there exists one edge in the network with 23 false crossings. Whether or not 23 false crossings is considered unacceptably high may depend on the circumstances. In this case, 23 false crossings is unacceptably high. An edge with a large number of false crossings is called a **wormhole edge**, and graphs with wormhole edges are not discrete-continuous dual.

In the asymptotically discrete-continuous dual space of Figure 15, there are several edges with a small number of false crossings, but no edges have a large number of false crossings. Finally, there are no false crossings in the strictly discrete-continuous dual space of Figure 16.

### 3.7 Tree-like Networks

It is crucial to keep in mind that discrete-continuous duality does not necessarily mean a discrete space  $\mathcal{D}$  embedded in a continuous space  $\mathcal{C}$ . In the case of asymptotic discrete-continuous duality the

discrete space  $\mathcal{D}$  is not embedded in the matched continuous space  $\mathcal{C}$ . In the case of strict discrete-continuous duality, the discrete space  $\mathcal{D}$  is embedded in the matched continuous space  $\mathcal{C}$ . However, a discrete space  $\mathcal{D}$  embedded in a continuous space  $\mathcal{C}$  does not necessarily form a strict discrete-continuous dual space. (To form a strict discrete-continuous dual space, the pair  $\{\mathcal{D}, \mathcal{C}\}$  must satisfy the requirements given in section 3.2.)

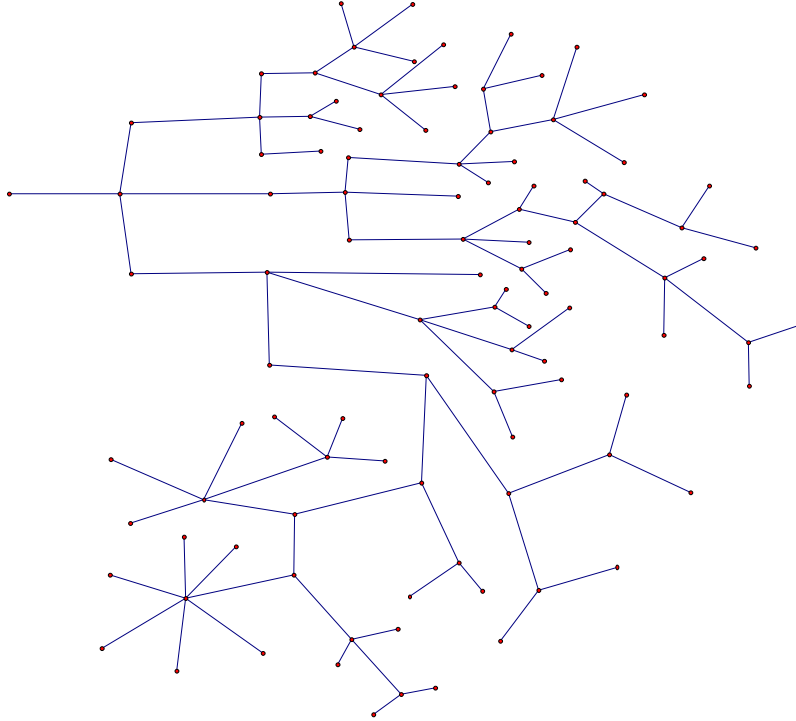


**Figure 17: A tree-like graph in which the branches are not gradual or smooth**  
*This graph is not discrete-continuous dual because the branches consist of a single edge.*

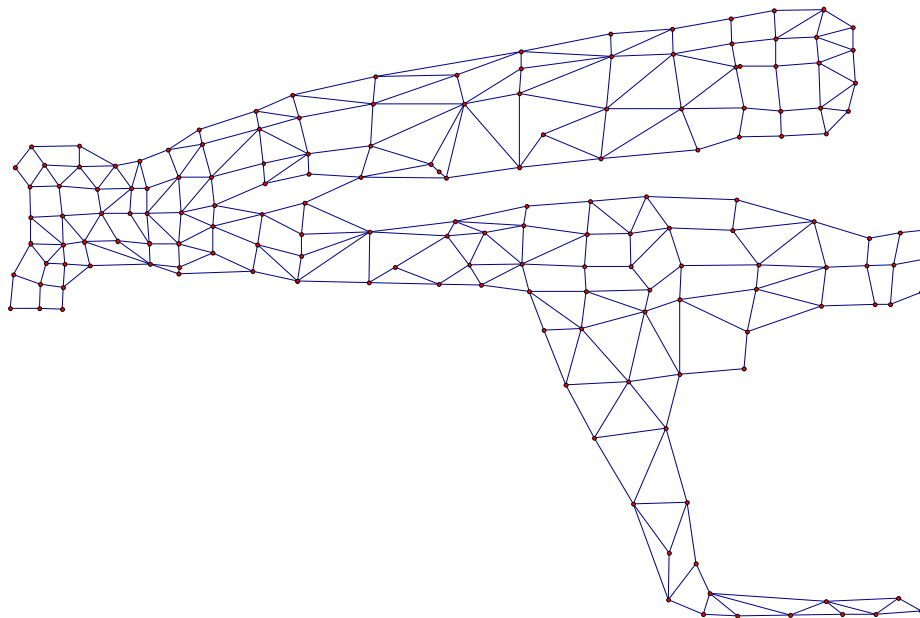


**Figure 18: A tree-like graph in which the branches are gradual and smooth**  
*This graph is discrete-continuous dual because the branches consist of many edges and approximate a smooth, continuous space.*

#### 4. COMPUTING THE CONNECTIVITY DIMENSIONALITY IN DISCRETE-CONTINUOUS DUAL SPACES

##### 4.1 Minimum Connectivity Radius for Computing the Connectivity Dimensionality

Consider a periodic lattice in which each vertex has degree  $k$  (i.e. each vertex is adjacent to  $k$  vertices). Next, consider the compact region  $\mathcal{R}_\zeta$  defined as the collection of edges and vertices with a connectivity distance less than or equal to  $\zeta$  from the vertex  $\mathbf{A}$ . When the connectivity radius equals one the number of included vertices equals  $k$ .

**Definition 20:** The **inclusive surface hypervolume** corresponding to connectivity radius  $\zeta$  is defined as

$$S[\zeta, \mathbf{A}] = C[\zeta, \mathbf{A}] - C[(\zeta - 1), \mathbf{A}]. \quad (54)$$

Since the degree of each vertex is  $k$ , the number of vertices adjacent to  $\mathcal{R}_\zeta$  for  $\zeta \geq 1$  cannot be greater than  $k - 1$  times the inclusive surface hypervolume  $S[\zeta, \mathbf{A}]$ . (The factor is  $k - 1$  since at least one of the vertices adjacent to any particular vertex included in  $\mathcal{R}_\zeta$  is also included in  $\mathcal{R}_\zeta$  for  $\zeta \geq 1$ .) This gives the bound

$$S[\zeta, \mathbf{A}] \leq (k - 1) \left( S[(\zeta - 1), \mathbf{A}] \right) \text{ for } \zeta \geq 2 \quad (55)$$

imposed by the vertex degree  $k$ . The asymptotically matched counterparts to equations (54) - (55) are:

$$\left\lceil S[\zeta, \mathbf{A}] \right\rceil = \left\lceil C[\zeta, \mathbf{A}] \right\rceil - \left\lceil C[(\zeta - 1), \mathbf{A}] \right\rceil, \quad (56)$$

and

$$\left\lceil S[\zeta, \mathbf{A}] \right\rceil \leq (k - 1) \left( \left\lceil S[(\zeta - 1), \mathbf{A}] \right\rceil \right). \quad (57)$$

Since each vertex in  $\mathcal{R}_\zeta$  is adjacent to  $k$  vertices, the total number of vertices in  $\mathcal{R}_\zeta$  plus the number of vertices adjacent to  $\mathcal{R}_\zeta$  is less than or equal to  $k$  times the number of vertices in  $\mathcal{R}_\zeta$ . Consequently, the count function satisfies the following inequality:

$$\ln \left[ C[(\zeta + 1), \mathbf{A}] \right] - \ln \left[ C[\zeta, \mathbf{A}] \right] \leq \ln[k] \text{ for } \zeta \geq 1. \quad (58)$$

$\zeta_{\min}$  is defined as the minimum connectivity radius needed to reliably compute the connectivity dimensionality. For large enough connectivity radius (i.e.  $\zeta \geq \zeta_{\min}$ ) the number of vertices enclosed in region  $\mathcal{R}_\zeta$  must scale approximately proportional to  $\zeta^N$  where  $N$  is the dimensionality of the lattice:

$$\mathcal{F}_{\text{vertexal}}[\mathcal{R}_\zeta] = \left\lceil C[\zeta, \mathbf{A}] \right\rceil \approx \mathcal{G} \zeta^N \text{ for } \zeta \geq \zeta_{\min} \quad (59)$$

where  $\mathcal{G}$  is called the **geometric hypervolume coefficient**. ( $\ln[\mathcal{G}]$  is the y-intercept on a  $\ln[\left\lceil C[\zeta, \mathbf{A}] \right\rceil]$  versus  $\ln[\zeta]$  plot.)

The number of pseudo-parallel edges to the surface of  $\mathcal{R}_\zeta$  is defined as the number edges connecting two vertices a connectivity distance of  $\zeta$  from vertex  $\mathbf{A}$ . The number of pseudo-perpendicular edges to the surface of  $\mathcal{R}_\zeta$  is defined as the sum of the number of (i) edges that connect a vertex with connectivity distance  $\zeta$  from vertex  $\mathbf{A}$  to a vertex with connectivity distance  $\zeta - 1$  from vertex  $\mathbf{A}$  and (ii) edges that connect a vertex with connectivity distance  $\zeta$  from vertex  $\mathbf{A}$  to a vertex with

connectivity distance  $\zeta + 1$  from vertex  $\mathbf{A}$ . The group (i) is called the inward pointing pseudo-perpendicular edges, while the group (ii) is called the outward pointing pseudo-perpendicular edges.

Since there are  $k$  edges per vertex, the average number of edges per connectivity dimension is  $\frac{k}{N}$ . We can define an ideal number of pseudo-parallel and pseudo-perpendicular edges by scaling the total number of edges by the percentages of independent directions parallel and perpendicular to the boundary of  $\mathcal{R}_\zeta$  when its dimensionality is well-developed. When the connectivity dimensionality is well-developed, the boundary of region  $\mathcal{R}_\zeta$  has a connectivity dimensionality of  $N-1$  giving  $k \left( \frac{N-1}{N} \right)$  as the ideal number of pseudo-parallel edges per vertex in the boundary. When the connectivity dimensionality is well-developed, there is one direction perpendicular to the boundary of region  $\mathcal{R}_\zeta$  giving  $\frac{k}{N}$  as the ideal number of pseudo-perpendicular edges per vertex in the boundary. Because some of the pseudo-perpendicular edges point inward, when the connectivity dimensionality is well-developed, the number of outward pointing pseudo-perpendicular edges per vertex will be less than  $\frac{k}{N}$ . Hence, the connectivity dimensionality of region  $\mathcal{R}_\zeta$  is well-developed (i.e. having an approximately  $N-1$  dimensional boundary and satisfying equation (59)) when

$$\left\lceil S[(\zeta + 1), \mathbf{A}] \right\rceil < \frac{k}{N} \left( \left\lceil S[\zeta, \mathbf{A}] \right\rceil \right) \text{ for } \zeta \geq \zeta_{\min} \quad (60)$$

For  $\zeta \geq \zeta_{\min}$ , the connectivity dimensionality is well-developed and equations (59) - (60) are valid. Following equations (54) and (59), one can write

$$\left\lceil S[(\zeta_{\min} + 1), \mathbf{A}] \right\rceil = \left\lceil C[(\zeta_{\min} + 1), \mathbf{A}] \right\rceil - \left\lceil C[\zeta_{\min}, \mathbf{A}] \right\rceil \cong \mathcal{G}(\zeta_{\min} + 1)^N - \mathcal{G}(\zeta_{\min})^N \quad (61)$$

and

$$\left\lceil S[(\zeta_{\min} + 2), \mathbf{A}] \right\rceil = \left\lceil C[(\zeta_{\min} + 2), \mathbf{A}] \right\rceil - \left\lceil C[(\zeta_{\min} + 1), \mathbf{A}] \right\rceil \cong \mathcal{G}(\zeta_{\min} + 2)^N - \mathcal{G}(\zeta_{\min} + 1)^N \quad (62)$$

Substituting equations (61) and (62) into (60), one obtains

$$\mathcal{G}(\zeta_{\min} + 2)^N - \mathcal{G}(\zeta_{\min} + 1)^N < \frac{k}{N} \left( \mathcal{G}(\zeta_{\min} + 1)^N - \mathcal{G}(\zeta_{\min})^N \right) \quad (63)$$

which simplifies to

$$\frac{(\zeta_{\min} + 2)^N - (\zeta_{\min} + 1)^N}{(\zeta_{\min} + 1)^N - (\zeta_{\min})^N} < \frac{k}{N}. \quad (64)$$

It is recommended to choose half-integer values for  $\zeta_i$  since this provides an average over connectivity radii having the same count function. (The continuous variable  $\zeta$  takes on the value of any nonnegative real number. The discrete variable  $\zeta_i$  takes on one of the values  $\frac{1}{2}, 1\frac{1}{2}, 2\frac{1}{2}, 3\frac{1}{2}, \dots$ ) Hence, I define

$\zeta_{\min}$  as the minimum number in the series  $\zeta_i = \frac{1}{2}, 1\frac{1}{2}, 2\frac{1}{2}, 3\frac{1}{2}, \dots$  that satisfies equation (64). That is,

$$\zeta_{\min} = \min_{\zeta \in \left\{ \frac{1}{2}, 1\frac{1}{2}, 2\frac{1}{2}, \dots \right\}} \text{ satisfying } \frac{(\zeta + 2)^N - (\zeta + 1)^N}{(\zeta + 1)^N - (\zeta)^N} < \frac{k}{N}. \quad (65)$$

For edge-vertex graphs having structural variability, average or typical or estimated values of  $k$  and  $N$  should be used for the purpose of estimating  $\zeta_{\min}$ .

Note that for  $\zeta < \zeta_{\min}$  the number of edges pseudo-parallel to the boundary of  $\mathcal{R}_{\zeta}$  is much less than  $k \left( \frac{N-1}{N} \right)$  and hence the inclusive surface of  $\mathcal{R}_{\zeta}$  appears to be much less than  $N-1$  dimensional.

In this case, the dimensionality of  $\mathcal{R}_{\zeta}$  is said to be underdeveloped. We have thus discovered an important and extremely fundamental principal: the development of the connectivity dimensionality of a discrete-continuous dual space requires a region exceeding a certain critical size, and this critical size corresponds to a connectivity radius of  $\zeta_{\min}$ .<sup>16</sup>

For example, consider spaces for  $N=1, 2, 3, 4, 5, 10$ , and  $100$  where  $k/N=2$ . The corresponding values for  $\zeta_{\min}$  are  $0.5, 1.5, 2.5, 3.5, 5.5, 12.5$ , and  $142.5$ , respectively. For a 2-dimensional space, equation (65) gives  $\zeta_{\min} = 0.5$  for  $2 < \frac{k}{N}$ ,  $\zeta_{\min} = 1.5$  for  $\frac{3}{2} < \frac{k}{N} \leq 2$ , and  $\zeta_{\min} = 2.5$  for  $\frac{4}{3} < \frac{k}{N} \leq \frac{3}{2}$ . Thus, a planar triangular lattice ( $k/N = 3$ ) has  $\zeta_{\min} = 0.5$ , a planar square lattice ( $k/N = 2$ ) has  $\zeta_{\min} = 1.5$ , and a planar hexagonal lattice ( $k/N = 1.5$ ) has  $\zeta_{\min} = 2.5$ .

What is the specific meaning of  $\zeta_{\min}$ ? Specifically, for  $\zeta < \zeta_{\min}$  the count function  $C[\zeta]$  is not approximately proportional to  $\zeta^N$  while for  $\zeta > \zeta_{\min}$  the count function  $C[\zeta]$  is approximately proportional to  $\zeta^N$ .<sup>17</sup> Therefore, when computing the connectivity dimensionality of a regular or irregular graph, connectivity distances greater than or equal to  $\zeta_{\min}$  should always be used.

**Minimum Connectivity Radius Principle:** The development of connectivity dimensionality in an edge-vertex graph requires a minimum connectivity radius. The value of the minimum connectivity radius depends both upon the value of the connectivity dimensionality and the degree distribution of the graph.

## 4.2 Estimating the Average Connectivity Dimensionality of a Local Region

Taking the logarithm of equation (59) gives

$$\ln[C[\zeta_i, \mathbf{A}]] \approx \ln[\mathcal{G}] + N \ln[\zeta_i] \text{ for } \zeta_i \geq \zeta_{\min}. \quad (66)$$

<sup>16</sup> The following explanation helps us to intuitively understand why there is a minimum connectivity radius  $\zeta_{\min}$  associated with measuring the connectivity dimensionality. When  $\zeta_i = 0.5$ , there is only one included vertex. Because the included vertex could just as well come from a 0-dimensional space, a 4-dimensional space, or a 100-dimensional space, we have no information about the connectivity dimensionality when  $\zeta_i = 0.5$ . When  $\zeta_i = 1.5$ , the number of included vertices is  $k + 1$ . If  $k=0$ , the space is zero-dimensional. If  $k=2$ , we are in a linear region of a space. If  $k>2$  then the whole space has a manifold covering dimension greater than or equal to 2 (while the particular region within  $\zeta_i = 1.5$  has a manifold covering dimension equal to 2). So now we have some (but still very little) information about the connectivity dimensionality. Accordingly, only when  $\zeta_i \geq 2$  can a graph region emerge that cannot be drawn properly on a plane; from this we infer that a space with three or more independent dimensions has  $\zeta_{\min} > 2$ . As we increase  $\zeta_i$  to larger and larger values, we learn more and more information about the connectivity dimensionality.

<sup>17</sup> We can write  $C[\zeta]$  instead of  $C[\zeta, \mathbf{A}]$  when the vertex of interest is unspecified.

Combining this equation for two different values of the connectivity radius gives

$$\ln[C[\zeta_i, \mathbf{A}]] - \ln[C[\zeta_j, \mathbf{A}]] \approx N \ln[\zeta_i] - N \ln[\zeta_j] \text{ for } \zeta_i, \zeta_j \geq \zeta_{\min}, \quad (67)$$

whence it follows that

$$N \approx \frac{\ln[C[\zeta_i, \mathbf{A}]] - \ln[C[\zeta_j, \mathbf{A}]]}{\ln[\zeta_i] - \ln[\zeta_j]} \text{ for } \zeta_i, \zeta_j \geq \zeta_{\min}. \quad (68)$$

This equation forms the basis for computing the connectivity dimensionality of graphs, networks, and discrete-continuous dual spaces.

Let us denote the smaller of  $\zeta_i$  and  $\zeta_j$  as  $\zeta_{\text{smaller}}$  and the larger simply as  $\zeta$ . Then, equation (68) can be written in the equivalent form

$$N[\zeta, \mathbf{A}] \approx \frac{\ln[C[\zeta, \mathbf{A}]] - \ln[C[\zeta_{\text{smaller}}, \mathbf{A}]]}{\ln[\zeta] - \ln[\zeta_{\text{smaller}}]} \text{ for } \zeta > \zeta_{\text{smaller}} \geq \zeta_{\min}. \quad (69)$$

$N[\zeta, \mathbf{A}]$  is an estimate of the average connectivity dimensionality for a region of connectivity radius  $\zeta$  about vertex  $\mathbf{A}$ .

For example, in an approximately 2-dimensional space with a typical/average vertex degree of four, one could use  $N \cong \frac{\ln[C[\zeta = 2.5]/C[\zeta = 1.5]]}{\ln[2.5/1.5]}$  to obtain an estimate of  $N$  since  $\zeta_{\min} = 1.5$ . If the typical/average vertex degree of an approximately 2-dimensional space is six then  $\zeta_{\min} = 2.5$  and hence  $N \cong \frac{\ln[C[\zeta = 3.5]/C[\zeta = 2.5]]}{\ln[3.5/2.5]}$  is the smallest combination of connectivity radii which could be used to obtain a good estimate of the connectivity dimensionality.

**Table 3: The minimum connectivity radius for evaluating the connectivity dimensionality**

$\zeta_i$	$S[\zeta_i, \mathbf{A}]$	$\frac{S[(\zeta_i + 1), \mathbf{A}]}{S[\zeta_i, \mathbf{A}]}$	$C[\zeta_i]$	Estimated Connectivity Dimensionality $\frac{\ln[C[\zeta_i + 1]/C[\zeta_i]]}{\ln[(\zeta_i + 1)/\zeta_i]}$
0.5	1	10	1	2.18
1.5	10	5	11	3.35
2.5	50	3.4	61	3.95
3.5	170	2.65	231	4.30
4.5	450	2.23	681	4.51
<b>5.5</b>	<b>1002</b>	<b>1.97</b>	<b>1683</b>	<b>4.64</b>
6.5	1970	1.79	3653	4.73
7.5	3530	--	7183	--

Consider a five-dimensional regular hypercubic lattice in which each vertex has degree 10. In this case, equation (65) gives  $\zeta_{\min} = 5.5$ . The computed inclusive surface values, count functions, and estimated connectivity dimensionalities are given in Table 3.<sup>18</sup> Note that for  $\zeta \geq \zeta_{\min}$  the estimated

<sup>18</sup> For a periodic lattice, the lattice companion graph should be used to compute the connectivity dimensionality. In this example, the count functions are computed from the lattice itself to illustrate the effects of measurement error.



connectivity dimensionality is closer to five (its true value) than any other integer; therefore,  $\zeta \geq \zeta_{\min}$  gives a reasonable estimate of the connectivity dimensionality. For  $\zeta < \zeta_{\min}$  the connectivity dimensionality is incorrectly estimated as either midway between four and five or closer to an integer smaller than five; therefore,  $\zeta < \zeta_{\min}$  does not give a reasonable estimate of the connectivity dimensionality. The data in Table 3 also shows the ratio  $\frac{S[(\zeta+1), \mathbf{A}]}{S[\zeta, \mathbf{A}]} < \frac{k}{N} = 2$  for  $\zeta \geq \zeta_{\min}$  but not for  $\zeta < \zeta_{\min}$ . Clearly this vindicates the above method for computing  $\zeta_{\min}$ .

### 4.3 When and Why the Connectivity Dimensionality Contains Inherent Uncertainty

The next few sections explain the following uncertainty principle associated with measuring the connectivity dimensionality:

**Connectivity dimensionality uncertainty principle:** The more precisely we want to know the average connectivity dimensionality in a region of space, the more elementary quantifiable geometric units that region of space must contain unless the space is zero-dimensional, one-dimensional, or a periodic lattice.

The origin of this uncertainty in the connectivity dimensionality stems directly from the definition of the connectivity dimensionality itself and properties of irrational numbers. Because this uncertainty principle is a general mathematical law, it applies to all kinds of spaces whether abstract or physical.

The term *quantifiable* means that we can index the individual elementary quantifiable geometric units by means of *variables* or *coordinates*. For an edge-vertex graph, the elementary quantifiable geometric units are the graph's vertices; in this case the vertices can be quantified by means of a counting number index. For a periodic lattice, the elementary quantifiable geometric units are the unit cells comprising the lattice. Some geometric constructs are unquantifiable. For example, in discrete-continuous dual graphs of non-integer dimensionality a set of variables or coordinates cannot be used to specify the individual points in the continuous representation; in this case the quantifiable points are the graph vertices while the continuously interpolated points between the graph vertices are unquantifiable. For a continuous space of integer dimensionality, each point in the space is an elementary quantifiable geometric unit because a set of coordinates can be used to quantify the location of each point in the space.

For a discrete or discrete-continuous dual space, the elementary quantifiable geometric units can be used to construct a graph representing the space. Each elementary quantifiable geometric unit is represented by a vertex. Two vertices are joined by an edge in the graph iff. the corresponding elementary quantifiable geometric units are adjacent to each other in the space. For an edge-vertex graph, this procedure gives the graph itself. For a periodic lattice, this procedure gives a lattice companion graph. (See Figure 19.)

We can use the connectivity radius  $\{\zeta_i\}$  and count function  $C[\zeta_i, \mathbf{P}]$  of the companion graph to estimate the average connectivity dimensionality of a local region following the procedures described in sections 4.1 and 4.2 above. We use half-integer values of the connectivity radius:  $\zeta_i \in \{\zeta_{\min}, \zeta_{\min} + 1, \zeta_{\min} + 2, \zeta_{\min} + 3, \dots\}$ . Let  $Q_i = C[\zeta_i, \mathbf{P}]$  denote the number of enclosed elementary quantifiable geometric units around position  $\mathbf{P}$  for a region of connectivity radius  $\zeta_i$ .

Let us hypothesize that the connectivity dimensionality of space enclosed in a region of connectivity radius  $\zeta_k \geq \zeta_{\min} + 1$  is some real number  $N$ ; then the predicted hypervolume enclosed in a region of connectivity radius  $\zeta_j$  where  $\zeta_k > \zeta_j \geq \zeta_{\min}$  is

$$Q_j = \left( \frac{\zeta_j}{\zeta_k} \right)^N Q_k \quad (\text{hypothesis}) \quad (70)$$

The values of  $Q_j$  and  $Q_k$  are integer because the count function always returns an integer value.

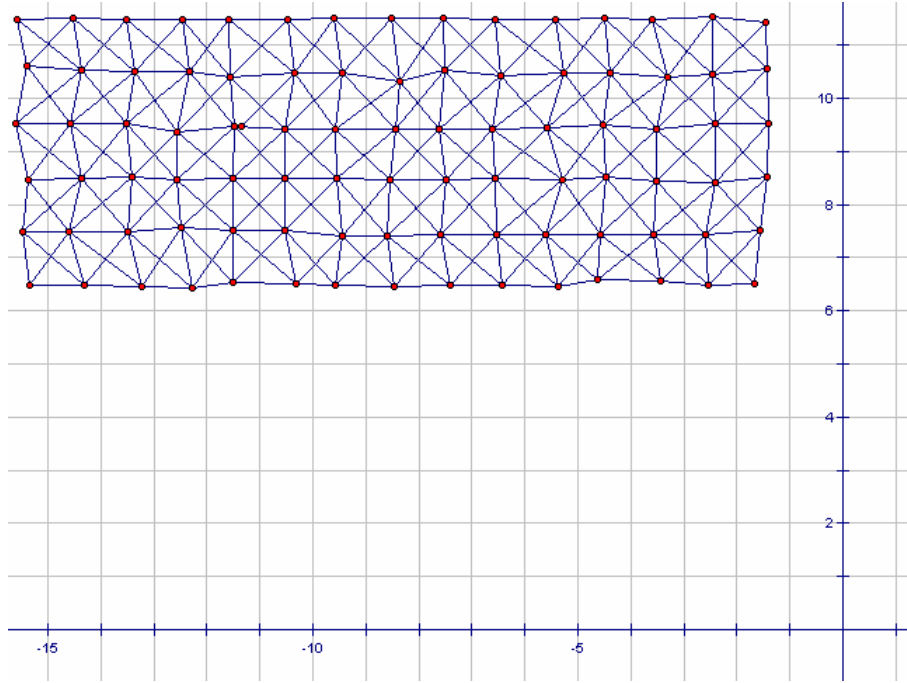


**Figure 19: A lattice companion graph superimposed on the lattice it represents**

*At the top of the figure is shown part of a lattice companion graph superimposed on the lattice it represents. There is one vertex per unit cell and two vertices are joined by an edge iff. the unit cells they represent are adjacent.*

If the connectivity dimensionality  $N$  is a real number, then equation (70) can be rearranged to give the equality

$$\frac{\zeta_j}{\zeta_k} = \sqrt[N]{\frac{Q_j}{Q_k}}. \quad (\text{hypothesis}) \quad (71)$$

We can rearrange equation (71) to give

$$\sqrt[m]{\frac{\zeta_j}{\zeta_k}} = \frac{Q_j}{Q_k} \quad \text{for } m = 1/N. \quad (\text{hypothesis}) \quad (72)$$

The quantity  $\frac{Q_j}{Q_k}$  is a rational number because it is the quotient of two integers. The quantity  $\frac{\zeta_j}{\zeta_k}$  is a rational number because it is the quotient of two half-integers. In order for equation (71) to be true  $\sqrt[N]{\frac{Q_j}{Q_k}}$

must be rational while for equation (72) to be true  $\sqrt[m]{\frac{\zeta_j}{\zeta_k}}$  must be rational.

**Box 1:****Cases in which the connectivity dimensionality field can be a constant real number not subject to inherent uncertainty**

In general, the Nth root of a rational number need not be rational unless  $N = 0$  or  $m=1/N$  is integer. If we demand that for arbitrarily chosen rational numbers  $p$  and  $q$ , both  $\sqrt[N]{p}$  and  $\sqrt[m]{q}$  are rational where  $N \geq 0$ , then it follows that  $N \in \{0, 1\}$ . Consequently, we can find a valid solution to equations (70) - (72) if the connectivity dimensionality  $N$  is 0 or 1. When  $N=0$ , we have the solution  $Q_j = Q_k$ . When  $N=1$ , we have the solution  $\{Q_i\} = \{2c\zeta_i\}$  where  $c$  is a counting number constant.

There exists another solution to equations (70) - (72). Namely, when  $N$  is an integer greater than 1,  $Q_j = c(2\zeta_j)^N$ , and  $c$  is a counting number constant. As shown later in this section, this case corresponds to the companion graph of a periodic lattice.

Finally, a valid solution to equations (70) - (72) can be found in the limit  $Q_j, Q_k \rightarrow \infty$  since for any positive number  $m$  we can asymptotically represent the rational or irrational number  $\sqrt[m]{\frac{\zeta_j}{\zeta_k}}$  by the quotient of two arbitrarily large integers. That is, a quotient of two arbitrarily large integers can be used to represent any rational or irrational positive number to any desired level of accuracy. In a continuous space of dimensionality  $N = \text{integer} \geq 2$ , each point is connected to an infinite number of other points; therefore, in such a space both  $Q_j$  and  $Q_k$  are infinitely large for any value of the connectivity radius  $\zeta_j, \zeta_k \geq \frac{3}{2}$ . We conclude that in a continuous space  $N = \text{integer} \geq 2$ , a solution to equations (70) - (72) is possible.

If the space is neither 0-dimensional, nor 1-dimensional, nor representative of a periodic lattice, nor a continuous space of integer dimensionality, then equations (70) - (72) cannot be universally valid because they try to equate the rational numbers  $\frac{Q_j}{Q_k}$  and  $\frac{\zeta_j}{\zeta_k}$  to the often irrational numbers  $\sqrt[m]{\frac{\zeta_j}{\zeta_k}}$  or  $\sqrt[N]{\frac{Q_j}{Q_k}}$ . In this case, our hypothesis (70) is incorrect. Another way of saying this is that the computed average connectivity dimensionality

$$N_{ave}[\zeta_j, \zeta_k] = \frac{\ln[C[\zeta_j, \mathbf{A}]] - \ln[C[\zeta_k, \mathbf{A}]]}{\ln[\zeta_j] - \ln[\zeta_k]} = \frac{\ln[Q_j] - \ln[Q_k]}{\ln[\zeta_j] - \ln[\zeta_k]} \quad (73)$$

is not a constant  $N$ .

We must figure out a way to correct equation (70). Clearly our mistake has been the assumption that  $N$  is a real number independent of the connectivity radius. Since  $N$  is not a real number independent of the connectivity radius, let us replace it by a real number  $\llbracket N \rrbracket$  plus a statistical uncertainty

$$N_{ave}[\zeta_j, \zeta_k] = \llbracket N \rrbracket + \hat{\mathfrak{A}}[N]. \quad (74)$$

(The notation  $\hat{\mathfrak{A}}$  will be used to represent an uncertainty operator.) This gives us

$$\frac{\zeta_j}{\zeta_k} = \left( \frac{Q_j}{Q_k} \right)^{\frac{1}{\llbracket N \rrbracket + \hat{\mathfrak{A}}[N]}}. \quad (75)$$

which can be rearranged to give

$$\llbracket N \rrbracket \sqrt[\llbracket N \rrbracket]{\frac{Q_j}{Q_k}} = \left( \frac{\zeta_j}{\zeta_k} \right) \cdot \left( \frac{\zeta_j}{\zeta_k} \right)^{\frac{\hat{\mathfrak{A}}[N]}{\llbracket N \rrbracket}}. \quad (76)$$

Now let's determine whether this modification fixes the previous problems. The quantity  $\hat{\mathfrak{A}}[N]$  is a residual that takes on different numeric values for different spaces, for different positions within a single space, and for different connectivity radii about a single location within a given space. Moreover, the

quantity  $\left( \frac{\zeta_j}{\zeta_k} \right)^{\frac{\hat{\mathfrak{A}}[N]}{\llbracket N \rrbracket}}$  need not be rational. Equation (76) states that the often irrational  $\llbracket N \rrbracket \sqrt[\llbracket N \rrbracket]{\frac{Q_j}{Q_k}}$  can be

expressed as the product of the rational number  $\left( \frac{\zeta_j}{\zeta_k} \right)$  and the often irrational  $\left( \frac{\zeta_j}{\zeta_k} \right)^{\frac{\hat{\mathfrak{A}}[N]}{\llbracket N \rrbracket}}$ . Because we are no longer trying to represent an irrational number by a rational quotient, equation (76) fixes the problem with equation (71).

Next, we further turn our attention to the fundamental reason that the connectivity dimensionality is subject to some inherent uncertainty. The measurements we take within the space allow us to determine a finite number of  $\frac{Q_j}{Q_k}$  associated with a finite number of chosen  $\frac{\zeta_j}{\zeta_k}$ . If we knew the particular values for the residuals  $\hat{\mathfrak{A}}[N]$  under these conditions, then we could obtain the real number  $\llbracket N \rrbracket$  via equation (76). On the other hand, if we knew the value of  $\llbracket N \rrbracket$ , we could use equation (76) to obtain the particular values of the residuals  $\hat{\mathfrak{A}}[N]$ . Except for those cases explained in Box 1, there are no independent measurements which we could perform that would allow us to separately determine either  $\llbracket N \rrbracket$  or  $\hat{\mathfrak{A}}[N]$ . Since  $\llbracket N \rrbracket$  and  $\hat{\mathfrak{A}}[N]$  are mathematically coupled and we cannot perform any measurements to completely uncouple them, all measurements that we perform to measure the connectivity dimensionality include effects of the uncertain and stochastic residual  $\hat{\mathfrak{A}}[N]$ . That is, the connectivity dimensionality contains inherent uncertainty.

#### 4.4 How Uncertainty in Average Connectivity Dimensionality Depends on Connectivity Radius

Next, let us consider the amount of uncertainty and how it depends upon the size of region observed. Clearly, the rational portion  $\left( \frac{\zeta_j}{\zeta_k} \right)$  on the right side of equation (76) is that part of the dimensionality measurement that is independent of the residual and therefore certain. Except in Box 1 cases where the residual is zero, the often irrational  $\left( \frac{\zeta_j}{\zeta_k} \right)^{\frac{\hat{\mathfrak{A}}[N]}{\llbracket N \rrbracket}}$  is that part of the dimensionality measurement that depends upon the residual and is uncertain because we cannot explicitly determine the residual's value. We define a stochastic variable

$$w = \left( \frac{\zeta_j}{\zeta_k} \right)^{\frac{\hat{\mathfrak{A}}[N]}{\llbracket N \rrbracket}} - 1. \quad (77)$$

The magnitude of the stochastic variable  $w$  depends upon how closely the rational number  $\varphi = \frac{\zeta_j}{\zeta_k}$  approaches the often irrational number  $\chi = \llbracket N \rrbracket \sqrt{\frac{Q_j}{Q_k}}$  as demonstrated by inserting equation (77) into (76) and rearranging to give

$$w = \frac{\chi}{\varphi} - 1. \quad (78)$$

Let an irrational number  $\chi' > 0$  be approximated by the rational quotient  $\varphi' = \frac{a}{b}$  where  $a$  and  $b$  are integers chosen to minimize the absolute error

$$|w'| = \left| \frac{\chi'}{\varphi'} - 1 \right| \quad (79)$$

subject to the constraints

$$0 < a \leq M \text{ and } 0 < b \leq M. \quad (80)$$

As the magnitudes of  $a$  and  $b$  increase by increasing  $M$ , the irrational number  $\chi'$  becomes better approximated by the rational quotient  $\varphi' = \frac{a}{b}$ . In the limit  $M$  becomes infinitely large, the absolute error

$|w'| = \left| \frac{\chi'}{\varphi'} - 1 \right|$  becomes arbitrarily small.

A direct corollary of this fundamental mathematical property of rational and irrational numbers is that the residual uncertainty component  $w = \frac{\chi}{\varphi} - 1$  is mathematically allowed to become smaller in magnitude as the integers  $2\zeta_j$  and  $2\zeta_k$  increase in magnitude, which corresponds to increasing the connectivity radius of the region for which the average connectivity dimensionality is being computed. Rearranging equation (77) we obtain an expression for the error in the computed average connectivity dimensionality

$$\hat{\mathfrak{A}}[N] = \frac{\llbracket N \rrbracket \ln[1+w]}{\ln[\zeta_j] - \ln[\zeta_k]}. \quad (81)$$

For sufficiently large connectivity radii we will have  $|w| < 0.5$  and hence we can approximate

$$\ln[1+w] \cong w + \dots \quad (82)$$

Substituting this into equation (81) one obtains

$$\frac{|\hat{\mathfrak{A}}[N]|}{\llbracket N \rrbracket} \cong \frac{|w|}{\ln[\zeta_{larger} / \zeta_{smaller}]} \quad (83)$$

where  $\zeta_{smaller}$  and  $\zeta_{larger}$  are smaller and larger values of  $\zeta_j$  and  $\zeta_k$ , respectively.

A soft upper bound on the absolute value of the relative error<sup>19</sup>  $w$  associated with approximating  $\sqrt[N]{\frac{Q_j}{Q_k}}$  by  $\frac{2\zeta_j}{2\zeta_k}$  can be derived as following. Since the discrete unit of the connectivity radius is 1 edge

we have  $\zeta_{p+1} = \zeta_p + 1$  and the set of possible  $\left\{ \frac{2\zeta_p}{2\zeta_q} \right\}$  values can be rewritten as

$$\left\{ \frac{2\zeta_p}{2\zeta_q} \right\} = \left\{ \left( \frac{\zeta_{3a}}{\zeta_{3b}}, \frac{\zeta_{3a}+1}{\zeta_{3b}}, \frac{\zeta_{3a}-1}{\zeta_{3b}}, \frac{\zeta_{3a}-1}{\zeta_{3b}-1}, \frac{\zeta_{3a}}{\zeta_{3b}-1}, \frac{\zeta_{3a}}{\zeta_{3b}+1}, \frac{\zeta_{3a}+1}{\zeta_{3b}+1}, \frac{\zeta_{3a}-1}{\zeta_{3b}+1}, \frac{\zeta_{3a}+1}{\zeta_{3b}-1} \right) \right\} \quad (84)$$

where  $p, q, a$ , and  $b$  are positive integers. The purpose of expanding the set  $\left\{ \frac{2\zeta_p}{2\zeta_q} \right\}$  in this way is to

obtain the size of the interval between different  $\frac{2\zeta_p}{2\zeta_q}$  for neighboring values of the connectivity radius.

On the right side of equation (84) the list enclosed in ( ) is an explicit representation of those values of  $\frac{2\zeta_p}{2\zeta_q}$  for connectivity radii which neighbor  $\zeta_{3a}$  and  $\zeta_{3b}$ . For some particular  $j$  and  $k$ , the often

irrational  $\sqrt[N]{\frac{Q_j}{Q_k}}$  must be approximated by a rational number  $\varphi$  where

$$\varphi \in \left\{ \frac{\zeta_{3a}}{\zeta_{3b}}, \frac{\zeta_{3a}+1}{\zeta_{3b}}, \frac{\zeta_{3a}-1}{\zeta_{3b}}, \frac{\zeta_{3a}-1}{\zeta_{3b}-1}, \frac{\zeta_{3a}}{\zeta_{3b}-1}, \frac{\zeta_{3a}}{\zeta_{3b}+1}, \frac{\zeta_{3a}+1}{\zeta_{3b}+1}, \frac{\zeta_{3a}-1}{\zeta_{3b}+1}, \frac{\zeta_{3a}+1}{\zeta_{3b}-1} \right\}. \quad (85)$$

The process of rationalizing  $\sqrt[N]{\frac{Q_j}{Q_k}}$  involves rounding  $C \cdot \sqrt[N]{Q_j}$  and  $C \cdot \sqrt[N]{Q_k}$  to some odd integers  $2\zeta_j$  and  $2\zeta_k$  where  $C$  is a real number. Because the smallest discrete interval in the connectivity radius is 1 edge, we can round  $C \cdot \sqrt[N]{Q_j}$  and  $C \cdot \sqrt[N]{Q_k}$  to the nearest odd integers to obtain the optimal values for  $2\zeta_j$  and  $2\zeta_k$ . Clearly, rounding to the nearest odd integer leads to a maximum possible change in value of  $\pm 1$ . (Example: 14.01 is rounded up to 15, but 13.99 is rounded down to 13.) If the rounding of  $C \cdot \sqrt[N]{Q_p}$  is uncorrelated over the set of possible  $p$  values then rounding up and down will occur randomly with equal probabilities; however, because  $Q_{smaller}$  is a subvolume of  $Q_{larger}$  the numbers  $C \cdot \sqrt[N]{Q_{smaller}}$  and  $C \cdot \sqrt[N]{Q_{larger}}$  are not uncorrelated.

If the rounding of  $C \cdot \sqrt[N]{Q_j}$  and  $C \cdot \sqrt[N]{Q_k}$  is completely correlated, then both are always rounded up or else both are rounded down. If both have been rounded down, the upper error associated with rationalizing  $\sqrt[N]{\frac{Q_j}{Q_k}}$  to  $\frac{2\zeta_j}{2\zeta_k}$  is given by the Taylor series expansion

<sup>19</sup> By relative error we mean the error divided by the magnitude of the quantity being approximated. The relative error times 100% is the percent error. A relative error of 0.1 corresponds to 10% error.



$$\sqrt[N]{\frac{Q_j}{Q_k}} \cong \frac{2\zeta_j + 1}{2\zeta_k + 1} = \left(\frac{\zeta_j}{\zeta_k}\right)^{1 + \frac{1}{2\zeta_j}} = \left(\frac{\zeta_j}{\zeta_k}\right) \left(1 + \frac{1}{2\zeta_j} - \frac{1}{2\zeta_k} + \dots\right) \quad (86)$$

If both have been rounded up, then

$$\sqrt[N]{\frac{Q_j}{Q_k}} \cong \frac{2\zeta_j - 1}{2\zeta_k - 1} = \left(\frac{\zeta_j}{\zeta_k}\right)^{1 - \frac{1}{2\zeta_j}} = \left(\frac{\zeta_j}{\zeta_k}\right) \left(1 - \frac{1}{2\zeta_j} + \frac{1}{2\zeta_k} + \dots\right). \quad (87)$$

Whence it follows that

$$\left| \sqrt[N]{\frac{Q_j}{Q_k}} - \frac{2\zeta_j}{2\zeta_k} \right| \cong \left(\frac{\zeta_j}{\zeta_k}\right) \left| \frac{1}{2\zeta_k} - \frac{1}{2\zeta_j} \right|. \quad (88)$$

Thus, in the case of correlated rounding, the approximate relative error is given by

$$|w_{\text{correlated}}| \cong \frac{1}{2\zeta_{\text{smaller}}} - \frac{1}{2\zeta_{\text{larger}}}. \quad (\text{upper estimate}) \quad (89)$$

Note that this corresponds to one-half of the relative interval between the members  $\frac{\zeta_{3a}}{\zeta_{3b}}$  and either

$\frac{\zeta_{3a}-1}{\zeta_{3b}-1}$  or  $\frac{\zeta_{3a}+1}{\zeta_{3b}+1}$  in the set (85). The factor of one-half occurs because the rounding error is one-half the size of the discrete rounding interval. (For example, rounding to the nearest 0.1 of a number yields a maximum possible change in value of 0.05. The number 10.549 gets rounded down to 10.5 while the number 10.551 gets rounded up to 10.6 giving an error of approximately 0.05 for these extremes.)

If the rounding of  $C \cdot \sqrt[N]{Q_j}$  and  $C \cdot \sqrt[N]{Q_k}$  is uncorrelated, then this rounding process can potentially lead to any of the members in set (85). In this case, we could approximate the error associated with rationalizing  $\sqrt[N]{\frac{Q_j}{Q_k}}$  to  $\frac{2\zeta_j}{2\zeta_k}$  by taking one-half the average absolute difference between each of the other members in the set (85) and  $\frac{\zeta_{3a}}{\zeta_{3b}}$ . (Again the factor of one-half occurs because the process of rounding gives an error one-half the interval size.) Expanding each of the members in set (85) as a Taylor series, subtracting each of the other members from  $\frac{\zeta_{3a}}{\zeta_{3b}}$ , taking the absolute value of each of these differences, averaging all of the absolute differences, multiplying by the factor of one-half, and expressing as a relative error one obtains the value

$$|w_{\text{uncorrelated}}| \cong \frac{3}{8\zeta_{\text{smaller}}} + \frac{1}{8\zeta_{\text{larger}}} \quad (\text{upper estimate}) \quad (90)$$

for the hypothetical case in which the rounding of  $C \cdot \sqrt[N]{Q_j}$  and  $C \cdot \sqrt[N]{Q_k}$  is uncorrelated.

Fortunately, for many values of  $\zeta_{\text{larger}} / \zeta_{\text{smaller}}$  the differences between  $|w_{\text{correlated}}|$  and  $|w_{\text{uncorrelated}}|$  are not large. For  $\frac{\zeta_{\text{larger}}}{\zeta_{\text{smaller}}} \geq 2$ , the difference between  $|w_{\text{uncorrelated}}|$  and  $|w_{\text{correlated}}|$  is less than 37.5%. As

$\frac{\zeta_{larger}}{\zeta_{smaller}} \rightarrow 1$ , the use of  $|w_{uncorrelated}|$  becomes dubious because in this limit  $Q_{smaller}$  and  $Q_{larger}$  represent the same hypervolume of space and therefore cannot act independently or be uncorrelated; for this limit the ratio  $|w_{uncorrelated}|/|w_{correlated}|$  becomes arbitrarily large.

The amount of underlying correlation between  $\sqrt[N]{Q_{smaller}}$  and  $\sqrt[N]{Q_{larger}}$  is directly related to the fraction of connectivity radius shared between them. In particular since  $Q_{smaller}$  is a subset of  $Q_{larger}$ , the relative fraction of  $\sqrt[N]{Q_{larger}}$  that is independent of (hence uncorrelated to)  $\sqrt[N]{Q_{smaller}}$  is  $\frac{\sqrt[N]{Q_{larger}} - \sqrt[N]{Q_{smaller}}}{\sqrt[N]{Q_{larger}}} \cong \left( \frac{\zeta_{larger} - \zeta_{smaller}}{\zeta_{larger}} \right)$  while the relative fraction of  $\sqrt[N]{Q_{larger}}$  that is due to  $\sqrt[N]{Q_{smaller}}$  (hence directly correlated to it) is  $\frac{\sqrt[N]{Q_{smaller}}}{\sqrt[N]{Q_{larger}}} \cong \left( \frac{\zeta_{smaller}}{\zeta_{larger}} \right)$ . We can use these fractions of correlated and uncorrelated effects to construct the following weighted average:

$$|w| = \left( \frac{\zeta_{larger} - \zeta_{smaller}}{\zeta_{larger}} \right) |w_{uncorrelated}| + \left( \frac{\zeta_{smaller}}{\zeta_{larger}} \right) |w_{correlated}| = \frac{1}{4} \frac{1}{\zeta_{larger}} + \frac{3}{8} \frac{1}{\zeta_{smaller}} - \frac{5}{8} \frac{\zeta_{smaller}}{\zeta_{larger}^2}. \quad (91)$$

Equation (91) states that the relative error  $|w|$  due to a combination of both correlated and uncorrelated roundoff can be approximated by multiplying the relative error due to uncorrelated roundoff times the fraction of the rounding which is uncorrelated and adding to this the relative error arising from correlated roundoff times the fraction of the rounding which is correlated. Also equation (91) uses the upper roundoff errors to obtain an upper estimate for  $|w|$ .

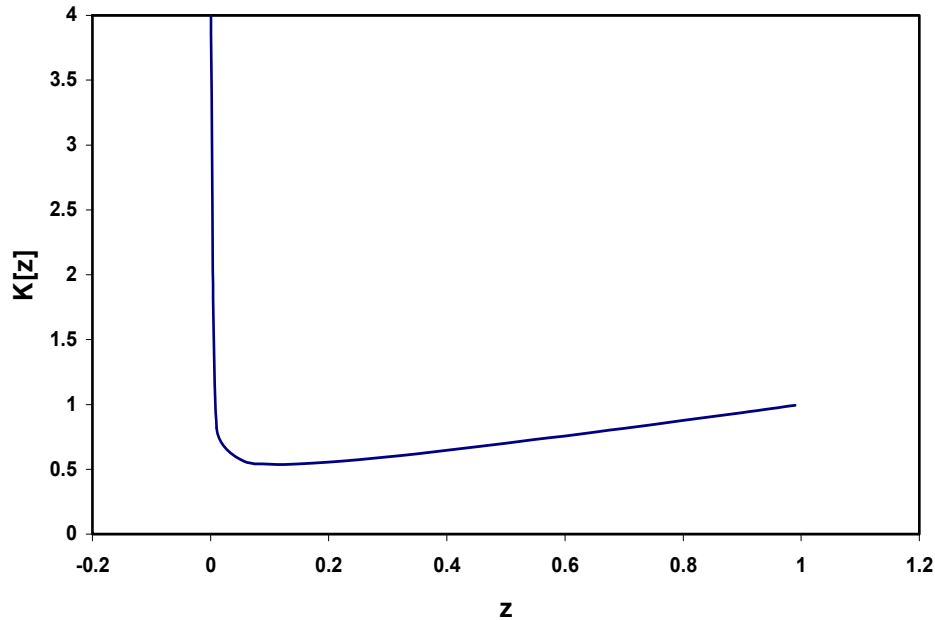


**Figure 20: A plot of the function  $K[z]$**

*In general, the larger the value of  $K[z]$ , where  $z = \zeta_{smaller} / \zeta_{larger}$ , the larger will be the estimated upper error on the computed average connectivity dimensionality if  $\sqrt{\zeta_{larger} \cdot \zeta_{smaller}}$  is held constant. See Figure 21 for a further discussion of this.*

Substituting equation (91) into (83) we obtain

$$\frac{|\hat{\mathfrak{A}}_{upper}[N]|}{\llbracket N \rrbracket} \cong \frac{1}{\ln[\zeta_{larger} / \zeta_{smaller}]} \left( \frac{1}{4} \frac{1}{\zeta_{larger}} + \frac{3}{8} \frac{1}{\zeta_{smaller}} - \frac{5}{8} \frac{\zeta_{smaller}}{\zeta_{larger}^2} \right) \quad (92)$$

which is valid for  $\zeta_{larger} > \zeta_{smaller} \geq \zeta_{min}$  and  $\llbracket N \rrbracket \notin \{0, 1\}$ . We now have an accurate method for estimating the upper uncertainty in computing the connectivity dimensionality. By defining the parameter

$$z = \zeta_{smaller} / \zeta_{larger} \quad (93)$$

we can rewrite equation (92) as

$$\frac{|\hat{\mathfrak{A}}_{upper}[N]|}{\llbracket N \rrbracket} \cong \frac{1}{\sqrt{\zeta_{larger} \cdot \zeta_{smaller}}} \frac{1}{\ln[1/z]} \left( \frac{1}{4} \sqrt{z} + \frac{3}{8} \frac{1}{\sqrt{z}} - \frac{5}{8} z^{3/2} \right) = \frac{K[z]}{\sqrt{\zeta_{larger} \cdot \zeta_{smaller}}} \quad (94)$$

A plot of  $K[z]$  over its entire range  $0 < z < 1$  is shown in Figure 20. We note that  $K[z]$  varies weakly except near  $z=0$  and is bound by the limits

$$0.539 \leq K[z] \leq 1 \text{ for } 0.0051 < z < 1. \quad (95)$$

We note that

$$\lim_{z \rightarrow 1} K[z] = 1, \quad (96)$$

while its minimum occurs for

$$K[0.11...] = 0.539... \quad (97)$$

Recall that equation (92) was developed using the estimated maximum values for the roundoff errors. That is, we considered a possible error of  $\pm 1$  in rounding to the nearest odd integer. However, we would also like to estimate the rms error in the computed average connectivity dimensionality. To do this, we compute the rms rounding error associated with rounding to the nearest odd integer

$$rms \text{ rounding error} = \sqrt{\int_0^1 s^2 ds} = \sqrt{\frac{1}{3}} = 0.577... \quad (98)$$

Hence the expected rms error in the computed connectivity dimensionality is approximately

$$\sqrt{\left\langle \left( \frac{\hat{\mathfrak{A}}[\llbracket N \rrbracket]}{\llbracket N \rrbracket} \right)^2 \right\rangle} \cong \frac{\sqrt{1/3}}{\ln[\zeta_{larger} / \zeta_{smaller}]} \left( \frac{1}{4} \frac{1}{\zeta_{larger}} + \frac{3}{8} \frac{1}{\zeta_{smaller}} - \frac{5}{8} \frac{\zeta_{smaller}}{\zeta_{larger}^2} \right) \cong \frac{\sqrt{1/3} \cdot K[z]}{\sqrt{\zeta_{larger} \cdot \zeta_{smaller}}} \quad (99)$$

Also, since

$$\frac{df}{f} = d \ln[f] \quad (100)$$

we have

$$\frac{\hat{\mathfrak{A}}[\llbracket N \rrbracket]}{\llbracket N \rrbracket} = \hat{\mathfrak{A}}[\ln[\llbracket N \rrbracket]]. \quad (101)$$

We now consider the question of “What is the minimum achievable uncertainty associated with measuring the connectivity dimensionality for a region of space having a connectivity radius  $\zeta_R$ ?” To answer this question, we re-write equation (94) in an alternate but completely equivalent way:

$$\frac{|\hat{\mathfrak{A}}_{upper}[\ln[\llbracket N \rrbracket]]|}{\llbracket N \rrbracket} = \frac{|\hat{\mathfrak{A}}_{upper}[N]|}{\llbracket N \rrbracket} \cong \frac{K[z]}{\sqrt{\zeta_{larger} \cdot \zeta_{smaller}}} = \frac{K[z] / \sqrt{z}}{\zeta_{larger}} \quad (102)$$

This allows us to suppress the explicit occurrence of  $\zeta_{smaller}$ . Next we choose those values of  $z$  and  $\zeta_{larger}$  which will minimize  $|\hat{\mathfrak{A}}_{upper}[\ln[\llbracket N \rrbracket]]|$ . The uncertainty will be a minimum for  $\zeta_{larger} = \zeta_R$ .

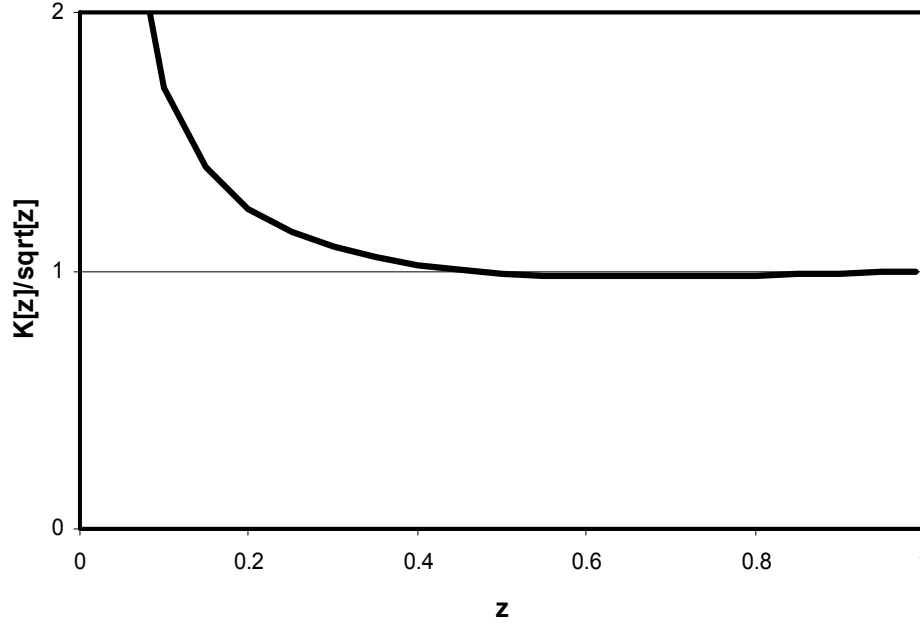


**Figure 21: A plot of the function  $K[z]/\sqrt{z}$**

For a region of a given radius, the relative upper error in computing the average connectivity dimensionality is proportional to the function  $K[z]/\sqrt{z}$  where  $z = \zeta_{\text{smaller}} / \zeta_{\text{larger}}$ . We note that for  $z > 0.4$ , the function  $K[z]/\sqrt{z}$  is approximately equal to 1 and may be treated as constant. From this we conclude the upper relative error in computing the average connectivity dimensionality for a region of space is approximately a function of radius only.

The function  $K[z]/\sqrt{z}$  is plotted in Figure 21. For larger values of  $z$ , this function is nearly constant:

$$0.975 < \frac{K[z]}{\sqrt{z}} < 1.025 \text{ for } 0.4 < z < 1 \quad (103)$$

Any value of  $z$  chosen in this range will lead to approximately the same inherent uncertainty  $\left| \hat{\mathfrak{A}}_{\text{upper}} \left[ \ln \left[ \left[ N \right] \right] \right] \right|$ . Choosing values  $z < 0.4$  leads to larger uncertainties in the computed connectivity dimensionality; therefore, it is recommended that for computing the average connectivity dimensionality of a region of space, one chooses any convenient value of  $z = \zeta_{\text{smaller}} / \zeta_{\text{larger}}$  satisfying  $0.4 < z < 1$ . When this is done, the uncertainty in computing the average connectivity dimensionality takes the especially simple form

$$\left| \hat{\mathfrak{A}}_{\text{upper}} \left[ \ln \left[ \left[ N \right]_{\mathfrak{B}_\zeta} \right] \right] \right| = \frac{\left| \hat{\mathfrak{A}}_{\text{upper}} \left[ \left[ N \right]_{\mathfrak{B}_\zeta} \right] \right|}{\left[ N \right]_{\mathfrak{B}_\zeta}} \cong \frac{1}{\zeta} \quad (104)$$

where  $\left[ N \right]_{\mathfrak{B}_\zeta}$  is the average connectivity dimensionality for the region  $\mathfrak{B}_\zeta$  of connectivity radius  $\zeta$ .

The expected rms error in the computed average connectivity dimensionality for this region is

$$\sqrt{\left\langle \left( \hat{\mathfrak{A}} \left[ \ln \left[ \left[ N \right]_{\mathfrak{B}_\zeta} \right] \right] \right)^2 \right\rangle} = \sqrt{\left\langle \left( \frac{\hat{\mathfrak{A}} \left[ \left[ N \right]_{\mathfrak{B}_\zeta} \right]}{\left[ N \right]_{\mathfrak{B}_\zeta}} \right)^2 \right\rangle} \cong \frac{\sqrt{1/3}}{\zeta} \quad (105)$$

because as derived previously the expected rms value of the uncertainty is approximately  $\sqrt{1/3}$  times its expected upper value. As explained previously, the Box 1 spaces are exempt from this inherent uncertainty.

Clearly, there are some inherent tradeoffs between getting more precise and more local information about the average connectivity dimensionality. If we want a more precise estimate of the average connectivity dimensionality, we must observe over a larger region which averages out local fluctuations in the connectivity dimensionality. Clearly as the size of the region becomes arbitrarily large it is possible to determine its average connectivity dimensionality  $\llbracket N \rrbracket$  with arbitrary precision. However this would not allow us to measure particular changes in the connectivity dimensionality within that region. If we want to measure local changes in the connectivity dimensionality we would have to compute the average connectivity dimensionalities for small regions of the space; accordingly, this would lead to higher uncertainties in the measurements.

#### 4.5 Hypergradients in the Connectivity Dimensionality

Figure 22 shows a graph containing a dimensionality hypergradient. Some of the vertices in the graph are labeled with the letters of the alphabet. The graph's discrete-continuous duality allows us to construct a matched continuous space, and this allows us to let the dimensionality  $N[\hat{P}]$  be a function of continuous position  $\hat{P}$ . Thus, it is meaningful to speak of the concept of a **dimensionality hypergradient** in a discrete-continuous dual space. (Hypergradient is the concept of gradient extended to a space whose connectivity dimensionality is variable. A gradient measures changes in a function with respect to a fixed whole number of connectivity dimensions (fixed number of independent variables) while a hypergradient measures changes in a function with respect to a variable number of connectivity dimensions.)

In Figure 22, the connectivity dimensionality varies from 1 in the upper right to just greater than 2 in the lower left of the graph. For vertices **A** and **B** in the upper right, the dimensionality is exactly 1 because these vertices lie in a perfectly linear region of the graph. Note that the amount of crosslinking also increases from the upper right to the lower left of the graph. In general, the more crosslinking, the higher the expected dimensionality for vertices in that region of the graph. A linear graph region contains no crosslinking and gives rise to a dimensionality of 1. When some crosslinking is added, but not too much, the graph regions are not linear but can still be drawn on a piece of paper without the edges crossing; for vertices in these graph regions we expect  $N[\hat{P}] \leq 2$ . From this we can infer that vertices **C** to **Q** in the graph should have dimensionalities between about 1 and 2. In the lower left of the graph, the amount of crosslinking has been increased such that some of the edges must necessarily be drawn crossed.

I invite you to try a simple exercise. Pick a few of the vertices in the graph and estimate their connectivity dimensionalities using equation (68). You will notice that the small number of vertices in the graph and the large dimensionality hypergradient makes accurate computation of the connectivity dimensionality more difficult. For all of the various parts of the graph in Figure 22, we have  $\zeta_{\min} \leq 5/2$ .

The estimated connectivity dimensionalities of the labeled vertices using  $N \cong \frac{\ln[C[7/2]] - \ln[C[5/2]]}{\ln[7/2] - \ln[5/2]}$

are given in Table 4. The estimated connectivity dimensionalities of these vertices confirm the presence of a connectivity dimensionality hypergradient within the graph.

The estimated connectivity dimensionalities do not precisely match their predicted values. We expect that the connectivity dimensionality of vertex **U** should be slightly greater than 2, but its computed estimate was only 1.8. On the other hand, we expect that the connectivity dimensionality of vertex **N** should be nearly exactly 2, but its computed estimate was 2.4. This suggests that the small range of  $\zeta$  values used to estimate the connectivity dimensionality led to an uncertainty as high as 0.4 dimensions in the connectivity dimensionality computation.

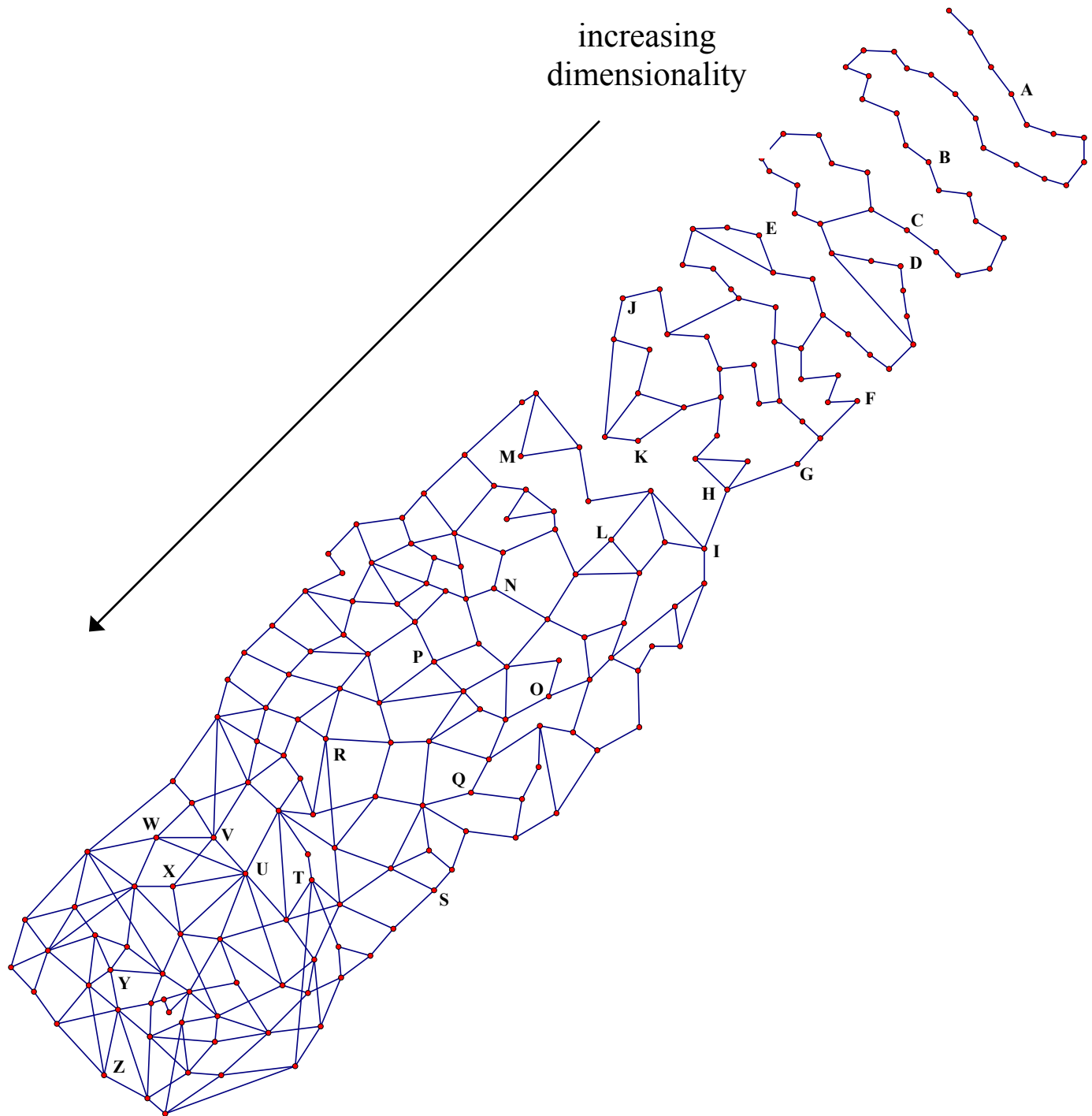


**Figure 22: Space containing a connectivity dimensionality hypergradient**

*The connectivity dimensionality increases from one for vertex A to slightly greater than 2 for later vertices, as shown in Table 4 below.*

**Table 4: Local average connectivity dimensionalities for the labeled vertices**

(Computed using  $\zeta = 5/2$  and  $7/2$ )

<b>A</b> 1	<b>E</b> 1	<b>I</b> 1.3	<b>M</b> 1	<b>Q</b> 1.9	<b>U</b> 1.8	<b>Y</b> 2.1
<b>B</b> 1	<b>F</b> 1.2	<b>J</b> 1.5	<b>N</b> 2.4	<b>R</b> 2.4	<b>V</b> 2.1	<b>Z</b> 1.8
<b>C</b> 1.5	<b>G</b> 1.7	<b>K</b> 1.5	<b>O</b> 2.1	<b>S</b> 2.2	<b>W</b> 2.1	
<b>D</b> 1	<b>H</b> 1.7	<b>L</b> 1.9	<b>P</b> 2.3	<b>T</b> 2.3	<b>X</b> 2.4	

Here we used the values  $\zeta_k = 3.5$  and  $\zeta_j = 2.5$ , which gives  $z=0.714$  and  $K[z]=0.825$ . Using equations (104) and (105) the estimated upper error is  $|\hat{\mathfrak{A}}_{upper}[\ln[\llbracket N \rrbracket]]| \cong 0.28$  while the estimated rms error is  $\left\langle \left( \hat{\mathfrak{A}}[\ln[\llbracket N \rrbracket]] \right)^2 \right\rangle = 0.16$ . This suggests that the errors in the computed dimensionalities for **Table 4** are approximately  $|\hat{\mathfrak{A}}_{upper}[\llbracket N \rrbracket]| \cong 0.56$  and  $\left\langle \left( \hat{\mathfrak{A}}[\llbracket N \rrbracket] \right)^2 \right\rangle \cong 0.32$  for those vertices with a connectivity dimensionality near 2. These values agree with the error estimates obtained by visual inspection of the graph. Visual inspection indicated that the computed connectivity dimensionalities were always accurate to within approximately  $\pm 0.4$  dimensions with an error of  $\pm 0.2$  dimensions being more typical.

Some regions of this graph are one-dimensional. In these cases, the quotient  $\sqrt[N]{\frac{\mathcal{Q}_j}{\mathcal{Q}_k}} = \frac{\mathcal{Q}_j}{\mathcal{Q}_k}$  is rational and the uncertainty in the connectivity dimensionality is predicted to be eliminated. This prediction agrees with what was observed for perfectly linear regions of the graph (e.g. vertices A, B, etc.) where the connectivity dimensionality was found to be exactly 1.

#### 4.6 How to Compute the Connectivity Dimensionality Field of Edge-Vertex Graphs

Thus far, we have discussed the average connectivity dimensionality for a region of connectivity radius  $\zeta_i$  about some vertex **A** in the discrete space  $\mathfrak{D}$ . Now we consider the problem of how to determine the connectivity dimensionality field  $N[\hat{P}]$  expressed as a continuous function of position in the matched continuous space  $\mathfrak{C}$ .

In order to graphically determine  $N[\hat{a}]$  from the count function  $C[\zeta_i, \mathbf{A}]$ , the first step is to plot  $\ln[C[\zeta_i, \mathbf{A}]]$  versus  $\ln[\zeta_i]$  for half-integer  $\zeta_i$ . The second step is to compute the average connectivity dimensionality  $N[\zeta_i, \mathbf{A}]$  from equation (69). (The average connectivity dimensionality is represented by  $N[\zeta, \mathbf{A}]$ ,  $N_{ave}[\zeta]$ , or  $\llbracket N \rrbracket$ .) For convenience,  $\zeta_{smaller}$  was set equal to the half-integer which satisfies the equation

$$2\zeta_{smaller}[\zeta_i] = \zeta_i + \frac{1}{2}. \quad (106)$$

For example,  $(\zeta, \zeta_{smaller}) = \dots(10.5, 5.5), (11.5, 5.5), (12.5, 6.5), \dots(25.5, 12.5) \dots$

Next,  $N[\zeta_i, \mathbf{A}]$  is plotted versus  $\zeta^p$  for some chosen value of  $p$  in the range  $0 < p \leq 1$ . In general, the exponent  $p$  is chosen such that small and large connectivity radii are both appropriately represented. This is done by compressing all of the  $\zeta$  values such that  $\zeta^p$  spans no more than about 1.5 orders of magnitude.<sup>20</sup> For example if we have data ranging from  $\zeta = 0.5$  to  $10000000000.5$  we might choose  $p=0.1$  or  $0.2$  to compress the data onto a plot for which  $\zeta^p$  ranged up to about 10 or 100. On the other

<sup>20</sup> If the  $\zeta^p$  values spanned many orders of magnitude, the small connectivity radii would get bunched up near the left axis and this would make it hard to see what happens at small connectivity radii. By using an appropriately chosen value of  $p$ , the small and large connectivity radii can both be visualized clearly on the same plot.



hand, if we have data over a smaller range of  $\zeta$  values, then  $p = 0.5$  or  $1$  would be sufficient to compress the data onto a reasonable scale.

The next step is to compute vertical error bars for all of the  $N[\zeta_i, \mathbf{A}]$  data points. These error bars are the upper uncertainty values computed via equation (104). Once the error bars are added, a smooth curve is fit to the  $N[\zeta_i, \mathbf{A}]$  versus  $\zeta^p$  plot. ***This curve should be as gradual and smooth as possible while intersecting nearly all of the error bars.*** This smooth curve is then extrapolated to  $\zeta \rightarrow 0$  to obtain the limit

$$N[\hat{a}] = \lim_{\zeta \rightarrow 0} \left[ \left\lfloor N[\zeta, \mathbf{A}] \right\rfloor \right] = \lim_{\zeta \rightarrow 0} \left[ \left\lfloor \frac{\ln[C[\zeta, \mathbf{A}]] - \ln[C[\zeta_{\text{smaller}}, \mathbf{A}]]}{\ln[\zeta] - \ln[\zeta_{\text{smaller}}]} \right\rfloor \right] \quad (107)$$

This provides an easy and accurate way to graphically determine the connectivity dimensionality field  $N[\hat{P}]$  from the count function. The main reason for using this method is that it allows for a robust, statistically accurate extrapolation to the  $\zeta \rightarrow 0$  limit.

You will notice that this method involves the preparation of two plots: (a.) a plot of  $\ln[C[\zeta_i, \mathbf{A}]]$  versus  $\ln[\zeta_i]$  for half-integer  $\zeta_i$ , and (b.) a plot of  $\left\lfloor N[\zeta, \mathbf{A}] \right\rfloor$  versus  $\zeta^p$  for some chosen value of  $p$  in the range  $0 < p \leq 1$ . There are reasons for preparing each of these plots. The slope of the  $\ln[C[\zeta_i, \mathbf{A}]]$  versus  $\ln[\zeta_i]$  plot is similar to the connectivity dimensionality. A dramatic change in the slope of the  $\ln[C[\zeta_i, \mathbf{A}]]$  versus  $\ln[\zeta_i]$  plot indicates a change in the number of independent connectivity dimensions with the scale of observation. On the other hand, if the  $\ln[C[\zeta_i, \mathbf{A}]]$  versus  $\ln[\zeta_i]$  plot has a nearly constant slope, the connectivity dimensionality is essentially independent of the scale of observation. The following examples demonstrate the utility of each of these two plots.

#### 4.7 Example: The Sierpiński Gasket

The Sierpiński gasket will now be used to illustrate the uncertainty in computing the connectivity dimensionality. To produce the Sierpiński gasket, one begins with a solid triangle. Next one connects the midpoints of the three sides of the triangle and removes the central area. This produces a structure comprised of three triangles. For each of these triangles, one connects the midpoints of the three sides and removes the central area. Now each of the three triangles has been divided into three smaller triangles giving a total of nine small triangles. This process is repeated with the nine triangles to produce 27 still smaller triangles, as illustrated in Figure 23 (a). This process is repeated again and again to produce an infinite number of infinitely small triangles. The resulting fractal is called the Sierpiński gasket. As commonly known, to produce the Sierpiński gasket one can start with Pascal's triangle and erase all of the binomial coefficients divisible by two. We note that the Sierpiński gasket is composed of three one-half magnification copies, with each one-half magnification copy located in a different corner of the Sierpiński gasket. With these properties in mind, we can create the Sierpiński gasket from three copies of Pascal's triangle having all the even binomial coefficients erased, as illustrated in Figure 23 (b). By placing a vertex at each of the odd binomial coefficients in Figure 23 (b) and connecting adjacent vertices with edges, the edge-vertex graph representation of the Sierpiński gasket shown in Figure 23 (c) is produced. (Only a portion of the graph is shown as it continues infinitely.) Every vertex in this graph has degree three (except the three corners which are located at infinity). The Sierpiński gasket is a strictly discrete-continuous dual space.

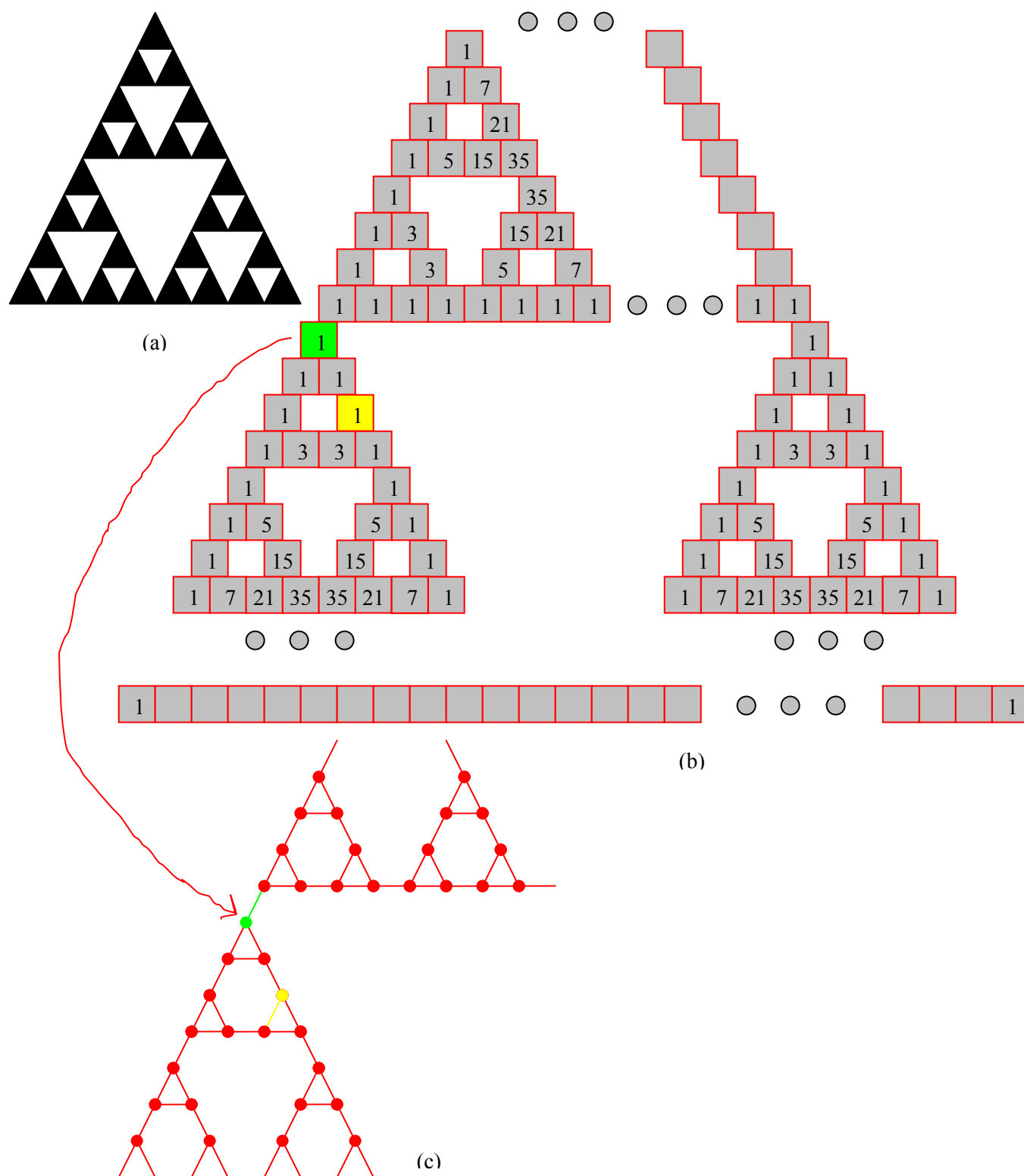


**Figure 23: The Sierpiński Gasket**

Shown above are three representations of the Sierpiński gasket: (a) space-filling model derived by repetitively deleting central triangular portions, (b) three Pascal triangles joined together with all of the even binomial coefficients removed, and (c) an edge-vertex graph representation in which each odd binomial coefficient in (b) is represented by a vertex in (c).

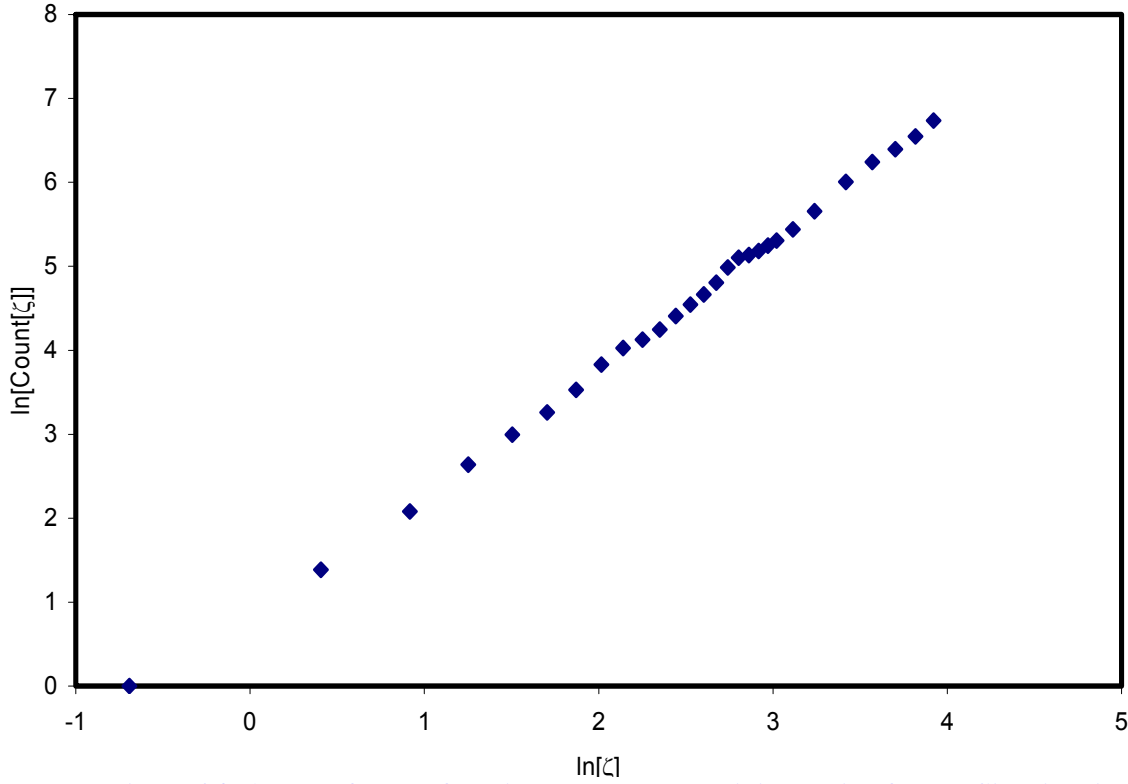


**Figure 24: A plot of count function versus connectivity radius for the Sierpiński gasket**  
*The origin is taken to be the green point in Figure 23. The trend of  $\ln[\text{Count}[\zeta]]$  versus  $\ln[\zeta]$  is nearly linear, which indicates the connectivity dimensionality field is well-developed and nearly constant with increasing connectivity radius.*

Using the methods described in this paper, we will now compute the connectivity dimensionality of the Sierpiński gasket. We take the vertex highlighted in green as our point of origin, which corresponds to the top of the lower left Pascal triangle. The binomial coefficient  $\binom{n}{p}$  occurs in row  $n$ , column  $p$  of Pascal's triangle. Each binomial coefficient is given by

$$\binom{n}{p} = \frac{n!}{(n-p)!p!}. \quad (108)$$

For a connectivity distance of  $\zeta_i$  (where  $\zeta_i = \frac{1}{2}, \frac{3}{2}, \frac{5}{2}, \dots$ ) from the green vertex, the maximum value of  $n$  reached in the lower left triangle is  $\zeta_i - 1/2$  while the maximum value of  $n$  reached in the top Pascal triangle is  $\zeta_i - 3/2$ . For a given value of  $n$ , all values of  $p$  are the same connectivity distance from the green vertex. We further note that

$$1 - (-1)^{\binom{n}{p}} = \begin{cases} 0 & \text{if } \binom{n}{p} \text{ is even} \\ 2 & \text{if } \binom{n}{p} \text{ is odd} \end{cases}. \quad (109)$$

From this it follows that the count function is given by

$$Count[\zeta_i] = \frac{1}{2} \left( \sum_{n=0}^{\zeta_i-1/2} \sum_{p=0}^n \left( 1 - (-1)^{\binom{n}{p}} \right) + \sum_{n=0}^{\zeta_i-3/2} \sum_{p=0}^n \left( 1 - (-1)^{\binom{n}{p}} \right) \right). \quad (110)$$

The factor of 1/2 occurs to cancel the factor of 2 in equation (109). The first term on the right side of equation (110) accounts for vertices in the lower left Pascal triangle while the second term accounts for the top Pascal triangle.

The first step in determining the connectivity dimensionality is to plot  $\ln[Count[\zeta]]$  versus  $\ln[\zeta]$  as shown in Figure 24. To estimate the connectivity dimensionality, we could fit the  $\ln[Count[\zeta]]$  versus  $\ln[\zeta]$  data to a straight line using a least squares fit. Doing this gives the line  $\ln[Count[\zeta]] = 1.5011 \cdot \ln[\zeta] + 0.7981$ , which corresponds to the value  $N \cong 1.5011$ . Using this estimate of the connectivity dimensionality and  $k=3$ , equation (65) gives  $\zeta_{\min} = \frac{1}{2}$ .

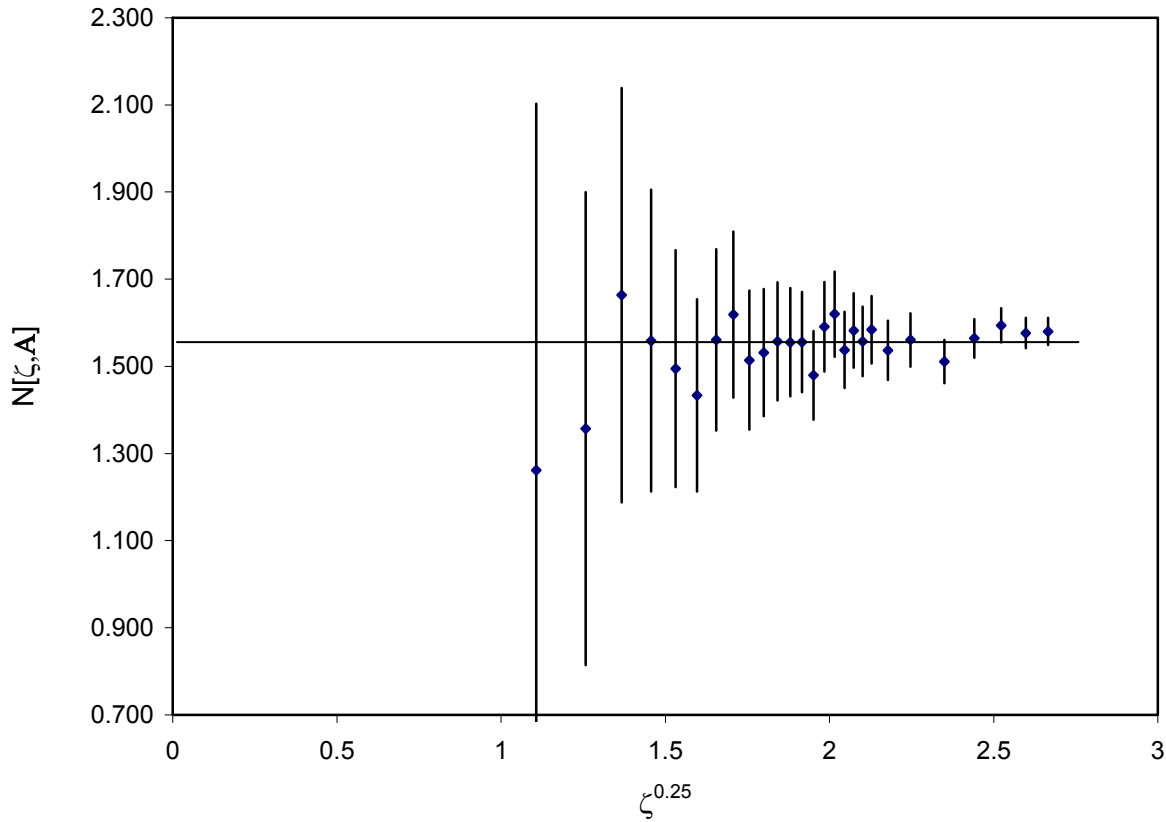


**Figure 25: Plot to determine the local connectivity dimensionality in the Sierpiński gasket**  
*In the above plot, the blue data points are the average connectivity dimensionalities computed for each value of the connectivity radius about the green vertex. The error bars represent the computed upper uncertainties on the computed average connectivity dimensionalities. The horizontal line intersecting all of the error bars is extrapolated to  $\zeta = 0$  to obtain the connectivity dimensionality of the green vertex.*

To achieve the best possible accuracy, a second plot is prepared in which  $N[\zeta, \mathbf{A}]$  is plotted versus  $\zeta^p$  for  $0 < p < 1$ . This is done in Figure 25. For each value of the connectivity radius, a higher and lower bound on the connectivity dimensionality was computed via

$$\begin{pmatrix} \text{lower bound} \\ \text{higher bound} \end{pmatrix} = \begin{pmatrix} N[\zeta, \mathbf{A}] - \mathfrak{A}_{\text{upper}}[N[\zeta, \mathbf{A}]] \\ N[\zeta, \mathbf{A}] + \mathfrak{A}_{\text{upper}}[N[\zeta, \mathbf{A}]] \end{pmatrix} \quad (111)$$

where the upper uncertainty in the average connectivity dimensionality was computed via equation (104); the numeric values are given in Table 5 and plotted as the error bars in Figure 25.

Of extreme interest, all of the error bars overlap because the highest lower bound (1.555) is less than the lowest higher bound (1.560). Consequently, a single horizontal line ( $N \cong 1.558 \pm 0.003$ ) can be drawn that falls within the range of uncertainty in the connectivity dimensionality for each connectivity radius. Based upon this procedure, the estimated value of the connectivity dimensionality field for the green vertex of the Sierpiński gasket is  $N[\text{green vertex}] \cong 1.558 \pm 0.003$ . This means the value of  $N \cong 1.501$  obtained by the simple linear regression of Figure 24 was too low.

**Table 5: Data for computing the local connectivity dimensionality in the Sierpiński gasket**

$\zeta_i$	$\ln[\zeta_i]$	$\text{Count}[\zeta_i]$	$\ln[\text{Count}[\zeta_i]]$	$N[\zeta, \mathbf{A}]$	$\mathfrak{A}_{\text{upper}}[N[\zeta, \mathbf{A}]]$	lower bound	higher bound
0.5	-0.69315	1	0	--	--	--	--
1.5	0.405465	4	1.386294	1.262	0.841	0.421	2.103
2.5	0.916291	8	2.079442	1.357	0.543	0.814	1.900
3.5	1.252763	14	2.639057	1.663	0.475	1.188	2.138
4.5	1.504077	20	2.995732	1.559	0.346	1.212	1.905
5.5	1.704748	26	3.258097	1.495	0.272	1.223	1.767
6.5	1.871802	34	3.526361	1.433	0.221	1.213	1.654
7.5	2.014903	46	3.828641	1.561	0.208	1.353	1.769
8.5	2.140066	56	4.025352	1.619	0.190	1.428	1.809
9.5	2.251292	62	4.127134	1.514	0.159	1.355	1.674
10.5	2.351375	70	4.248495	1.532	0.146	1.386	1.678
11.5	2.442347	82	4.406719	1.557	0.135	1.422	1.693
12.5	2.525729	94	4.543295	1.555	0.124	1.431	1.680
13.5	2.60269	106	4.663439	1.556	0.115	1.441	1.671
14.5	2.674149	122	4.804021	1.480	0.102	1.378	1.582
15.5	2.74084	146	4.983607	1.591	0.103	1.488	1.694
16.5	2.80336	164	5.099866	1.620	0.098	1.522	1.718
17.5	2.862201	170	5.135798	1.538	0.088	1.450	1.626
18.5	2.917771	178	5.181784	1.582	0.086	1.497	1.668
19.5	2.970414	190	5.247024	1.557	0.080	1.477	1.637
20.5	3.020425	202	5.308268	1.584	0.077	1.507	1.661
22.5	3.113515	230	5.438079	1.537	0.068	1.468	1.605
25.5	3.238678	286	5.655992	1.561	0.061	1.499	1.622
30.5	3.417727	406	6.006353	1.511	0.050	1.461	1.560
35.5	3.569533	514	6.242223	1.564	0.044	1.520	1.608
40.5	3.701302	598	6.393591	1.594	0.039	1.555	1.633
45.5	3.817712	698	6.548219	1.576	0.035	1.542	1.611
50.5	3.921973	842	6.73578	1.580	0.031	1.549	1.612

The upper uncertainty in the connectivity dimensionality can be defined as the range of uncertainty which allows almost all of the error bars in the  $N[\zeta, \mathbf{A}]$  versus  $\zeta^p$  plot to intersect a smooth curve whose slope varies slowly (or is constant). In this particular example, the smooth curve is a straight line. We notice that if the upper uncertainty is decreased then it is no longer possible to draw a slowly varying smooth curve that intersects all of the error bars. For example, when the upper uncertainty is multiplied

by 94% in this example then it is no longer possible to draw a horizontal line which intersects all of the error bars.

Moreover, equation (104) predicts the upper uncertainty should scale proportionally to  $1/\zeta$ . To test this, the quantity  $|1.558 - N[\zeta, \mathbf{A}]|$  has been plotted versus connectivity radius in Figure 26. The red line in the figure shows the computed upper uncertainty values. (See Table 5.) The distribution of points under the curve suggests the scaling of upper uncertainty versus connectivity radius is reasonable.

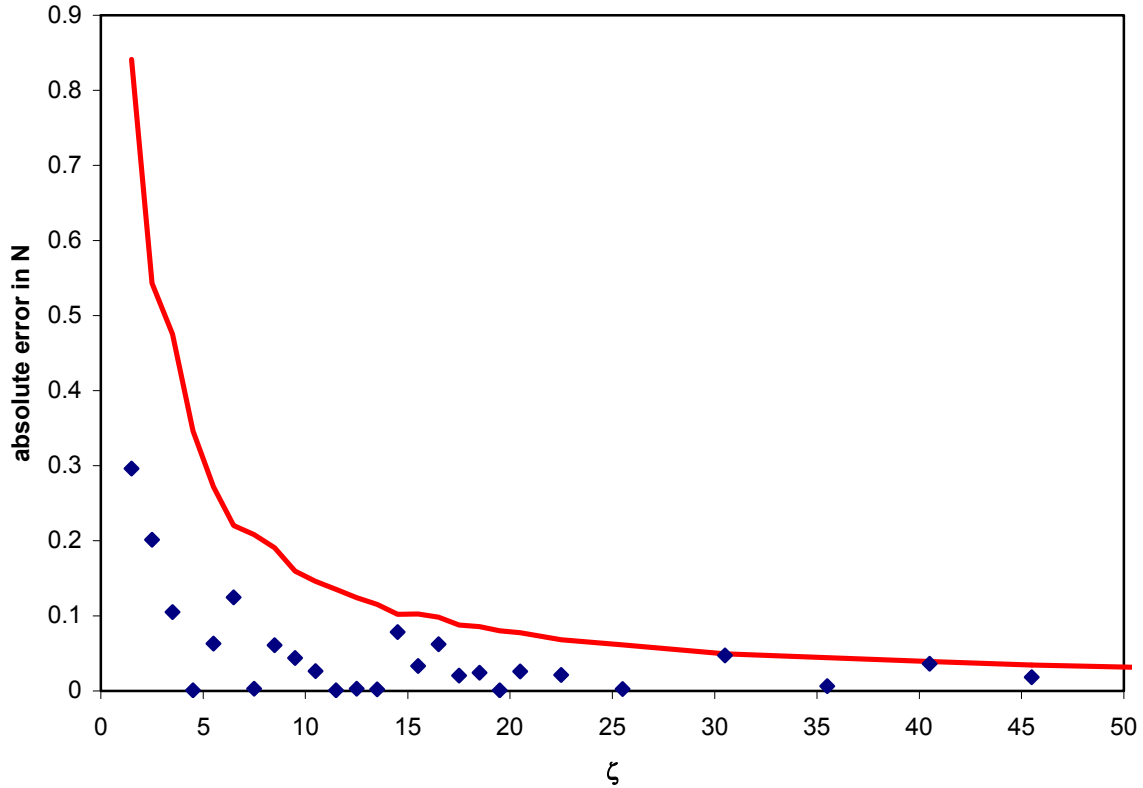


**Figure 26: The upper uncertainty in the average connectivity dimensionality**

The red line in the above plot shows the computed upper uncertainty values in the average connectivity dimensionality. The blue points show the computed absolute errors in the average connectivity dimensionality for each connectivity radius. The blue points fall below the red line, suggesting the computed upper uncertainty is valid.

Finally, let us turn our attention to the rms error in the computed connectivity dimensionality. Multiplying both sides of equation (105) by  $\zeta$  gives:

$$\sqrt{\left\langle \left( \frac{\zeta \cdot \hat{\alpha}[\llbracket N \rrbracket]}{\llbracket N \rrbracket} \right)^2 \right\rangle} \cong \sqrt{1/3} = 0.577... \quad (112)$$

We can test the validity of this equation by computing

$$\sqrt{\left( \frac{1}{(27-1)} \sum \left( \frac{(1.558 - N[\zeta, \mathbf{A}])\zeta}{1.558} \right)^2 \right)} = 0.428 \quad (113)$$

where the summation is conducted over the 27 data points in Table 5. Equation (113) has a form analogous to the square root of the bias-corrected sample variance commonly employed in statistics:

$$s_{T-1}^2 = \frac{1}{T-1} \sum_{i=1}^T (y_i - \llbracket y \rrbracket) \quad (114)$$

where  $T$  is the total number of data points in the sample. A comparison of the right sides of equations (112) and (113) shows reasonable agreement.

What else can we learn from the Sierpiński gasket example? Not all vertices in the Sierpiński gasket have equivalent environments. For example, there are 20 vertices within  $\zeta = 4.5$  of the green vertex but only 18 vertices within  $\zeta = 4.5$  of the yellow vertex in Figure 23. Because different vertices in the Sierpiński gasket have different environments, different vertices can have different connectivity dimensionalities. Consequently, the connectivity dimensionality field of the Sierpiński gasket is not constant.

The macroscopically averaged connectivity dimensionality (that is the connectivity dimensionality averaged over all vertices) of the Sierpiński gasket can be computed in the following manner. Suppose we have a geometric object of ‘diameter’ (or edge length)  $b$  whose macroscopic connectivity dimensionality is  $N$ . If the ‘diameter’ (or edge length) of the geometrical object is increased to  $2b$  then we expect the hypervolume of the object to increase by a factor of  $2^N$ . In the case of the Sierpiński gasket, the edge length can be increased by a factor of two by creating two identical copies of the Sierpiński gasket. The original and two copies are placed at the three corners of an equilateral triangle leaving an identically sized region blank in the center of the larger triangle. This resulting object is identical to the original Sierpiński gasket except that it has twice the edge length and three times the hypervolume (because it contains one original and two copies of the original space). Thus, we clearly have  $3 = 2^N$  giving the macroscopically averaged connectivity dimensionality of  $N = \frac{\ln[3]}{\ln[2]} = 1.58496...$  for the Sierpiński gasket.

Since the above computed connectivity dimensionality was so close to the macroscopically averaged value we might in fact be led to conclude the computed connectivity dimensionality of  $N \cong 1.558 \pm 0.003$  was mistakenly computed too low by 0.027. However, this presumption is flawed. The reason is because the computed connectivity dimensionality  $N \cong 1.558 \pm 0.003$  refers to the region of space in the vicinity of the green vertex of Figure 23 and for a connectivity radius less than or equal to  $\zeta = 50.5$ . On the other hand, the macroscopically averaged connectivity dimensionality refers to the connectivity dimensionality averaged over all of the vertices contained in the Sierpiński gasket. As already pointed out, the environments of different vertices in the Sierpiński gasket are different; therefore, the connectivity dimensionality field of the Sierpiński gasket need not be a constant. Consequently, there is no reason to presume that the connectivity dimensionality field of the Sierpiński gasket should equal its macroscopically averaged connectivity dimensionality.

In fact, a difference between the local average value of the connectivity dimensionality and the macroscopic value is predicted due to the inherent uncertainty in the connectivity dimensionality field. The Sierpiński gasket is expected to have local patches with higher or lower connectivity dimensionalities than the macroscopic average. From equation (105), the average connectivity dimensionality of a region in a not Box 1 space is expected to have an rms deviation from the macroscopic average of  $\frac{\sqrt{1/3}N}{\zeta}$ .

(This is the inherent uncertainty in the connectivity dimensionality for such a region.) For a connectivity radius  $\zeta = 50.5$  (the size of the region investigated) this gives an expected rms deviation of 0.02 between the average connectivity dimensionality of the region and the macroscopic connectivity dimensionality of the space. In this example, the actual difference between  $N \cong 1.558 \pm 0.003$  and

$N = \frac{\ln[3]}{\ln[2]} = 1.58496...$  is 0.027, which indicates the deviation is very close to the expected deviation for a region of this size.



In summary, the difference between  $N \cong 1.558 \pm 0.003$  and  $1.58496\dots$  is not an error in the computation but rather a manifestation of inherent dimensional fluctuation in a fractional-dimensional space. This dimensional fluctuation is actually *present* in the space, and when we measure this fluctuation we are measuring something that is real. That is, the dimensionality field of the Sierpiński gasket is actually nonconstant and we have managed to find a local region whose average connectivity dimensionality is less than the macroscopic average by about  $0.027 \pm 0.003$  dimensions.

In general, the fitted line in the  $N[\zeta, \mathbf{B}]$  versus  $\zeta^p$  plot can be nonlinear. A nonlinear curve is warranted when both of the following conditions are met: (a) the  $N[\zeta, \mathbf{B}]$  values display a noticeable upward or downward trend as  $\zeta^p$  increases and (b) the upward or downward trend is significant enough that a straight horizontal line cannot be drawn which intersects all of the error bars. In the example of [Figure 25](#) a straight horizontal line could be drawn which intersected all of the error bars so there was no need to introduce nonlinearity.

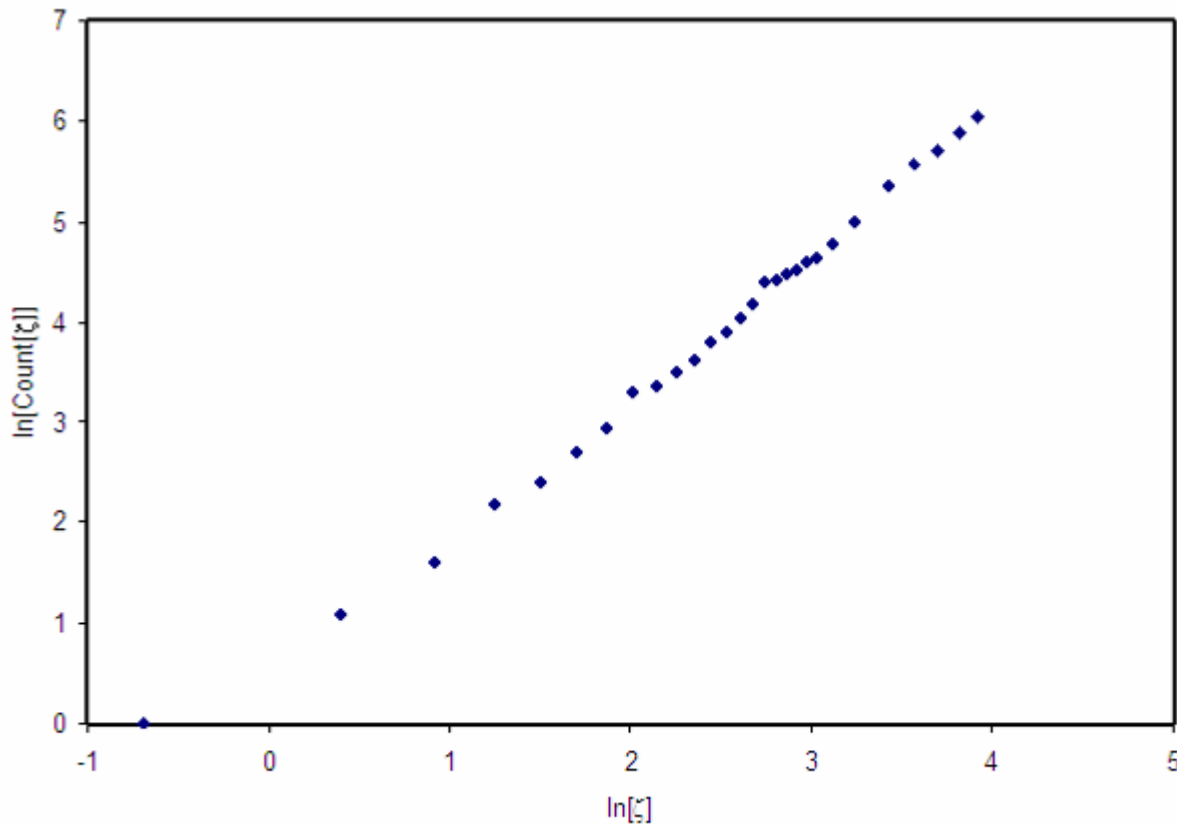


**Figure 27: A plot of count function versus connectivity radius for a corner vertex in the Sierpiński gasket**

Now let's repeat the above analysis taking one of the three corners of the Sierpiński gasket as our point of origin. In this case, the count function is given by

$$Count[\zeta] = \frac{1}{2} \left( \sum_{n=0}^{\zeta^{-1/2}} \sum_{p=0}^n \left( 1 - (-1)^{\binom{n}{p}} \right) \right). \quad (115)$$

The plot below shows how the logarithm of the count function varies with the logarithm of the connectivity radius. This curve has a slightly smaller slope at smaller connectivity radii.

In a similar manner as before, we compute the average connectivity dimensionalities for different connectivity radii and plot them with error bars. (See [Figure 28](#).) In this case, a single horizontal line cannot be drawn to intersect all of the error bars. An attempt has been made to draw a smooth curve

through all of the error bars; however, there are two outlying points whose error bars do not intersect the curve. The smooth curve is given by

$$N_{red}[\zeta] = \frac{\frac{\ln[3]}{\ln[2]} \zeta + 3.2}{\zeta + 3.2}. \quad (116)$$

Because the error bars for two of the points do not intersect the red curve, we conclude the error in the computed average connectivity dimensionality can exceed the upper uncertainty. We infer the upper uncertainty is a soft (i.e. typical) upper bound on the computed average connectivity dimensionality, and it can be exceeded in some cases.

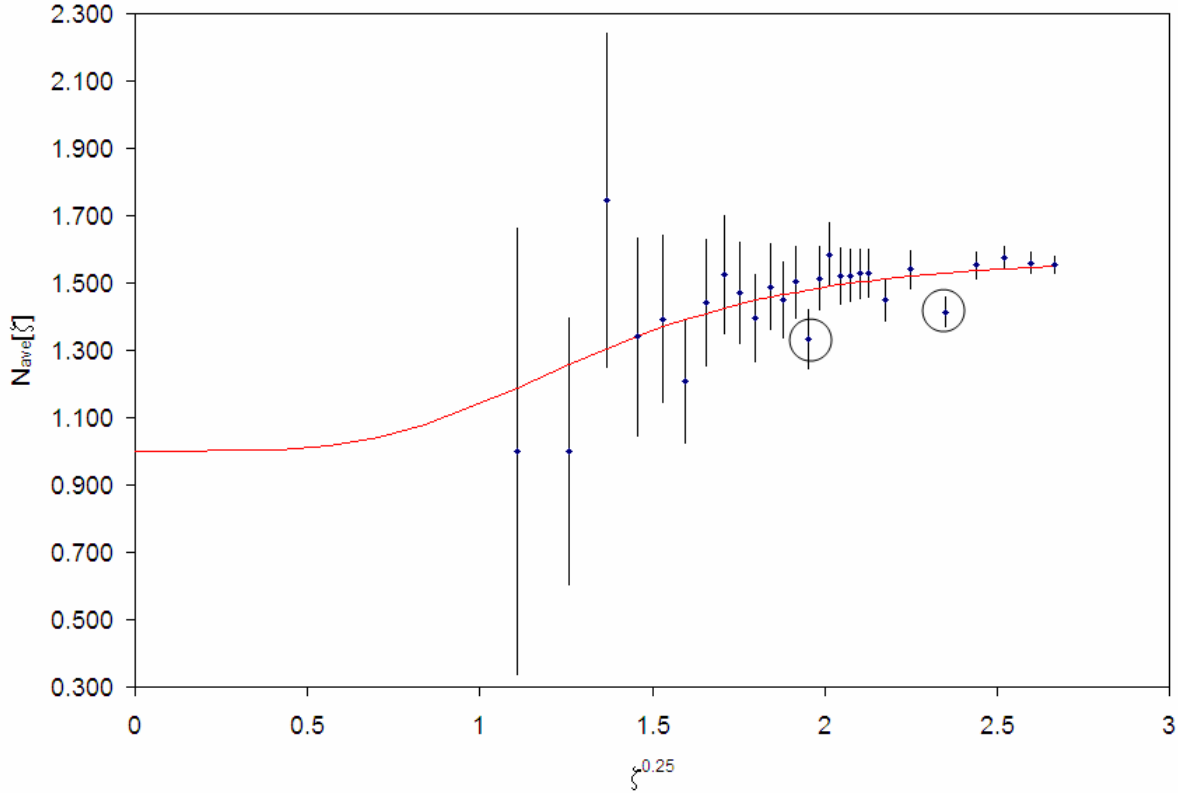


**Figure 28: Plot to determine the connectivity dimensionality of a corner vertex in the Sierpiński gasket**

*In the above plot, the blue data points are the average connectivity dimensionalities computed for each value of the connectivity radius about the corner vertex. The error bars represent the computed upper uncertainties on the computed average connectivity dimensionalities. The red line represents a smooth curve that has been drawn through the data. The red curve intersects most of the error bars, but there are two outliers (circled points).*

According to the recommended procedure for computing the connectivity dimensionality field, the connectivity dimensionality at the corner point is given by the limit

$$N[\text{corner vertex}] = \lim_{\zeta \rightarrow 0} \frac{\frac{\ln[3]}{\ln[2]} \zeta + 3.2}{\zeta + 3.2} = 1. \quad (117)$$

On the other hand, the macroscopically averaged connectivity dimensionality is recovered in the limit of arbitrarily large connectivity radius:

$$\mathbb{N} = \lim_{\zeta \rightarrow \infty} \frac{\frac{\ln[3]}{\ln[2]} \zeta + 3.2}{\zeta + 3.2} = \frac{\ln[3]}{\ln[2]}. \quad (118)$$

Why does the corner vertex have a connectivity dimensionality of only one? The reason is because the count function starts off in the same pattern as a straight line:

$$\text{Count}[\zeta = 1/2] = 1, \text{Count}[\zeta = 3/2] = 3, \text{ and } \text{Count}[\zeta = 5/2] = 5.$$

To compute the rms deviation factor, we use the equation

$$\sqrt{\left( \frac{1}{(27-1)} \sum \left( \frac{(N_{red}[\zeta] - N[\zeta, \mathbf{B}]) \zeta}{N_{red}[\zeta]} \right)^2 \right)} = 0.536 \quad (119)$$

where  $N_{red}[\zeta]$  is the connectivity dimensionality given by the smooth curve (red line). The rms deviation factor of 0.536 is in reasonable agreement with the predicted factor of  $\sqrt{1/3} = 0.577\dots$

As explained in the previous section, dimensional perturbations of this nature are inherent to the structure of discrete-continuous dual spaces except when the connectivity dimensionality is zero or one, when the structure of the connectivity is representable by a periodic lattice, or when the number of quantifiable geometric units per unit hypervolume is infinite.

#### 4.8 Isolated Point and Straight Line

For an isolated point,  $C[\zeta, \mathbf{A}] = 1$  for all  $\zeta$ . Thus,

$$N = \lim_{\zeta \rightarrow 0} \frac{d \ln \left[ \left[ \left[ C[\zeta, \mathbf{A}] \right] \right] \right]}{d \ln[\zeta]} = \lim_{\zeta \rightarrow 0} \frac{d \ln[1]}{d \ln[\zeta]} = 0. \quad (120)$$

Therefore the connectivity dimensionality of an isolated point equals zero identically.

For a straight line,  $C[\zeta_i, \mathbf{A}] = 2\zeta_i$  where  $\zeta_i$  is half-integer. Thus,

$$N = \lim_{\zeta \rightarrow 0} \frac{d \ln \left[ \left[ \left[ C[\zeta, \mathbf{A}] \right] \right] \right]}{d \ln[\zeta]} = \lim_{\zeta \rightarrow 0} \frac{d \ln[2\zeta]}{d \ln[\zeta]} = 1. \quad (121)$$

Therefore the connectivity dimensionality of a straight line equals one identically. As predicted, there is no uncertainty in the connectivity dimensionality for these two cases.

#### 4.9 Tilings and Lattices

##### 4.9.1 Types of Lattices

**Definition 21:** Here a **lattice** is defined as a discrete space that is strictly discrete-continuous dual to a continuous differential manifold.

Lattices are a special type of discrete-continuous dual space. In particular, the interpolated continuous space of a lattice has a constant integer dimensionality within the limits of measurement uncertainty in the connectivity dimensionality. (The connectivity dimensionality of a manifold is always a constant integer value. Continuous spaces whose connectivity dimensionality varies as a function of position and/or is noninteger are not classified as manifolds.)

Every differential manifold can be discretized by constructing a discrete lattice within it. The mathematics of manifolds and lattices are dual to each other with lattices being the discrete counterpart of

the continuous manifolds. Since the lattice can be properly drawn in the manifold (i.e. drawn without any false crossings), the lattice and manifold are strictly dual to each other.

Lattices are classified according to the following four basic criteria:

1. The connectivity dimensionality of the lattice—for example, whether the lattice is 1-dimensional, 2-dimensional, 3-dimensional, 4-dimensional, etc.
2. The type of manifold which the lattice is dual to—for example, whether the lattice is dual to a Euclidean space, a hypersphere, a toroid, a Klein bottle, etc.
3. Whether or not the lattice possesses translational symmetry—lattices possessing translational symmetry are called **periodic lattices** and the periodic unit is called the **unit cell**, while those which do not possess translational symmetry are called **aperiodic lattices**
4. Whether or not the lattice is constructed from a small number of repeated shapes—lattices constructed from a small number of shapes repeated over and over are called **tiled lattices**, while those which are not constructed from a small number of repeated shapes are called **untiled lattices**

All periodic lattices are tiled lattices. Examples of periodic lattices include the crystal structures of many solids. On the other hand, some tiled lattices are aperiodic, and these are called **Penrose tilings**. Glasses are lattices which are neither periodic nor tiled.

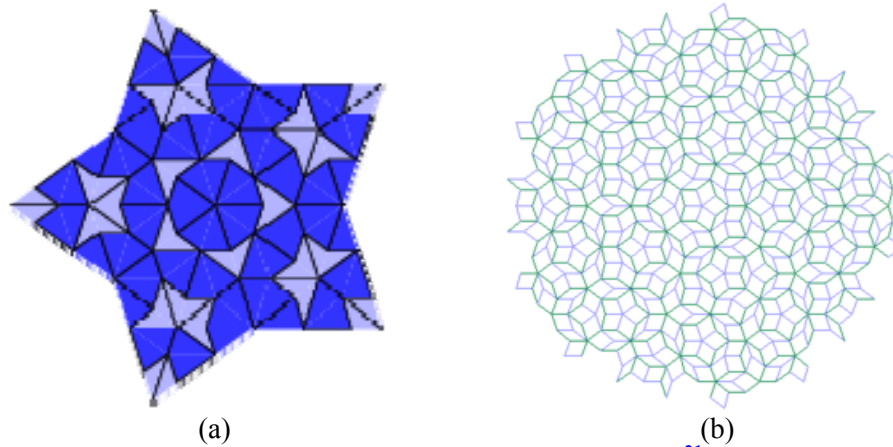


**Figure 29: Examples of Penrose tilings<sup>21</sup>**

*A Penrose tiling contains a few basic tile shapes that are arranged to cover a surface without translational symmetry (i.e. in an aperiodic pattern).*

An important property characterizing lattices and other types of networks is the degree distribution. The degree distribution  $f[k]$  is the probability that a randomly chosen vertex in a graph will have degree  $k$ . In this article, a **regular lattice** means a periodic lattice that spans a Euclidean space and for which every vertex of the lattice has the same degree and every edge has the same length. A 1-dimensional regular lattice has vertices of degree 2. Two-dimensional regular lattices have vertex degrees of 3 (hexagon lattice), 4 (square lattice), or 6 (triangle lattice). Some examples of three dimensional regular lattices are degree 6 (cubic lattice) and 12 (hexagonal close packed and cubic close packed).

<sup>21</sup> Left and right images (Public Domain) downloaded from <http://mathworld.wolfram.com/PenroseTiles.html> and [http://en.wikipedia.org/wiki/Penrose\\_tiling](http://en.wikipedia.org/wiki/Penrose_tiling) on 12/23/06.

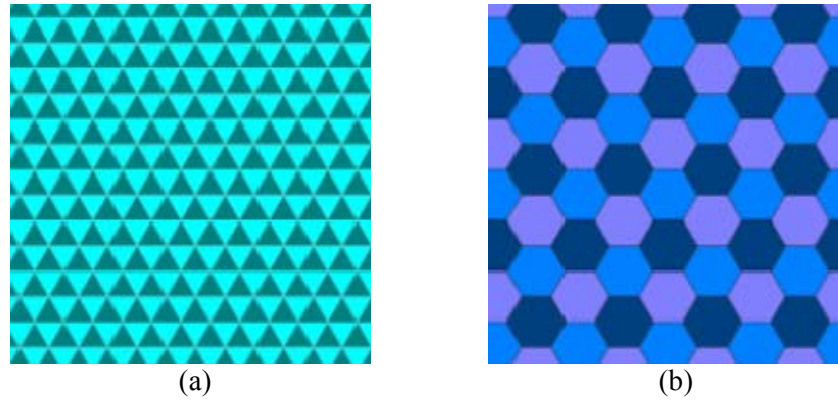


**Figure 30: Examples of regular lattices<sup>22</sup>**

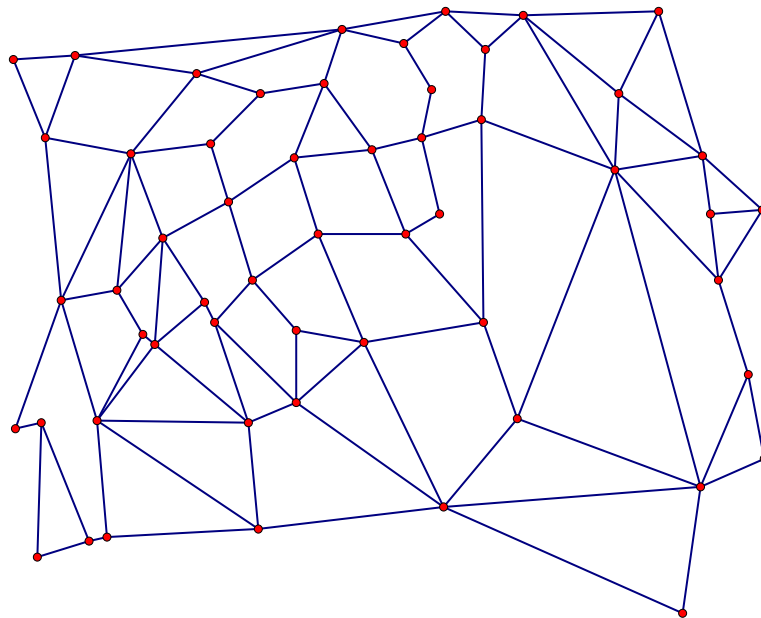


**Figure 31: Section of an untiled lattice**

*An **untiled lattice**, also called a **glass**, is an aperiodic lattice that is not constructed from a small set of repeated shapes.*

#### 4.9.2 Removing the Connectivity Dimensionality Error for Periodic Lattices

In a regular lattice, the environment around every vertex is identical. Consequently, every vertex in a regular lattice must have the same connectivity dimensionality. Since every vertex in the regular lattice has the same connectivity dimensionality, the connectivity dimensionality field of the regular lattice is constant and equal to its average connectivity dimensionality. Recall that a regular lattice is strictly dual to a manifold of integer dimensionality. Clearly, the average connectivity dimensionality of the regular lattice must equal the average connectivity dimensionality of the continuous space to which it is strictly dual. From this it follows that the connectivity dimensionality of every regular lattice is integer. Since the connectivity dimensionality of a regular lattice is exactly integer, for regular lattices it is possible to remove all uncertainty in computing the connectivity dimensionality.

<sup>22</sup> Images (Public Domain) downloaded from [http://en.wikipedia.org/wiki/Hexagonal\\_lattice](http://en.wikipedia.org/wiki/Hexagonal_lattice).

Now let us consider all periodic lattices. To each such periodic lattice we can assign a translational unit cell. Let two unit cells be called adjacent iff. they share one or more points in space. For example, two unit cells sharing a face, edge, or corner are adjacent to each other. We can construct a companion graph for the periodic lattice in which every unit cell is represented by a vertex and two vertices are joined by an edge in the graph iff. the two corresponding unit cells are adjacent in the periodic lattice. (See Figure 19.) The lattice companion graph is then used to compute the connectivity dimensionality of the periodic lattice.

A lattice companion graph ( $N \geq 2$ ) has many edges that appear to cross at points which are not vertices. Because the edges appear to cross, the lattice companion graph cannot be properly drawn in the manifold strictly dual to the lattice represented by the lattice companion graph. For this reason, a lattice companion graph is not itself a lattice. The lattice companion graph is clearly periodic since each vertex in the graph has an equivalent environment and the graph is translationally invariant. Just as there are lattices that are not periodic, so also there are periodic graphs that are not lattices.

Consider a 2-dimensional periodic lattice. Associated with this periodic lattice are two translation vectors which we shall call  $\vec{v}_a$  and  $\vec{v}_b$ . The position of each unit cell can be represented by integer coordinates along these two translation vectors. For example, the unit cell  $(5, -2)$  is formed by translating the  $(0, 0)$  unit cell 5 times by  $\vec{v}_a$  and 2 times by  $-\vec{v}_b$ . The unit cells adjacent to  $(a, b)$  are  $(a+1, b)$ ,  $(a-1, b)$ ,  $(a, b+1)$ ,  $(a, b-1)$ ,  $(a+1, b+1)$ ,  $(a-1, b+1)$ ,  $(a-1, b-1)$ , and  $(a+1, b-1)$ .

Interestingly, the count function  $C[\zeta, \mathbf{A}]$  is the same for all companion graphs of periodic lattices with the same connectivity dimensionality. For a connectivity distance of  $\zeta_i$  one extends to  $\pm \left( \zeta_i - \frac{1}{2} \right)$  along each translation vector, which gives a total of  $2\zeta_i$  possible coordinate values along each translation vector. For example, for  $\zeta_i = \frac{11}{2}$  the possible coordinates along each translation vector are  $-5, -4, -3, -2, -1, 0, 1, 2, 3, 4, 5$ , which gives a total of 11 possible values along each translation vector. For an N-dimensional space there are N coordinate vectors giving a total of  $(2\zeta_i)^N$  possible coordinate sets within a connectivity distance  $\zeta_i$  from unit cell  $\mathbf{A}$ . Therefore, we have

$$C[\zeta_i, \mathbf{A}] = (2\zeta_i)^N \text{ for a periodic lattice.} \quad (122)$$

Because this count function scales perfectly, the connectivity dimensionality of the periodic lattice has no uncertainty and can be computed without error.

In the case of an aperiodic lattice, no translational unit cell can be defined and there is inherent uncertainty associated with computing the connectivity dimensionality field. As an example, consider the center vertex of the Penrose tiling in Figure 29(b). The associated count function is given in the second column of Table 6. Another column gives the count function for the companion graph of a 2-dimensional periodic lattice. The Nth root (in this case square root) of the count function is often irrational for the aperiodic lattice but always rational for the companion graph of the periodic lattice. Using values of  $\zeta_1 = 3.5$  and  $\zeta_2 = 4.5$ , the computed average connectivity dimensionalities by equation (68) are 3.53 and 2 for the region in the Penrose tiling and 2-dimensional periodic lattice, respectively. When values of  $\zeta_1 = 2.5$  and  $\zeta_2 = 4.5$  are used, the computed average connectivity dimensionalities become 2.61 and 2 for the region in the Penrose tile and 2-dimensional periodic lattice, respectively. The change in value means there is uncertainty in computing the connectivity dimensionality of the region in the Penrose tile. On the other hand, there is no uncertainty associated with computing the connectivity dimensionality for the region in the periodic lattice companion graph.

**Table 6: Count function for a Penrose tile compared to a 2-dimensional periodic lattice.**

connectivity radius	center vertex in the Penrose tile of Figure 29(a)		2-dimensional periodic lattice companion graph	
$\zeta$	$C[\zeta, \mathbf{A}]$	$\sqrt{C[\zeta, \mathbf{A}]}$	$C[\zeta, \mathbf{A}]$	$\sqrt{C[\zeta, \mathbf{A}]}$
$\frac{1}{2}$	1	rational	1	rational
$1\frac{1}{2}$	6	irrational	9	rational
$2\frac{1}{2}$	11	irrational	25	rational
$3\frac{1}{2}$	21	irrational	49	rational
$4\frac{1}{2}$	51	irrational	81	rational

What is the connectivity dimensionality for the center vertex in the Penrose tile of Figure 29(a)? To answer this question, one must prepare plots like those in Figure 25 - Figure 28. This exercise is left to the reader. In general, different vertices in the Penrose tile can have different connectivity dimensionalities. Moreover, even after such plots are constructed there will be a small residual uncertainty in the connectivity dimensionality for each vertex of the Penrose tile.

#### 4.10 Tree-like Networks

Consider a graph which starts as a single edge between two vertices. Next, suppose the graph spawns two new edges and vertices from one end. Then, consider each of these new edges in turn spawning two new edges and vertices. Continuing this process indefinitely produces the infinite tree shown in Figure 32 below.

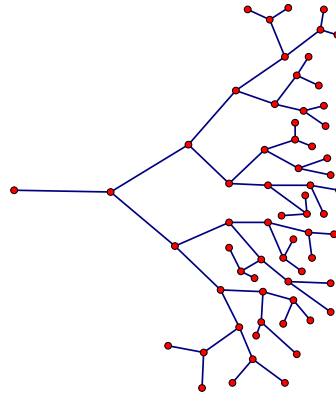


**Figure 32: Noncrosslinked infinite tree**  
(only 6 generations shown)

*A noncrosslinked tree contains no hyperbubbles and has a high quartropy.*

Let's try to compute the connectivity dimensionality of vertices in this graph. In this particular example, the count function is given by the formula

$$C[\zeta, \mathbf{P}] = 3(2^W) - 2 \quad (123)$$

where  $W$  is the largest integer such that

$$W \leq \zeta. \quad (124)$$

The asymptotically matched count function must satisfy

$$\mathcal{F}_{\text{vertexal}}[0, \widehat{P}] = \left\lfloor C[0, \mathbf{P}] \right\rfloor = 0 \text{ for } N[\widehat{P}] > 0. \quad (125)$$



Applying the constraint of equation (125) is particularly important. It specifies that the asymptotically matched count function approaches zero as the radial distance approaches zero. This constraint appears automatically when the count function scales like  $\left[ C[\zeta, \mathbf{P}] \right] \propto \zeta^n$  such as was the case in most of the previous examples. Infinite trees have count functions with exponential dependence on the radial distance, and equation (123) displays this behavior.

For a noncrosslinked infinite tree in which each edge spawns  $G$  new vertices and edges, the asymptotically matched value of the count function can be expanded as a sum of the form

$$\mathcal{F}_{\text{vertexal}}[\zeta, \widehat{P}] = \left[ C[\zeta, \mathbf{P}] \right] = \sum_j a_j G^{b_j \zeta}. \quad (126)$$

Applying equation (125) gives

$$\mathcal{F}_{\text{vertexal}}[0, \widehat{P}] = \sum_j a_j = 0. \quad (127)$$

We have

$$d \ln \left[ \sum_j a_j G^{b_j \zeta} \right] = \frac{\sum_j a_j b_j \ln[G] G^{b_j \zeta}}{\sum_j a_j G^{b_j \zeta}}. \quad (128)$$

Near  $\zeta = 0$ , we can expand the exponentials as

$$G^{b_j \zeta} = 1 + b_j \ln[G] \zeta + O[\zeta^2] \quad (129)$$

Near  $\zeta = 0$ , equations (129) and (127) give

$$\sum_j a_j G^{b_j \zeta} = \sum_j a_j + \sum_j a_j b_j \ln[G] \zeta + O[\zeta^2] = \sum_j a_j b_j \ln[G] \zeta + O[\zeta^2] \quad (130)$$

and

$$\sum_j a_j b_j \ln[G] G^{b_j \zeta} = \sum_j a_j b_j \ln[G] + O[\zeta]. \quad (131)$$

Also, we have

$$\frac{1}{d \ln[\zeta]} = \frac{1}{1/\zeta} = \zeta. \quad (132)$$

Combining these results we obtain

$$\begin{aligned} N[\widehat{P}] &= \lim_{\zeta \rightarrow 0} \frac{d \ln \left[ \sum_j a_j G^{b_j \zeta} \right]}{d \ln[\zeta]} = \lim_{\zeta \rightarrow 0} \left[ \frac{\sum_j a_j b_j \ln[G] G^{b_j \zeta}}{\sum_j a_j G^{b_j \zeta}} \right] \zeta, \\ &= \lim_{\zeta \rightarrow 0} \left[ \frac{\sum_j a_j b_j \ln[G]}{\sum_j a_j b_j \ln[G] \zeta} \right] \zeta = 1 \end{aligned} \quad (133)$$

which shows the connectivity dimensionality of the infinite tree is exactly 1.

One should note that the infinite tree represents a challenging scenario for computing the connectivity dimensionality due to the exponential dependence of the count function on the connectivity radius. The noncrosslinked infinite tree contains no closed paths. A space of dimensionality  $N > 1$  normally has some crosslinks and contains multiple closed paths. The absence of crosslinks and closed paths is the main feature causing the connectivity dimensionality of the infinite tree to be 1.

Some possible configurations of a system over time can be represented by a tree-like graph called a **decision tree**. A decision tree embodies the process of a system that chooses between different possible outcomes, where each branch of the tree represents a different outcome. A series of consecutive quarter

flips has a decision tree that looks like Figure 32, where the two branches at each step correspond to the quarter landing heads or tails up. Because the tree has no crosslinks, there are no interactions between different branches of the tree. As the quarter passes through the tree, its state (heads or tails) may change, but the quarter only moves along one continuous coordinate ('time'). We can represent a series of quarter flips by a binary number letting 0 = tails and 1 = heads. Then HTHHTHHTTT... = 1011011000... . In such case, the number produced forms a one-dimensional sequence and this explains the one-dimensionality of the decision tree. In decision trees, the quartropy plays an extremely important role as the system must choose between different possible discrete states. For example, consider the task of choosing one particular linear path from the left to the right of Figure 32. There are 32 possible choices giving a quartropy of  $\log_2[32] = 5$  for this decision process.

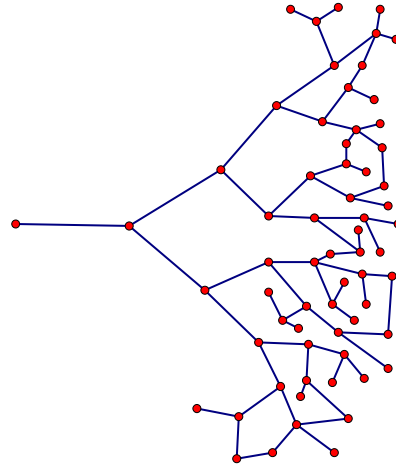


**Figure 33: A partially crosslinked tree**

*In a partially crosslinked tree, there are connections between the branches. A partially crosslinked tree contains hyperbubbles.*

## 5. DISCRETE-CONTINUOUS DUAL MATCHING

### 5.1 The Need for a New Field of Mathematics Studying Discrete-Continuous Dual Spaces

Variable-based mathematics is the name given to all kinds of mathematics that can be represented and solved by means of variables. Each component of a scalar, matrix, tensor, vector, etc. is a variable. Furthermore, variables may be either discrete or continuous. Variables may be either independent or dependent or constant parameters. Algebra, calculus, tensor analysis, differential geometry, etc. are examples of variable-based mathematics.

In mathematics, an independent real variable has exactly one degree of freedom, while a dependent variable has no additional degrees of freedom outside the degrees of freedom already accounted for by the independent variables. Any combination of independent and dependent variables always yields a nonnegative integer number of degrees of freedom. **Quantifiable forms** represent a nonnegative integer number of degrees of freedom; therefore, quantifiable forms can be represented by variables. **Unquantifiable forms** represent fractional degrees of freedoms; therefore, unquantifiable forms cannot be represented by variables. Unquantifiable forms are said to transcend variable-based mathematics.

Positions in the continuous representation  $\mathfrak{C}$  can be described by a set of independent continuous coordinate variables iff. the connectivity dimensionality field of  $\mathfrak{C}$  is constant and integer. For example, in a 3-dimensional space one might represent independent positions by means of three independent coordinate variables  $v_1$ ,  $v_2$ , and  $v_3$  giving the representation  $\{\widehat{P}\} = \{(v_1, v_2, v_3)\}$ . If the connectivity dimensionality is 3.198782 then one would hypothetically need 3.198782 independent continuous coordinate variables to describe the set of positions in the continuous representation  $\mathfrak{C}$ . Because a

fractional independent variable is not explicitly constructible, positions in the continuous representation  $\mathbb{C}$  transcend variable based mathematics when the connectivity dimensionality field is not a whole number:

**Theorem 4:** Discrete-continuous dual spaces in which the connectivity dimensionality field is not precisely equal to a nonnegative integer transcend variable-based mathematics.<sup>23</sup>

Discrete-continuous dual mathematics is the area of mathematics that studies the properties of discrete-continuous dual spaces. The continuous forms pointing to the independent positions  $\{\widehat{P}\}$  in a discrete-continuous dual space are called **hypercoordinates**. A vector-like object constructed in a discrete-continuous dual space is called a **hypervector**. A tensor-like object constructed in a discrete-continuous dual space is called a **hypertensor**. An integral-like object constructed in a discrete-continuous dual space is called a **hyperintegral**. A derivative-like object constructed in a discrete-continuous dual space is called a **hyperderivative**. A differential-equation-like object constructed in a discrete-continuous dual space is called a **hyperdifferential equation**. Hypercoordinates, hypervectors, hypertensors, hyperintegrals, hyperderivatives, and hyperdifferential equations will be explained more fully in future articles. Some properties of these objects are unquantifiable while other properties of these objects are quantifiable. A scalar property of one of these objects is quantifiable in principle because a scalar property represents a single degree of freedom and can be represented by a single variable. For example, the absolute value of the determinant of a hypertensor is a scalar and quantifiable in principle. A hypervector in a 5.123897-dimensional space has 5.123897 degrees of freedom and is thus an unquantifiable form; however, the length of this hypervector is a scalar and quantifiable form. There is no existing mathematical framework for describing the unquantifiable forms of discrete-continuous dual spaces having a connectivity dimensionality field not precisely equal to a nonnegative integer. The new mathematics governing such spaces will be called hypercalculus. Hypercalculus studies hypercoordinates, hypergradients, hypervectors, hypertensors, hyperintegrals, and hyperdifferential equations. Because hypercalculus is discrete-continuous dual, it sits at the interface between discrete mathematics and continuous mathematics.

The following example helps us understand the physical meaning of hypervectors, hypertensors, hyperderivatives, hyperintegrals, and hyperdifferential equations. Consider a solid cube of metal. Suppose that we apply a voltage difference between two opposite sides of the cube by electrically connecting one side of the cube to the '+' terminal of a car battery while connecting the opposite side to the '-' terminal of the battery. This will cause an electric current to flow through the cube of metal, and this current will generate heat because of the resistance of the metal. Because the metal cube is three-dimensional, positions within the cube can be described by 3 coordinates. The current density within the cube is vector. A dielectric tensor can be used to represent the dielectric properties of a solid material. Differential equations (Maxwell's equations) can be used to describe various relationships between the electric field, magnetic field, charge density, current density, etc.; these equations can be represented in either

<sup>23</sup> **Proof:** (1) A variable-based system of mathematics contains by definition a nonnegative integer number of independent variables. (2) The mathematical dimensionality of a mathematical system is equal to the number of independent continuous variables in one of its self-consistent solutions. (3) From (1) and (2) it follows that the mathematical dimensionality of a variable-based system is integer. (4) The connectivity dimensionality field is the effective number of independent directions in a space and thus represents the effective number of independent continuous variables needed to specify a position in the space. (5) When the connectivity dimensionality is noninteger, the number of independent continuous variables is effectively noninteger. (6) From (1) and (5) it follows that when the connectivity dimensionality field is not a nonnegative integer the system cannot be described by a variable-based system of mathematics. (7) A system that cannot be described by a variable-based system of mathematics is said to transcend variable-based mathematics. (8) From (6) and (7) it follows that when the connectivity dimensionality field is not a nonnegative integer the system transcends variable-based mathematics.

derivative or integral form. Suppose we replace the cube of metal with a discrete-continuous dual space comprised of a network of carbon nanotubes. This network can be represented by an edge-vertex graph. A vertex represents a location where two or more carbon nanotubes are in direct contact, and an edge represents a section of carbon nanotube between two adjacent contacts. Whereas the connectivity dimensionality field of the cube of metal was exactly 3 everywhere, the connectivity dimensionality field of the network of carbon nanotubes need not be constant or integer. (The connectivity dimensionality field of the network of carbon nanotubes can be computed using the methods described previously in this article.) When two distant points of the network of carbon nanotubes are connected to opposite terminals of the car battery, a current will flow through the network. The current will flow between two adjacent contacts in the network by traveling through the nanotubes connecting the contacts; that is, the current flows from vertex to vertex by following the edges of the graph. Instead of keeping track of the individual carbon nanotubes and their contacts in the form of a discrete network, we might choose a continuous space to model the behavior of the system where the continuous space provides a continuum approximation to the underlying discrete space. Because the current flows along the independent directions contained in the network and the number of independent directions can be fractional and vary with location, the current within the network is described in the continuum approximation by a hypervector instead of by a vector. Because the number of independent directions in the network is fractional, constructs involving two different network directions form hypertensors instead of tensors. The hypergradient of the electric potential describes how the asymptotically matched (aka smoothed) electric potential changes for a differential change in continuously interpolated position for the network. The hypervectors, hypertensors, and hypergradients are related to each other through hyperdifferential equations. Finally, hyperintegrals can be used to recover the total current through the network from the local current density, or to recover the total voltage drop across the network from the local hypergradient of the electric potential. In this manner, hypervectors, hypertensors, hyperintegrals, hypergradients, and hyperdifferential equations have roles in discrete-continuous dual spaces that are analogous to the roles of vectors, tensors, integrals, gradients, and differential equations in differential manifolds.

Hypercalculus should not be confused with fractional calculus. In fractional calculus, the order of derivatives and integrals with respect to an independent variable can be fractional (noninteger) but the number of independent variables is integer. In hypercalculus the opposite is true; namely, the order of derivatives and integrals with respect to an independent direction is integer but the number of independent directions can be fractional (noninteger). Fractional calculus utilizes quantifiable forms while hypercalculus utilizes both quantifiable and unquantifiable forms; fractional calculus is a type of variable-based mathematics while hypercalculus transcends variable-based mathematics.

Hypercalculus is not the same as fractal mathematics. Fractal mathematics is primarily concerned with the fractal dimensionality rather than the connectivity dimensionality field. For some fractals the connectivity dimensionality is integer, while for other fractals the connectivity dimensionality field is noninteger. The positions in some fractals can be described by means of continuous variables, while those in other fractals cannot. Some fractals transcend variable-based mathematics while others do not. Hypercalculus is principally concerned with discrete-continuous duality whereas fractal mathematics is not. Some objects described by hypercalculus are fractals while other objects described by hypercalculus are nonfractals. In short, there is some overlap between hypercalculus and fractal mathematics, but these are two different subject areas in mathematics.

## 5.2 What is Discrete-Continuous Dual Matching?

**Definition 22: Discrete-continuous dual matching** is the process of finding a continuous representation  $\mathbb{C}$  endowed with a continuous distance function given a discrete representation  $\mathbb{D}$  of a discrete-continuous dual space such that distances in the discrete and continuous representations are asymptotically matched and  $\{\mathbb{D}, \mathbb{C}\}$  forms a discrete-continuous dual space.

There are two types of discrete-continuous dual matching: strict and asymptotic. Strict discrete-continuous dual matching produces a strictly discrete-continuous dual space whereas asymptotic discrete-continuous dual matching produces an asymptotically discrete-continuous dual space. In strict discrete-continuous dual matching, positions in the discrete space are a subset of positions in the continuous space and the connectivity dimensionality fields of the continuous and discrete spaces are indistinguishable.<sup>24</sup> A strictly discrete-continuous dual space contains something like a discrete grid, lattice, or network whose interpolated positions form the continuous space. In asymptotic discrete-continuous dual matching, positions in the discrete and continuous space representations do not have a precise correspondence, although they have an approximate correspondence. For example, a particular discrete graph whose connectivity dimensionality is approximately 2 and which has an overall structure resembling a plane might be discrete-continuous dual matched to a 2-dimensional continuous plane. If some of the edges of the discrete graph cannot be properly drawn on the plane, the discrete-continuous dual matching is not strict; on the other hand, if all of the edges can be properly drawn on the plane, the discrete-continuous dual matching is strict.

Herein we consider a few examples of discrete-continuous dual matching to illustrate some of the key concepts, but a full exposition of discrete-continuous dual matching lies beyond the scope of this article. Consider the graph shown in Figure 34 below. Vertices and edges with a zero connectivity distance from vertex A are shown in orange. Vertices and edges with a connectivity distance  $\leq 1$  from vertex A are shown in black. Similarly, connectivity distances  $\leq 2$  are red,  $\leq 3$  are light green, and  $\leq 4$  are blue. Since the graph is 2-dimensional, the surface of the sheet of paper (or computer monitor) upon which the graph is drawn is the corresponding continuous space.

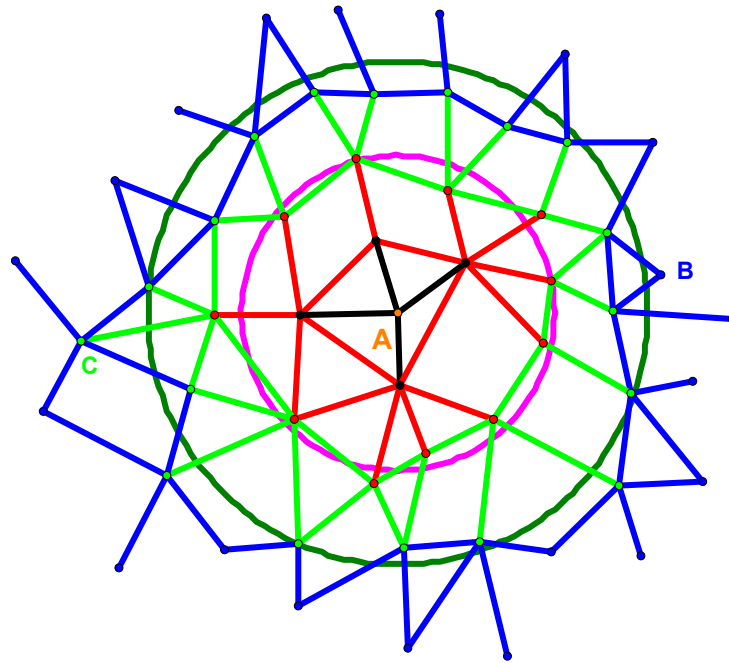


**Figure 34: Connectivity versus hypercoordinate radius**

*This graph illustrates how discrete-continuous dual matching is performed around a particular location in a space.*

Our job is to create a continuous distance function which asymptotically matches the underlying discrete connectivity distance. (Even in strict discrete-continuous dual matching the discrete and continuous distance functions are asymptotically matched.) To begin, I have drawn two circles, a pink one

<sup>24</sup> The term 'indistinguishable' means that the fields are the same within the limits of measurement uncertainty.

and a dark green one around the vertex A. What radial hypercoordinate distance  $R$  do these two circles correspond to? This can only be determined after choosing a particular rational for constructing a hypercoordinate basis. Let us choose to construct the hypercoordinate basis in such a manner that every vertex in the graph has a hypervolume of 1 unit and the vertexal density in the chosen hypercoordinate basis is identically one; this is called the **isovortexal hypercoordinate basis**. Clearly, the graph shown in Figure 34 has a connectivity dimensionality close to 2 and a compact cross-section of one; therefore, the hypervolume enclosed by each of the circles asymptotically approaches  $V[2, R] = \pi R^2$ . Inside the pink circle are located 13 vertices; therefore, the hypercoordinate radius corresponding to the pink circle is  $R = \sqrt{\frac{13}{\pi}} = 2.03$ . Inside the dark green circle are located 31 vertices; therefore, the hypercoordinate

radius associated with the dark green circle is  $R = \sqrt{\frac{31}{\pi}} = 3.14$ .

Notice that increasing connectivity radius is associated on average with increasing isovortexal hypercoordinate radius. However, we can find pairs of vertices (A,B) and (A,C) such that the connectivity distance is larger from A to B than from A to C while the isovortexal hypercoordinate distance is slightly smaller from A to B than from A to C. In the above graph, the connectivity radius from A to B is four, the connectivity radius from A to C is three, the isovortexal hypercoordinate distance from A to B is about

$R = \sqrt{\frac{32}{\pi}} = 3.19$ , and the isovortexal hypercoordinate distance from A to C is about  $R = 3.6$ .

This example illustrates concretely that starting with a discrete-continuous dual edge-vertex graph we can construct an asymptotically matched continuous distance function. The asymptotically matched continuous distance function allows us to do continuous mathematics in the continuous space that is dual to the associated discrete space. **In such discrete-continuous dual mathematics, the continuous space provides a continuum approximation of the statistical properties of the associated discrete space.**

It is important to realize that the asymptotically matched continuous distance function contains inherent uncertainty. The uncertainty in the isovortexal hypercoordinate radius associated with the pink circle in the figure above can be estimated as following. There were 13 vertices found inside the pink circle. If the graph had been drawn slightly differently, or if the radius of the pink circle had been increased or decreased by a small amount, the number of vertices enclosed within the pink circle could have increased by three or decreased by several vertices. The smallest conceivable change in hypervolume corresponds to  $\pm 1$  vertex, from which we infer that the isovortexal hypercoordinate radius satisfies the following uncertainty principle:

$$\hat{\Delta} \left[ \mathcal{V}_{\text{vertexal}} \left[ R, \hat{P} \right] \right] = \left( \frac{d\mathcal{V}_{\text{vertexal}} \left[ R, \hat{P} \right]}{dR} \right) \hat{\Delta} \left[ R, \hat{P} \right] \geq 1 \quad (134)$$

where  $\mathcal{V}_{\text{vertexal}} \left[ R, \hat{P} \right]$  is the hypervolume (in the isovortexal hypercoordinate basis) within a hypercoordinate radius  $R$  of the point  $\hat{P}$ . Defining

$$S_{\text{vertexal}} \left[ R, \hat{P} \right] = \left( \frac{d\mathcal{V}_{\text{vertexal}} \left[ R, \hat{P} \right]}{dR} \right) \quad (135)$$

as the boundary hypervolume (aka hyperarea), one obtains

$$\hat{\Delta} \left[ R, \hat{P} \right] \geq \frac{1}{S_{\text{vertexal}} \left[ R, \hat{P} \right]}. \quad (136)$$

In other words, the uncertainty in the isovortexal hypercoordinate radius associated with a hypersphere drawn in a discrete-continuous dual space is greater than or equal to the reciprocal of the hyperarea of that

same hypersphere. This gives a minimum uncertainty of  $\hat{\Delta}[R] = \frac{1}{2\pi R} = \frac{1}{2\pi \sqrt{\frac{13}{\pi}}} = 0.08$  for the pink

circle in Figure 34. The meaning, of course, is that hypercoordinate radius in a discrete-continuous dual space cannot be measured to infinite precision but contain a residual uncertainty:

$$R = \langle R \rangle \pm \hat{\Delta}[R, \hat{P}]. \quad (137)$$

For a one-dimensional space, we have  $S[1, R] = 2$ , whence it follows immediately that the isovortexal hypercoordinate radius between two points A and B in a one-dimensional space has the residual uncertainty

$$\hat{\Delta}[R, \hat{P}] = \frac{1}{2}. \quad (138)$$

For example, if we computed a hypercoordinate radius of 3 in a one-dimensional space, this would need to be expressed as  $R = 3 \pm 0.5$ . Equation (138) also represents the inherent uncertainty in hypercoordinate distance associated with a shortest path between two points in a discrete-continuous dual space.

### 5.3 An Example Space with a Fractional Connectivity Dimensionality Field

Many of my friends have commented that they have trouble visualizing spaces with fractional connectivity dimensionality. We are very familiar with 0, 1, 2, 3, and 4-dimensional spaces, but what do spaces with fractional connectivity dimensionality look like? To help out with this common problem, I have prepared a graph in Figure 9 on page 24 with a connectivity dimensionality between 1 and 2. Table 7 gives the count function for different connectivity radii. In this case, the minimum connectivity radius for computing the connectivity dimensionality is  $\zeta_{\min} = 1/2$ .

**Table 7: Count function for the graph of Figure 9**

$\zeta_i$	$C[\zeta_i, \mathbf{P}]$
0.5	1
1.5	5
2.5	11
3.5	18

This data was used to prepare the plot of  $\left[ \left[ \ln[C[\zeta, \mathbf{P}]] \right] \right]$  versus  $\ln[\zeta]$  shown in Figure 35. The data was strictly linear with a slope of  $N[\mathbf{P}] \cong 1.4875$ . Since  $\left[ \left[ \ln[C[\zeta, \mathbf{P}]] \right] \right]$  versus  $\ln[\zeta]$  was strictly linear, the dimensionality is constant in this case. The fitted line gives the function

$$\left[ \left[ C[\zeta, \mathbf{P}] \right] \right] = e^{1.0248} \zeta^{1.4875} = 2.7865 \cdot \zeta^{1.4875}. \quad (139)$$

Note that

$$\left[ \left[ C[\zeta, \mathbf{P}] \right] \right] \cong V[N, \llbracket R \rrbracket_{\zeta}] \text{ for } N[\hat{\mathbf{P}}] = N = \text{const and } t \quad (140)$$

in an unbranched space with a compact cross-section equal to one. Here  $\llbracket R \rrbracket_{\zeta}$  is the average hypercoordinate distance for a connectivity radius  $\zeta$ . From equation (20), we have

$$V[1.4875, R] = \frac{\pi^{0.74375}}{0.74375 \cdot \Gamma[0.74375]} \cdot R^{1.4875} = 2.553 \cdot R^{1.4875} \quad (141)$$

Combining equations (139) - (141) gives the following asymptotic scaling relationship



$$\zeta \approx 1.4875 \sqrt{\left( \frac{2.553}{2.7865} \right)} \llbracket R \rrbracket_{\zeta} = 0.9429 \llbracket R \rrbracket_{\zeta} \quad (142)$$

between the connectivity radius  $\zeta$  and the average hypercoordinate radius  $\llbracket R \rrbracket_{\zeta}$ .

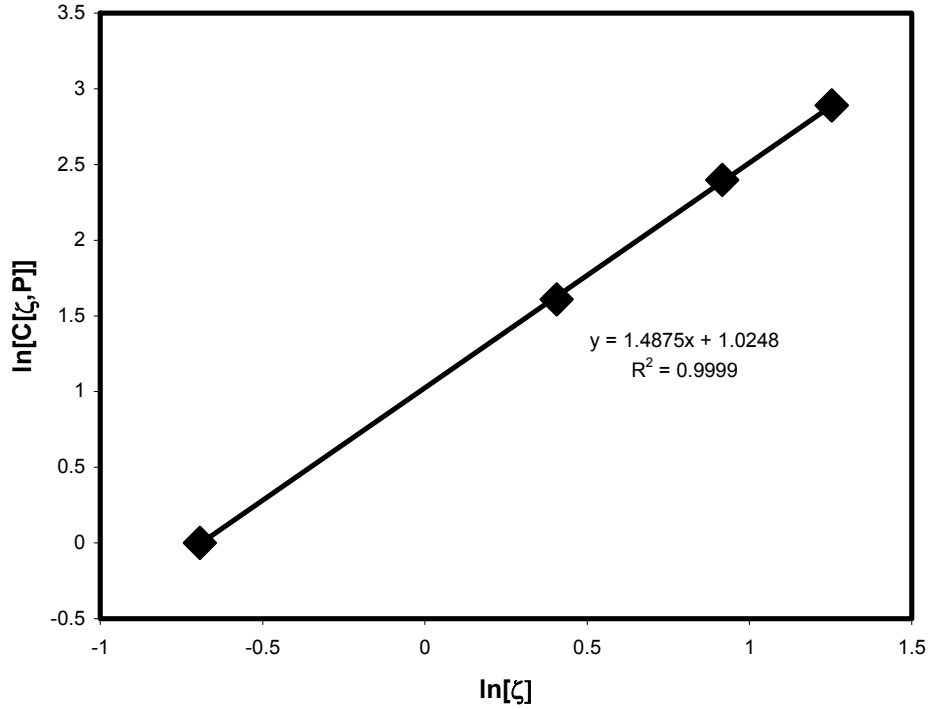


**Figure 35: Plot used to determine the connectivity dimensionality of vertex P in Figure 9**

It is important to keep in mind that there is not a one-to-one map between  $R$  and  $\zeta$ . Consider a unit square grid forming an  $xy$ -Cartesian coordinate system. Moving two units along the  $+x$  direction gives a connectivity distance of 2 and a coordinate distance of 2. Moving one unit along  $+x$  followed by one unit along  $+y$  gives a connectivity distance of 2 and a coordinate distance of  $\sqrt{2}$ . In both cases the connectivity distance was 2; however, the coordinate distances were different in each case. Moving 5 units in the  $+x$  direction gives a coordinate distance of 5 and a connectivity distance of 5. Moving 3 units in the  $+x$  direction followed by 4 units in the  $+y$  direction gives a coordinate distance of 5 and a connectivity distance of 7. In both cases the coordinate distance was 5; however, the connectivity distances were different in each case. From these examples, it follows the map between  $R$  and  $\zeta$  is many-to-many. The reason the map between  $R$  and  $\zeta$  is many-to-many is that the shortest connectivity distance path is usually not the same as the shortest hypercoordinate distance path.

#### 5.4 Other Hypercoordinate Bases and Vertexal Density Variations

In the isovortexal hypercoordinate basis, there is one vertexal per unit hypervolume:

$$\rho_{\text{vertexal}} = 1. \quad (143)$$

Other schemes for constructing a hypercoordinate basis are possible. Suppose that for some nonisovortexal hypercoordinate basis the vertexal density in a 2-dimensional discrete-continuous dual space varies with hypercoordinate radius  $\tilde{R}$  around some particular point  $\widehat{P}_A$  as

$$\rho_{\text{vertexal}}[\tilde{R}] = \rho_0 - \kappa \tilde{R} \quad (144)$$

where the squiggly lines indicate these quantities are measured in a nonisovortexal hypercoordinate basis. The vertexal hypervolume function for this space is thus given by

$$\mathcal{V}_{\text{vertexal}}[\tilde{R}, \widehat{P}_A] = \int_0^{\tilde{R}} \rho_{\text{nodal}} d\tilde{V} = \int_0^{\tilde{R}} (\rho_0 - \kappa r) 2\pi r dr = \rho_0 \pi \tilde{R}^2 - \frac{2}{3} \pi \kappa \tilde{R}^3. \quad (145)$$

(The vertexal hypervolume  $\mathcal{V}_{\text{vertexal}}[\tilde{R}, \widehat{P}_A]$  is asymptotically equal to the number of enclosed vertices within a hypercoordinate radius  $\tilde{R}$  of the point  $\widehat{P}_A$ .) The connectivity dimensionality of the continuous representation can be computed by

$$N[\widehat{P}_A] = \lim_{\tilde{R} \rightarrow 0} \frac{d \ln[\mathcal{V}_{\text{vertexal}}[\tilde{R}, \widehat{P}_A]]}{d \ln[\tilde{R}]}. \quad (146)$$

Equation (146) is the general method for computing the connectivity dimensionality field of the continuous representation in an arbitrary hypercoordinate basis. Expanding

$$d \ln[\mathcal{V}_{\text{vertexal}}[\tilde{R}, \widehat{P}_A]] = \frac{d\mathcal{V}_{\text{vertexal}}[\tilde{R}, \widehat{P}_A]}{\mathcal{V}_{\text{vertexal}}[\tilde{R}, \widehat{P}_A]} = \frac{(\rho_0 - \kappa \tilde{R}) 2\pi \tilde{R}}{\rho_0 \pi \tilde{R}^2 - \frac{2}{3} \pi \kappa \tilde{R}^3} \quad (147)$$

and

$$d \ln[\tilde{R}] = \frac{1}{\tilde{R}}. \quad (148)$$

Inserting (147) - (148) into (146) gives

$$N[\widehat{P}_A] = \lim_{\tilde{R} \rightarrow 0} \frac{(\rho_0 - \kappa \tilde{R}) 2\pi \tilde{R}^2}{\rho_0 \pi \tilde{R}^2 - \frac{2}{3} \pi \kappa \tilde{R}^3} = 2. \quad (149)$$

As required, this recovers the exact dimensionality of the space in the presence of vertexal density variations.

The connectivity dimensionality field is a measure of the number of independent directions in a space. The vertexal density and hypercoordinate basis are means of assigning distances to those independent directions. A different choice of vertexal density or hypercoordinate basis just leads to a different distance metric, it does not effect the number of independent directions in the space. From this we conclude a method for computing the connectivity dimensionality field must be independent of the choice of hypercoordinate basis and vertexal density to be mathematically viable. The methods described in this paper achieve such independence by taking the  $\zeta \rightarrow 0$  or  $\tilde{R} \rightarrow 0$  limit. Note that without the  $\tilde{R} \rightarrow 0$  limit in equation (146), the correct connectivity dimensionality would not have been obtained in equation (149). This example illustrates the importance of taking such limits when computing the connectivity dimensionality field.

## 5.5 Compact and Hidden Dimensions

A graphical feature may have a different dimensionality depending upon whether we view it from close up or far away. A speck of dirt is a useful analogy. When viewed at large distances, the speck of dirt might appear like a point particle floating around in space. However, when viewed at close distances with a microscope the speck of dirt appears to have a much richer structure. The speck of dirt has a spatial dimensionality  $n_s = 0$  for observation distances much greater than its radius, but  $n_s = 3$  for observation distances much smaller than its radius. Another useful analogy is a sheet of paper. When viewed over distances much larger than its thickness, a sheet of paper gives an effective spatial dimensionality of

$n_s = 2$ . However, when viewed over distances much smaller than its thickness, the effective spatial dimensionality of the paper is  $n_s = 3$ .

This gives rise to an interesting complication; namely, certain dimensions may only be operational over limited distance scales. Dimensions of this type are called compact dimensions. For each compact dimension, we can define a corresponding compaction length  $\lambda_d$  such that the dimension is operational over a distance  $\lambda_d$ . In the above examples, the compaction lengths approximately correspond to the diameter of the dirt particle and the thickness of the sheet of paper. Dimensions that have extremely large  $\lambda_d$  or which do not compact at all are called long-range dimensions. Dimensions that have extremely small  $\lambda_d$  are called short-range dimensions.

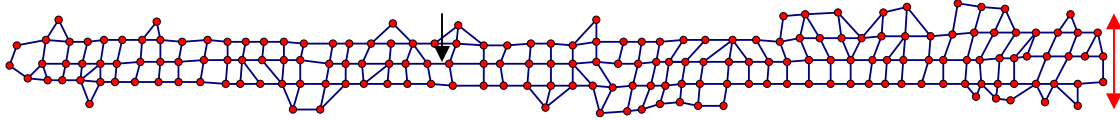


**Figure 36: Space containing a compact dimension**

*A compact dimension is a dimension that is operational over a limited distance. In this figure, there is a compact dimension that is operational along the direction of the red double arrow for distances less than the strip height.*

The graph in Figure 36 contains one compact dimension with  $\lambda_d \cong 2.5$  (the average height of the strip) and one compact dimension with  $\lambda_d \cong 54$  (the average length of the strip). The count function for the vertex indicated by the arrow in Figure 36 is given in Table 8. The value of  $\zeta_{\min}$  was estimated to be  $3/2$  using equation (65).

**Table 8: Count function for the indicated vertex in Figure 36**

$\zeta_i$	$C[\zeta_i]$	$\zeta_i$	$C[\zeta_i]$	$\zeta_i$	$C[\zeta_i]$	$\zeta_i$	$C[\zeta_i]$
1.5	5	4.5	27	7.5	51	10.5	72
2.5	13	5.5	34	8.5	58	11.5	79
3.5	20	6.5	42	9.5	65	12.5	86

The log-log count function plot for this network is shown in Figure 37. We notice that the slope of the function  $\ln[C[\zeta]]$  versus  $\ln[\zeta]$  changes from approximately 2 at small connectivity distances to approximately 1 at larger connectivity distances, indicating a change in the connectivity dimensionality with observation distance. Two straight lines have been superimposed on the plot, one showing the asymptotic linear behavior at small connectivity radii and the other showing the asymptotic linear behavior at larger connectivity radii. These two lines intersect at the knee point occurring at  $\ln[\zeta] = 0.52$ , as indicated by the broken line on the figure. The knee point  $\zeta_{knee}$  indicates the center of the transition region over which the compact dimension becomes compacted. Clearly for  $\zeta \leq \frac{\lambda_d}{2}$  there is absolutely no compaction whereas for  $\zeta \geq 2\lambda_d$  there is clearly compaction. This means that

$$\frac{\lambda_d}{2} < \zeta_{knee} < 2\lambda_d \quad (150)$$

or equivalently

$$\frac{\zeta_{knee}}{2} < \lambda_d < 2\zeta_{knee}. \quad (151)$$

In this case,  $\zeta_{knee} = 3.3$  from whence follows  $1.65 < \lambda_d < 6.6$ .

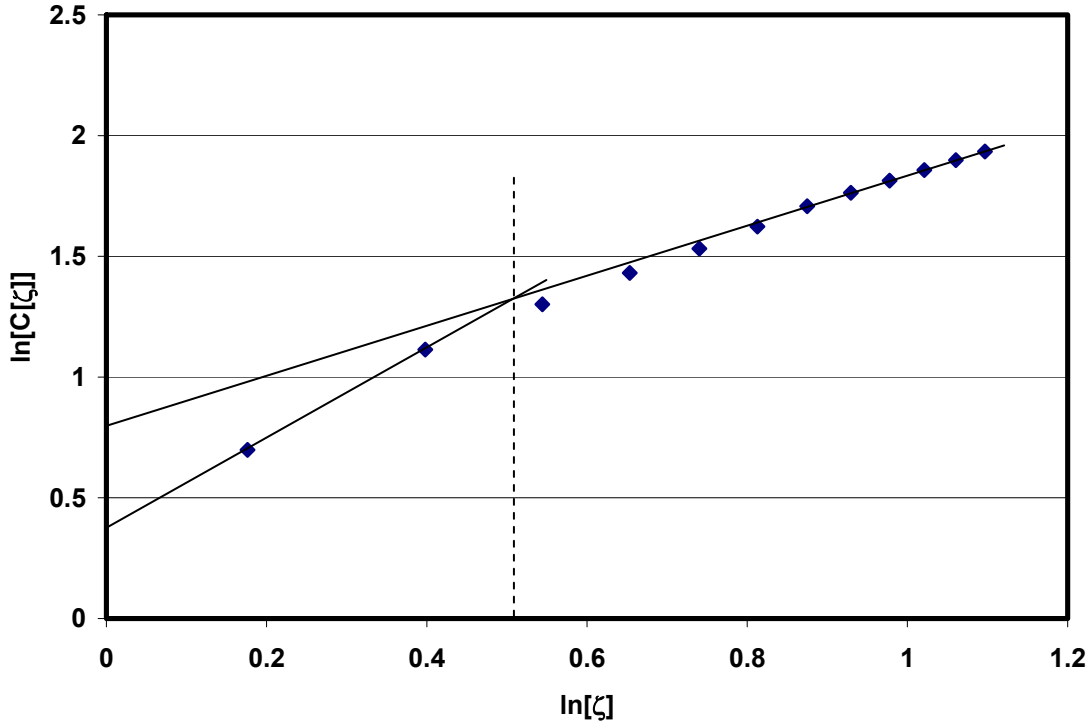


**Figure 37: Plot of the count function for a space containing a compact dimension**

When one or more compact dimensions are present in a space, the slope of  $\ln[C[\zeta]]$  versus  $\ln[\zeta]$  transitions from a higher value at lower distances to a lower value at higher distances. This change in slope indicates there are additional connectivity dimensions that operate only over small distances (i.e. compact dimensions). The knee point marks the center of the compaction transition and occurs where the high and low distance linear asymptotes intersect.

The y-intercept of the larger distance linear asymptote on the log-log count function plot is  $\ln[\mathcal{G}_{large}]$ , while the y-intercept of the smaller distance linear asymptote is  $\ln[\mathcal{G}_{small}]$ . Also, the count function at larger distances scales like

$$C[\zeta] \cong \mathcal{G}_{large} \zeta^N \text{ for } \zeta \geq 2\lambda_d \quad (152)$$

while that for smaller distances scales like

$$C[\zeta] \cong \mathcal{G}_{small} \zeta^{N+\Gamma} \text{ for } \zeta \leq \lambda_d / 2 \quad (153)$$

where  $\Gamma$  is the number of short-range dimensions. For the graph of Figure 37, the values are approximately

$$\mathcal{G}_{large} \cong 6.3 \text{ and } \mathcal{G}_{small} \cong 2.5. \quad (154)$$

It is useful for us to construct  $N$  long-range hypercoordinates. For example, in the graph of Figure 36, let us choose a coordinate called  $y$  to represent measurements along the direction parallel to the long-range dimension. Clearly, since the average height of the graph is 3.5 vertices, the hypervolume of a section of the graph scales like

$$\mathcal{V}_{vertexal} = 3.5 \cdot 2R \quad (155)$$

where  $2R$  is the hypercoordinate length of the section along the long-range dimension. (The factor of 2 occurs because  $R$  is the radius of the section along the long-range dimension, giving a total length of  $2R$ .) To complete this analysis, we need to consider the projection of  $\zeta$  onto the coordinate  $y$ . Comparing equations (152), (154), and (155) for  $N=1$ , we obtain the asymptotic matching condition

$$R \cong 0.9\zeta. \quad (156)$$

Because the vertexal hypervolume of each vertex is 1 and the long-range dimensionality of the graph is 1, the increase in hypervolume of the graph section must scale over large distances like  $2R$  times the compact cross-section giving

$$\frac{d\mathcal{V}_{\text{vertexal}}}{dR} = 2\mathcal{K} \text{ for this particular graph,} \quad (157)$$

where  $\mathcal{K} \cong 3.5$  is the graph's compact cross-section.

**Definition 23:** The **compact cross-section** of a discrete-continuous dual space is the hypervolume along the short-range dimensions for a constant location in the long-range dimensions. The compact cross-section is a field defined over the long-range dimensions.

In addition, since this particular graph has one long-range dimension, the vertexal hypervolume for large distances also scales like twice the connectivity radius times the graph's compact cross-section:

$$\frac{d\mathcal{V}_{\text{vertexal}}}{d\zeta} = 2\mathcal{K} \text{ for this particular graph.} \quad (158)$$

A comparison of equations (157) and (158) gives the rigorously correct asymptotic matching condition

$$\frac{dR}{d\zeta} = 1 \text{ for large distances.} \quad (159)$$

The slight discrepancy between equations (156) and (159) was introduced by the graphical analysis which involved measurement errors in the slopes, intercepts, etc.

The concept of a space's compact cross-section  $\mathcal{K}$  is developed to account for the presence and effects of short-range dimensions. For  $R \gg \lambda_d$  where  $\lambda_d$  is the compaction length of the hidden dimension, the hypervolume enclosed in region of radius  $R$  centered about some point  $\hat{P}$  in a space of constant dimension  $n$  asymptotically approaches

$$\mathcal{V}_{\text{vertexal}}[R, \hat{P}] = \mathcal{K}V[n, R] = \mathcal{K} \frac{2 \cdot \pi^{n/2}}{n \cdot \Gamma[n/2]} \cdot R^n \quad (160)$$

Consider a long copper wire having a cross-sectional area of  $0.001 \text{ cm}^2$ . In this case, the volume of the wire is given by  $0.001 \text{ cm}^2$  times the length of the wire; therefore, the compact cross-section of the wire is  $\mathcal{K} = 0.001 \text{ cm}^2$ . Here, the compact cross-section has been expressed in metric units, but we could also express it as a dimensionless number by multiplying  $0.001 \text{ cm}^2$  by the average number of vertices per square centimeter in the wire's cross-section. The dimensionless form is needed whenever the number of dimensions is nonconstant.

In general the compact cross-section of a space must be treated as a field that varies as a function of position  $\hat{P}$  in the long-range dimensions; that is,  $\mathcal{K} = \mathcal{K}[\hat{P}]$ . The vertexal hypervolume enclosed in a region of particular radius depends on  $\mathcal{K}[\hat{P}]$ ,  $N[\hat{P}]$ , and the vertexal density  $\rho_{\text{vertexal}}[\hat{P}]$ . The compact cross-section  $\mathcal{K}[\hat{P}]$  is formally defined as

$$\mathcal{K}[\hat{P}] = \lim_{\mathcal{V}_{\text{vertexal}}[R, \hat{P}] \rightarrow 1} \left[ \mathcal{V}_{\text{vertexal}}[R, \hat{P}] \left( \frac{N[\hat{P}] \cdot \Gamma[N[\hat{P}]/2]}{2 \cdot \pi^{N[\hat{P}]/2} \cdot R^{N[\hat{P}]}} \right) \right] \quad (161)$$

where  $R$  is hypercoordinate radius measured in an isovetexal hypercoordinate basis,  $\mathcal{V}_{\text{vertexal}}[R, \hat{P}]$  has been obtained by asymptotic matching for  $R > \lambda_d$  (i.e. long-range asymptote), and  $N[\hat{P}]$  is derived

from asymptotic matching over  $R > \lambda_d$  via equation (146) or graphical analysis of equation (107). (Equation (161) involves extrapolating functions asymptotically matched for large  $R$  to the hypothetical limit corresponding to a hypervolume enclosing a single vertex.) Obtaining an accurate value for the compact cross-section  $\mathcal{K}[\widehat{P}]$  is a challenging problem because equation (161) requires one to know the vertices enclosed within a particular hypercoordinate radius  $R$  rather than within a particular connectivity radius  $\zeta$ . Equation (161) applies to all types of discrete-continuous dual spaces regardless of the structural variations contained within those spaces; that is, equation (161) applies whether or not there are short-range dimensions, hyperbubbles, dimensionality hypergradients, branches, and/or intrinsic curvature in the vertexal density.<sup>25</sup>

Let's use equation (161) to compute the compact cross-section of the graph in Figure 36. For spaces with 1 long-range dimension, the long-range asymptotic matching condition is usually  $\frac{dR}{d\zeta} = 1$  (162). Next, the long-range asymptotic scaling behavior is represented as  $C[\zeta] \cong \mathcal{G}_{large}\zeta$  (163), and by using  $\zeta = 12.5$  we obtain  $\mathcal{G}_{large} = 86/12.5 = 6.83$  (164). Combining equations (162) - (164), we obtain the long-range asymptotic condition  $\mathcal{V}_{vertexal}[R, \widehat{P}] = 6.83R$  (165). Putting this into equation (161), one obtains  $\mathcal{K}[\widehat{P}] = \lim_{6.83R \rightarrow 1} \left[ 6.83R \left( \frac{1 \cdot \Gamma[1/2]}{2 \cdot \pi^{1/2} \cdot R^1} \right) \right] = 3.41$  (166). This gives a nearly perfect match to the actual compact cross-section of the strip near the vertex of interest.

## 5.6 Hyperbubbles and Porous Spaces

A continuous space is said to contain a **hole** if a closed curve drawn in the space cannot be contracted to a point without leaving the space. A discrete-continuous dual space is said to contain a hole if the continuous representation of that space contains a hole; in such cases, the discrete representation is also said to contain a hole.

**Hyperbubbles** are higher-dimension analogs of holes. A simple closed curve is topologically equivalent to a circle, and a circle is a 1-dimensional hypersphere. A hole is called a hyperbubble of order 1, because a simple closed curve drawn around the hole in the space cannot be contracted to a point without leaving the space. If a 2-dimensional hypersphere (or topologically equivalent surface) can be drawn in the continuous space but not contracted to a point without leaving the space, the space is said to contain a hyperbubble of order 2. More generally, if an  $n$ -dimensional hypersphere (or topologically equivalent surface) can be drawn in the space but not contracted to a point without leaving the space, the space is said to contain a hyperbubble of order  $n$ . A discrete-continuous dual space is said to contain a hyperbubble of order  $n$  iff. the continuous representation contains a hyperbubble of order  $n$ ; in such case, the discrete representation is also said to contain a hyperbubble of order  $n$ .

The number of hyperbubbles in a continuous space  $\mathbb{S}$  is equal to the number of hyperspheres that satisfy all three of the following conditions: (i) the dimension of each hypersphere is a nonnegative integer (but not necessarily the same nonnegative integer for different hyperspheres), (ii) each hypersphere (or topologically equivalent surface) can be drawn in the space  $\mathbb{S}$  but not contracted to a single point without leaving the space  $\mathbb{S}$ , and (iii) the drawn hyperspheres form a set such that each drawn hypersphere (or topologically equivalent surface) in the set cannot be deformed into any other without leaving the space  $\mathbb{S}$ .

<sup>25</sup> Intrinsic curvature in the vertexal density occurs when the space has intrinsic curvature in the isovortexal hypercoordinate basis, and in such case the intrinsic curvature is a scalar field whose value may vary with position.

A **hard boundary** abruptly terminates a direction of motion within the space while a **soft boundary** does not. Hyperbubbles with a hard boundary are called **intrusive hyperbubbles**, while hyperbubbles with a soft boundary are called **latent hyperbubbles**.

It is useful to think of the hyperspheres as being composed of rubber which may be deformed and contracted at will. For example, an ellipse is topologically equivalent to a circle and an ellipsoid is topologically equivalent to a sphere. Thus an ellipse contains exactly one hyperbubble and this hyperbubble is of order 1 and latent. An ellipsoid contains exactly one hyperbubble and this hyperbubble is of order 2 and latent. A toroid contains two latent hyperbubbles of order 1. A sphere contains one latent hyperbubble of order 2. The figure '8' contains two hyperbubbles of order 1. The letter 'P' contains one hyperbubble of order 1. A typical coffee mug contains two latent hyperbubbles of order 1.

A porous material like a foam contains numerous intrusive hyperbubbles. For a porous material, the bulk density  $\rho_{bulk}$  is related to the true density  $\rho$  and the void fraction  $f_{void}$  by

$$\rho_{bulk} = (1 - f_{void}) \rho. \quad (167)$$

In this case, the compact cross-section is given by

$$\mathcal{K} = (1 - f_{void}). \quad (168)$$

For example, consider a can of soda pop in which carbon dioxide bubbles give 10 % void fraction in the pop:  $f_{void} = 0.1$ . In this case, the fraction of space occupied by the liquid equals 1 minus the void fraction giving a compact cross-section of  $\mathcal{K} = 0.9$ . Since the mass density of water is  $1 \text{ g/cm}^3$ , the bulk density of the soda pop is  $0.9 \text{ g/cm}^3$ .

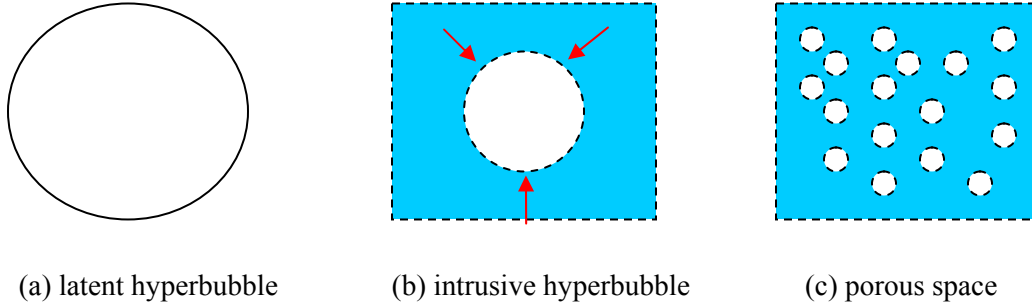


**Figure 38: Hyperbubbles and porous spaces**

*(a) A latent hyperbubble has a soft boundary and does not terminate an active direction; (b) an intrusive hyperbubble terminates one or more active directions (indicated by the red arrows); (c) a porous space contains numerous hyperbubbles.*

The presence of short-range dimensions increases the compact cross-section while porosity decreases the compact cross-section. For  $\mathcal{K} > 1$ , short-range dimensions are more dominant than pores. For  $\mathcal{K} < 1$ , pores are more dominant than short-range dimensions. For  $\mathcal{K} = 1$ , the space either lacks short-range dimensions and porosity or else the hypervolume contributions of pores and short-range dimensions cancel each other.

The discrete-continuous dual matching procedure for a porous space is analogous to that for a space containing short-range dimensions. Let the typical or characteristic pore size be denoted by  $\lambda_p$  such that for  $\zeta \gg \lambda_p$  the count function scales as

$$C[\zeta] \cong \mathcal{G}_{large} \zeta^N, \quad (169)$$

while for  $\zeta \ll \lambda_p$  the count function scales as

$$C[\zeta] \cong \mathcal{G}_{small} \zeta^{N+\Gamma}. \quad (170)$$



For a porous space, the number of short-range dimensions  $\Gamma$  can be positive, negative, or zero. For example, if the space appears 2-dimensional over short distances but 3-dimensional over larger distances, then  $N = 3$  and  $\Gamma = -1$ ; a honeycomb structure with arbitrarily thin walls is an example of such a space.

## 6. CONCLUSIONS

**The major conclusions of this work are:**

1. A new type of dimensionality measure, called the connectivity dimensionality field, is needed to quantify the effective number of independent directions passing through a location in space. The connectivity dimensionality field is a completely different concept than the topological dimensionality and fractal dimensionalities. Fractal dimensionalities depend upon both a space's connectivity and its crumpledness while the connectivity dimensionality field depends upon a space's connectivity but not its crumpledness. The connectivity dimensionality field is topologically invariant while fractal dimensionalities are not necessarily topologically invariant. While the topological dimensionality is a nonnegative integer referring to properties of the space as a whole, the value of the connectivity dimensionality field can vary smoothly with position and need not be a whole number.
2. There exist spaces called discrete-continuous dual spaces which exhibit complementary discrete and continuous representations. These spaces give rise to some very interesting and important new mathematics. Of particular importance, discrete-continuous dual spaces contain a connectivity dimensionality field that may vary as a continuous function of position.
3. There are two different types of discrete-continuous dual spaces: (a.) strictly discrete-continuous dual spaces and (b.) asymptotically discrete-continuous dual spaces. In a strictly discrete-continuous dual space the continuous representation provides a perfect interpolation of the discrete structure. In an asymptotically discrete-continuous dual space, the continuous representation provides a good, albeit imperfect, interpolation of the discrete structure. The process of mapping locations between the discrete and continuous representations of a discrete-continuous dual space is called discrete-continuous dual matching. Strict discrete-continuous dual matching is associated with strictly discrete-continuous dual spaces whereas asymptotic discrete-continuous dual matching is associated with asymptotically discrete-continuous dual spaces.
4. Meaningful computation of the connectivity dimensionality requires a region whose connectivity radius exceeds a minimum value,  $\zeta_{\min}$ . A formula for estimating  $\zeta_{\min}$  has been derived.
5. First principles were used to derive a general method for computing the connectivity dimensionality field in discrete, continuous, and discrete-continuous dual spaces. This method has the following advantages:
  - a) **The method accurately evaluates the connectivity dimensionality of a space in the presence of curvature (metric variations) and vertexal density variations.**
  - b) **The method accurately evaluates the connectivity dimensionality of a space in the presence of dimensionality gradients.**
  - c) **The method accurately evaluates the connectivity dimensionality of a space in the presence of stochastic structural variations by using the asymptotically matched value of the count function to provide an average over vertices.**
  - d) **The method accurately evaluates the connectivity dimensionality of branched spaces.**

- e) The method provides a dimensionality measure  $N[\hat{P}]$  that varies continuously and smoothly (differentially) with respect to position  $\hat{P}$  by being based on the continuous and differentiable functions obtained through asymptotic matching.
  - f) The method works together with the concepts of hidden dimensions, hyperbubbles, and a space's compact cross-section to explain differences in the short-range and long-range dimensionalities of a space.
6. Strictly discrete-continuous dual spaces for which the continuous representation has a nonnegative integer of connectivity dimensions are called lattices. It is well-established that lattices may be either periodic (having a translational unit cell) or aperiodic and either tiled or untiled.
  7. The presented method for computing the connectivity dimensionality gives exactly correct values in those three cases where an exact computation of the connectivity dimensionality is mathematically allowed: (a.) when the connectivity dimensionality is zero or one, (b.) when the space is continuous (contains an infinite number of quantifiable points per unit hypervolume), and (c.) when the space is representable by a periodic lattice. It has been shown that for other types of spaces the connectivity dimensionality field contains inherent uncertainty. Moreover, by making use of the fundamental properties of irrational numbers, it has been shown that the inherent uncertainty in the average connectivity dimensionality of a region is inversely proportional to the connectivity radius of that region.
  8. Numerous examples were considered for computing the connectivity dimensionality in discrete, continuous, or discrete-continuous dual spaces, spaces of constant or variable dimensionality, branched or unbranched spaces, and spaces with compact dimensions or hyperbubbles. These numerous examples gave results in good agreement with predictions of the theory.
  9. The study of discrete-continuous dual spaces in which the connectivity dimensionality field is not a constant nonnegative integer transcends variable-based mathematics. A new subject area of mathematics called hypercalculus utilizes various types of unquantifiable forms (mathematical objects that cannot be quantified by numeric values or a nonnegative integer number of variables) to describe the properties of discrete-continuous dual spaces.

## 7. GLOSSARY

**additive distance function** – a distance function for which the total distance along a shortest path equals the sum of distances along the various parts of that shortest path.

**asymptotically discrete-continuous dual space** – a discrete-continuous dual space in which positions in the discrete and continuous representations are asymptotically matched.

**compact cross-section** – the hypervolume of a space per unit hypervolume of the macroscopic (hyper)coordinates.

**compact dimension** – a dimension which operates over a limited distance.

**complementarity** – “The concept that the underlying properties of entities (especially subatomic particles) may manifest themselves in contradictory forms at different times, depending on the conditions of observation; thus, any physical model of an entity exclusively in terms of one form or the other will be necessarily incomplete.” (American Heritage Science Dictionary, 2005)

**connected space** – a space in which any two points contained in the space can be joined by a connected path that doesn't leave the space.

**connectivity dimensionality field** – an effective and smooth measure of the number of linearly independent directions passing through each location in a space.

**connectivity dimensionality uncertainty principle** – the principle that measurement of the connectivity dimensionality involves inherent uncertainty unless the space is 0-dimensional, 1-dimensional, representative of a periodic lattice, or contains an infinite number of quantifiable points per unit hypervolume.

**connectivity distance** – the minimum number of edges in a connected path between two chosen vertices in an edge-vertex graph.

**connectivity radius** – a radius-like quantity based on the connectivity distance. The connectivity radius is used to specify a collection of positions that are the same connectivity distance away from a chosen position.

**continuous space** – a space in which positions can be varied differentially.

**count function** – the number of vertices contained in a region of space.

**differential manifold** – a continuous space for which (i) the connectivity dimensionality field is a constant nonnegative integer and (ii) the notion of differentiation with respect to position changes is defined.

**discrete space** – a space in which positions cannot be varied differentially.

**discrete-continuous dual matching** – the process of asymptotically or strictly matching continuous positions and continuous distances in the continuous representation of a discrete-continuous dual space to the discrete positions and discrete distances in the discrete representation of that discrete-continuous dual space.

**discrete-continuous dual space** – a space with two complementary representations: (i) a continuous representation in which positions can be varied differentially, and (ii) a discrete representation in which positions cannot be varied differentially.

**discrete-continuous duality** – exhibiting complementarity of discrete and continuous behaviors.

**elementary vertexal compartment** – a continuous region of unit hypervolume in the continuous representation of a discrete-continuous dual space which signifies the hypervolume spanned by a vertex in the discrete representation.

**Euclidean covering dimensionality of connected space  $\mathbb{S}$**  – the minimum topological dimensionality of a Euclidean space needed to properly draw one space  $\mathbb{S}'$  that is topologically equivalent to  $\mathbb{S}$ . The Euclidean covering dimensionality is always a nonnegative integer and refers to the space  $\mathbb{S}$  as a whole.

**expectation value** – the average of expected outcomes, which equals the value of each outcome times the relative probability of observing that outcome.

**false crossing** – a place in the drawing of a graph where two edges appear to cross but there is no vertex at the crossing.

**fractal** – “any of various extremely irregular curves or shapes for which any suitably chosen part is similar in shape to a given larger or smaller part when magnified or reduced to the same size.”<sup>26</sup>

**fractal dimensionality** – a measure of the self-similar scaling behavior of fractals and other objects: the capacity, Hausdorff, and box counting dimensionalities are various measures of the fractal dimensionality.

**half-integer** – a number  $X$  is half-integer if and only if  $(X + \frac{1}{2})$  is an integer.

**hard boundary** – a boundary that terminates one or more active directions within a space.

---

<sup>26</sup> Merriam-Webster Online Dictionary: <http://www.m-w.com/dictionary/fractal>

**hidden dimension** – a compact dimension with a compaction length smaller than the chosen observation scale.

**homeomorphism** – a continuous bijective map between two spaces.

**hyperability** – the number of continuous boundary conditions and continuous parameters that must be specified to give a particular self-consistent solution to a mathematical system.

**hyperbubble** – a region that may be surrounded by a hypersphere (or topologically equivalent surface) that cannot be contracted to a point without leaving the space.

**hypercoordinates** – the continuous forms pointing to the independent positions in a discrete-continuous dual space.

**hypercoordinate distance** – a continuous invariant distance measure associated with changes in hypercoordinate positions.

**hypercoordinate radius** – a radius-like quantity based on the hypercoordinate distance. The hypercoordinate radius is used to specify a collection of positions that are the same hypercoordinate distance away from a chosen position.

**hyperderivative** – a derivative-like object constructed in a discrete-continuous dual space.

**hyperdifferential equation** – a differential-equation-like object constructed in a discrete-continuous dual space.

**hypergradient** – a gradient-like object constructed in a discrete-continuous dual space.

**hyperintegral** – an integral-like object constructed in a discrete-continuous dual space.

**hypermatrix** – a matrix-like object constructed in a discrete-continuous dual space.

**hypertensor** – a tensor-like object constructed in a discrete-continuous dual space.

**hypervector** – a vector-like object constructed in a discrete-continuous dual space.

**intrusive hyperbubble** – a hyperbubble with a hard boundary.

**invariant distance parameter or invariant distance measure** – a parameter used to measure distance that is independent of reference frame or coordinate system.

**isovertexal hypercoordinate basis** – a hypercoordinate basis in which the vertexal density is everywhere equal to 1.

**large-world network** – a network comprised of many vertices connected in such a way that the connectivity distance between most pairs of vertices is large.

**latent hyperbubble** – a hyperbubble with a soft boundary.

**lattice** – (a) a strictly discrete-continuous dual space in which the continuous representation is a differential manifold, or (b) the discrete representation of (a).

**lattice companion graph** – an edge-vertex graph associated with a periodic lattice in which each vertex represents a unit cell and two vertices are joined by an edge iff. the unit cells are adjacent.

**manifold covering dimensionality of a connected space  $\mathbb{S}$**  – the minimum topological dimensionality of a smooth manifold needed to properly draw one space  $\mathbb{S}'$  that is topologically equivalent to  $\mathbb{S}$ . The manifold covering dimensionality is always a nonnegative integer and refers to the space  $\mathbb{S}$  as a whole.

**mathematical dimensionality** – the number of independent continuous variables in a self-consistent solution of a mathematical system.

**minimum connectivity radius** – the minimum connectivity radius needed to calculate a meaningful estimate of the connectivity dimensionality.

**noncompact dimension** – a dimension which operates over a virtually unlimited distance.

**nonfractal** – an object or function that is not a fractal.

**nonnegative extensive property** – a property that is zero for the null set, positive for any region of space with positive hypervolume, and for which the property value of the union of two nonintersecting regions equals the sum of property values for those two regions.

**periodic lattice** – a lattice with a translational unit cell and periodic structure.

**properly drawn graph** – a graph drawing with no false crossings.

**quantifiable forms** – forms that can be quantified by numeric values or a nonnegative integer number of variables.

**quartropy** – the base 2 logarithm of the number of discrete possibilities in the family of possible solutions out of which one particular must be chosen in order to specify a self-consistent solution to the mathematical system.

**relatively well-defined** – defined but potentially containing inherent uncertainty.

**small-world network** – a network comprised of many vertices connected in such a way that the connectivity distance between any two vertices is small.

**soft boundary** – a boundary that does not terminate any active directions within a space.

**strictly discrete-continuous dual space** – a discrete-continuous dual space in which the positions in the discrete representation are strictly matched to a subset of positions in the continuous representation.

**topological dimensionality (or Lebesgue covering dimension)** – “A space has Lebesgue covering dimension  $m$  if for every open cover of that space, there is an open cover that refines it such that the refinement has order at most  $m + 1$ . Consider how many elements of the cover contain a given point in a base space. If this has a maximum over all the points in the base space, then this maximum is called the order of the cover. If a space does not have Lebesgue covering dimension  $m$  for any  $m$ , it is said to be infinite dimensional.”<sup>27</sup>

**topologically equivalent** – two spaces are topologically equivalent iff. they are related to each other by a homeomorphism.

**transcending variable-based mathematics** – requiring the mathematics of unquantifiable forms.

**unquantifiable forms** – forms that cannot be quantified by numeric values or a nonnegative integer number of variables.

**variable-based mathematics** – mathematics involving quantifiable forms but not unquantifiable forms.

**vertex-labeled graph** – an edge-vertex graph in which each vertex is labeled with a scalar value.

**vertexal density** – the number of vertices per unit hypervolume.

**vertexal hypervolume** – hypervolume in the isovortexal hypercoordinate basis.

## REFERENCES

J. R. Carr and W. B. Benzer, “On the practice of estimating fractal dimension,” *Mathematical Geology* 23 (1991) 945-958. doi:10.1007/BF02066734

“complementarity,” *The American Heritage® Science Dictionary*, (Houghton Mifflin Company, 2005; ISBN: 978-0618455041).

---

<sup>27</sup> Eric W. Weisstein. "Lebesgue Covering Dimension." From *MathWorld*--A Wolfram Web Resource. <http://mathworld.wolfram.com/LebesgueCoveringDimension.html>

A. Corana, G. Bortolan, and A. Casaleggio, "Most probable dimension value and most flat interval methods for automatic estimation of dimension from time series," *Chaos, Solitons, and Fractals* 20 (2004) 779-790. doi: 10.1016/j.chaos.2003.08.012

C. D. Cutler, "A Review of the Theory and Estimation of Fractal Dimension," *Dimension Estimation and Models, Nonlinear Time Series and Chaos*, H. Tong (editor), Vol. 1, (World Scientific, 1994; ISBN:978-9810213534), pp. 1-107.

"fractal dimensionality," *McGraw-Hill Dictionary of Scientific and Technical Terms*, 4th edition, (McGraw-Hill, 1989; ISBN: 0070452709) p. 757.

L. C. Freeman, "Spheres, Cubes, and Boxes: Graph Dimensionality and Network Structure," *Social Networks* 5 (1983) 139-156.

F. Hausdorff, *Grundzüge der Mengenlehre* (von Veit, 1914; ISBN: 978-3540422242). English version published as *Set Theory, 2nd ed.* (Chelsea, 1962; ISBN: 978-0828401197).

J. Li, A. Arneodo, and F. Nekka, "A practical method to experimentally evaluate the Hausdorff dimension: An alternative phase-transition-based methodology," *Chaos* 14 (2004) 1004-1017. doi:10.1063/1.1803435

B.B. Mandelbrot, "Self-Affine Fractals and Fractal Dimension," *Phys. Ser.* 32 (1985) 257-260. doi:10.1088/0031-8949/32/4/001

O. Nairz, M. Arndt, and A. Zeilinger, "Quantum interference experiments with large molecules," *Am. J. Phys.* 71 (2003) 319-325. doi: 10.1119/1.1531580

D. M. Y. Sommerville, *An Introduction to the Geometry of  $n$  Dimensions* (Dover, 1958; ISBN: 978-0486604947) 135-137.

J. Theiler, "Estimating fractal dimension," *J. Opt. Soc. Am.* 7 (1990) 1055-1073.

J. Travers and S. Milgram, "An Experimental Study of the Small World Problem," *Sociometry* 32 (1969) 425-443. doi:10.2307/2786545

W. J. Wang and J. Chen, "Estimation and Application of Correlation Dimension of Experimental Time Series," *Journal of Vibration and Control* 7 (2001) 1035-1047. doi:10.1177/107754630100700705